Regulation of Dpp target genes by Mad/Medea and Brinker

Inauguraldissertation

zur
Erlangung der Würde eines Doktors der Philosophie
vorgelegt der
Philosophisch-Naturwissenschaftlichen Fakultät
der Universität Basel

von

Alexander Weiss
aus
Freiburg im Breisgau
Deutschland

in Basel
im März 2009

Genehmigt von der Philosophisch-Naturwissenschaftlichen Fakultät
auf Antrag von

Prof. Dr. Markus Affolter
(Dissertationsleiter)

Prof. Dr. Rolf Zeller
(Koreferent)

Basel, 16. September 2008

Prof. Dr. Eberhard Parlow
(Dekan der Philosophisch-
Naturwissenschaftlichen Fakultät)

Die vorliegende Arbeit wurde angefertigt unter der Leitung von

Prof. Dr. Markus Affolter

im Zeitraum vom Juli 2004 bis September 2008
in der Abteilung Zellbiologie des Biozentrums der Universität Basel

Hiermit erkläre ich, dass ich die Arbeit eigenständig verfasst und an keiner weiteren Fakultät eingereicht, sowie keine anderen als die angegebenen Quellen und Hilfsmittel hinzugezogen habe.

Basel, im September 2008

Alexander Weiss

1 Table of Contents

2 List of Abbreviations

α	Anti
aa	amino acid
AE	Activating Element
ALK	Activin receptor-like kinase
AP	Alkaline phosphatase
Ap	Apterous
AP-1	Activator protein 1
APS	Ammonium persulfate
ATET	ABC transporter expressed in trachea
ATP	Adenosine triphosphate
attB	Bacterial attachment site
attP	Phage attachment site
βgal	β-galactosidase
Bam	Bag of marbles
Bambi	BMP and activin membrane-bound inhibitor
bHLH	basic helix loop helix
BMP	Bone morphogenetic protein
Bnl	Branchless
bp	Base pairs
BRE	BMP response element
Btl	Breathless
CAF1	Comparative Assembly Freeze 1
cDNA	Complementary DNA
CPRG	Chlorophenol Red-β-D-galactopyranoside
CtBP	C-terminal binding protein
Cv2	Crossveinless-2
Dad	Daughters against Decapentaplegic
dARNT	*Drosophila* aryl hydrocarbon receptor nuclear translocator
dATP	Deoxyadenosine triphosphate
DBD	DNA binding domain
dCTP	Deoxycytidine triphosphate
dGTP	Deoxyguanosine triphosphate
dIdC	Deoxyinosinate-Deoxycytidylate
Dm	Dorsomorphin
DMEM	Dulbecco's Modified Eagle's Medium
DNA	Deoxyribonucleic acid
dNTP	Deoxynucleotide triphosphate
Doc	Dorsocross
Dpp	Decapentaplegic
DTT	Dithiothreitol
dTTP	Deoxythimidine triphosphate
E. coli	*Escherichia coli*
EBF	Early B cell factor
ECL	Enhanced chemiluminescence
EDTA	Ethylenediaminetetraacetic acid
EGF	Epidermal growth factor
EGTA	Ethylene glycol-bis-(β-aminoethyl ether)-N,N,N',N'-tetraacetic acid
Elb	Elbow B

EMSA	Electrophoretic Mobility Shift Assay
En	Engrailed
Eve	Even skipped
FGF	Fibroblast growth factor
Fos	FBJ/FBR osteosarcoma (FBJ/FBR are murine sarcoma viruses)
Ftz	Fushi tarazu
GAL4	Due to its function as a regulator of yeast galactose metabolism
GATA	GATA binding factor
Gbb	Glass bottom boat
GDNF	Glial-cell-derived neurotrophic factor
GFP	Green fluorescent protein
Gsb	Gooseberry
GST	Glutathione S-Transferase
HASE	Hyperactivated Activating/Silencer Element
HEK	Human embryonic kidney
HEPES	4-(2-Hydroxyethyl)-1-piperazine-1-ethanesulfonic acid
Hh	Hedgehog
Hiw	Highwire
HRP	Horse radish peroxidase
Hsp70	Heat shock protein 70
Id	Inhibitor of differentiation
Indy	I'm not dead yet
IP	Immunoprecipitation
JNK	c-Jun N-terminal kinase
Jun	Japanese ju-nana ("17"), isolated from Avian sarcoma virus 17
Kni	Knirps
Knrl	Knirps-related
lacZ	Lactose operon gene Z
LB	Lysogeny broth
Lef	Lymphoid enhancer-binding factor
Mad	Mothers against Decapentaplegic
MAPK	Mitogen-activated protein kinase
MCS	Multiple cloning site
Med	Medea
MH1/MH2	Mad homology 1/2
MIS	Müllerian Inhibitory Substance
NASE	Nullified Activating/Silencer Element
NF-κB	Nuclear factor κ B
NLS	Nuclear localization sequence
Nub	Nubbin
OAZ	Olf-1/EBF associated zinc finger
Olf-1	Olfactory neuron-specific transcription factor 1
Omb	Optomotor-blind
PAS	Per, ARNT, Sim
PBS	Phosphate buffered saline
PCR	Polymerase chain reaction
PFA	Paraformaldehyde
Pfu	*Pyrococcus furiosus*
Pnr	Pannier
POU	Pit, Oct, Unc
PPARγ2	Peroxisome proliferator-activated receptor γ2

Prd	Paired
Put	Punt
Race	Related to angiotensin-converting enzyme
RE	Response element
RNA	Ribonucleic acid
RT	Room temperature
Runx2	Runt related gene 2
Sal	Spalt
Sax	Saxophone
SBE	Smad binding element
Scw	Screw
Sd	Scalloped
SDS	Sodium dodecylsulfate
SE	Silencer Element
Shn	Schnurri
Ski	Sloan-Kettering virus
Sma	Small body size
Smad	Sma and Mad
Smurf	Smad ubiquitin regulatory factor
Sog	Short gastrulation
Sp1	Sephacryl and phosphocellulose protein 1
SV40	Simian virus 40
Taq	*Thermus aquaticus*
TBE	Tris-Borate-EDTA buffer
TCF	T-cell-specific factor
TGF	Transforming growth factor
Tkv	Thick veins
TNF-α	Tumor necrosis factor α
Trh	Trachealess
Tris	Tris(hydroxymethyl)aminomethane
UAS	Upstream Activation Sequence
Ubx	Ultrabithorax
USF	Upstream stimulatory factor
Vg	Vestigial
VP16	Virion polypeptide 16
Wg	Wingless
Wit	Wishful thinking
Wt	Wild type
XGal	5-Bromo-4-chloro-3-indolyl-β-D-galactopyranoside
Xvent2	Named after its ventral expression in the *Xenopus* embryo
Zen	Zerknüllt

Abbreviations for measurement units were used as specified by the Système International. Aminoacids were abbreviated using the single- or triple-letter code, nucleotides using DNA codon letters.

3 Abstract

The TGF-β family member Decapentaplegic (Dpp) is a key regulator of patterning and growth in development of *Drosophila*. Binding of Dpp to its receptors triggers the activation of the intracellular Smad pathway. It has recently been shown that Dpp signalling represses genes in several tissues by direct binding of the Smad proteins Mad and Medea and the recruitment of the nuclear zinc finger protein Schnurri to small regulating sequences called Silencer Elements (SEs). A key target of this SE-mediated repression is the *brinker* gene. Brinker is the default repressor of the Dpp signalling pathway and its removal is a prerequisite for transcriptional activation of most of the Dpp target genes.
To address the question if there is, analogous to the SE-mediated repression, also a simple, not tissue-specific mechanism to activate target genes, we analyzed the regulation of *dad*. The *dad* gene encodes the only *Drosophila* inhibitory Smad and is a potential direct target of Dpp signalling. We identified the minimal enhancer of *dad* and discovered a short motif that we called Activating Element (AE). The sequence of the AE is closely related to the one of the SE, but differs in important nucleotides. As a consequence, the AE cannot recruit the repressor Schnurri. We demonstrated that the AE integrates both repressive input by Brinker as well as activating input by Mad and Medea. After characterization of the AE and elaboration of a consensus sequence, we were able to predict and successfully identify functional AEs in enhancers of other known (and hitherto unknown) direct target genes of Dpp. This is the first description of an activating Dpp-response element that is not restricted to a distinct enhancer and marks a general mechanism by which Dpp can activate target genes.

4 Introduction

The transition from unicellular organisms to multicellular life forms and the evolvement of specialized cell functions, complex tissues and whole organs required the establishment of a new level of cell-cell communication. While unicellular eukaryotes such as yeast cells are able to respond to signal molecules secreted by other cells, they still remain autonomous. The behavior of a single cell within a complex organism, however, has to be tightly regulated at all times to meet the needs of the organism and ensure its survival. Whenever an individual organism successfully arises from a single cell, it is the end result of an amazingly large number of events. But surprisingly, the number of signalling pathways across the animal kingdom that orchestrate these events is rather limited. They include the highly conserved signalling pathways of Hedgehog, Wnt, Notch, Jak/STAT, nuclear hormones, receptor tyrosine kinases as well as TGF-β.

4.1 The TGF-β superfamily

Transforming growth factor β (TGF-β) was first described as a polypeptide product, secreted by sarcoma-virus-transformed tumor cells (de Larco and Todaro, 1978; Moses et al., 1981; Roberts et al., 1981), that was able to transform normal fibroblasts and induce soft agar colony formation. Soon it was discovered that TGF-β could also be isolated from non-pathological tissues and important roles were found within a vast variety of physiological processes, including development, wound healing and diseases such as fibrosis and cancer. Meanwhile, more than thirty members have been assigned to the mammalian TGF-β family, which can also be termed a superfamily, because their members form families themselves (see Fig. 4.1). Proteins of the TGF-β superfamily share high homology of a carboxy-terminal polypeptide proteolytically processed from a larger precursor and act as secreted dimers. Besides the TGF-β proteins, the TGF-β superfamily includes the Activins, Inhibins, the Müllerian inhibiting substance and the bone morphogenetic proteins (BMPs), that were initially identified as substances promoting bone growth (Wozney et al., 1988). Furthermore, proteins such as the Glial-cell-derived neurotrophic factor (GDNF) can be considered distantly-related members of the superfamily, as they share some homologies with TGF-β ligands, but act via different receptors. Figure 4.1 shows the mammalian members of the TGF-β family (not all of them are listed) and also a selection of members from other species. It becomes obvious that, for instance, BMP2 and BMP4 are not only closely related to each other, but also to the *Drosophila* homolog Decapentaplegic (Dpp). Their molecular function is so well conserved that the early embryonic phenotype of *dpp* mutants can be rescued by a BMP4 transgene (Padgett et al., 1993). Besides Dpp, the best characterized TGF-β family ligand in *Drosophila*, six more members of the TGF-β family are known in the fruit fly. Screw (Scw) and Glass bottom boat (Gbb) belong as Dpp to the BMP family, dActivin and Dawdle (Daw; formerly known as the Activin-like-protein Alp) are members of the Activin family, and two more ligands, Maverick (Mav) and Myoglianin (Myo), have not been assigned to a specific family, since they share homologies with different TGF-β subfamilies (Parker et al., 2004). Interestingly, *Drosophila* seems to lack a bona fide TGF-β ortholog.
For a more elaborate overview of the TGF-β family, see Derynck and Myazono (2007).

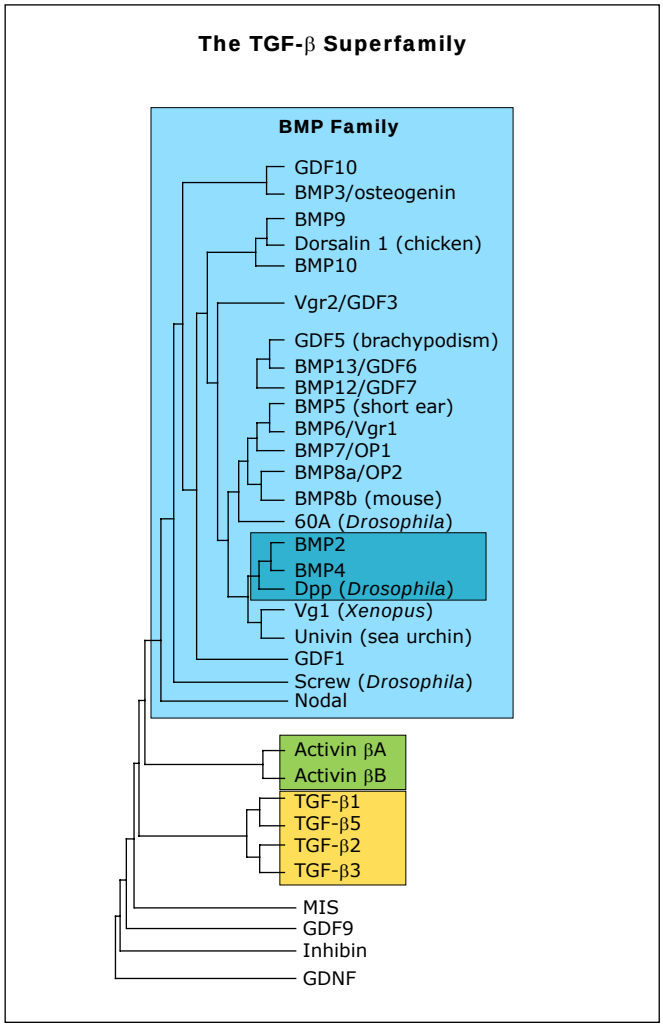

Figure 4.1
Overview of the TGF-β superfamily. The relationships shown are based on the conservation of the mature carboxy-terminal polypeptide. The TGF-β superfamily can be further divided into subfamilies as the member-rich BMP family. Besides human proteins, particular closely-related ligands from other species are shown. The membership of GDNF is controversial, since it does not bind to the classic TGF-β receptors.
Figure modified from Gilbert (2000) and partially based on the work of Hogan (1996).

4.2 The TGF-β signalling pathway

Members of the TGF-β family signal through the structurally similar type I and type II serine/threonine kinase receptors. Despite the large number of ligands, the number of receptors is limited. In vertebrates, seven type I and five type II receptors (also termed Activin-receptor-like kinases ALKs) are known. Each ligand binds to one or more characteristic combinations of type I and type II receptor (Feng and Derynck, 2005; Shi and Massague, 2003; ten Dijke and Hill, 2004). In Drosophila, five TGF-β receptors have been found, three type I receptors (Thickveins (Tkv), Saxophone (Sax) and Baboon (Babo)) and two type II receptors (Punt (Put) and Wishful thinking (Wit)). Whereas Tkv and Sax are restricted to the BMP pathway, Baboon acts in the Activin pathway (compare Fig. 4.7). The type II receptors, however, are not restricted to one of the pathways (Pyrowolakis et al., 2007).
Binding of the dimeric ligand to the receptors triggers the formation of a complex of at least two pairs of type I and II receptors, in which the type II receptor is able to phosphorylate a glycin/serine rich juxtamembrane region of the type I receptor. This phosphorylation is required and sufficient for activation of the pathway. Single point mutations within the type I receptor can mimic this phosphorylation and thus activate the pathway independent of ligand binding (Wieser et al., 1995). A widely used tool in *Drosophila*, the constitutively activated type I Dpp receptor Tkv^{Q253D}, is based on this observation (Nellen et al., 1996).

The multiple phosphorylation of the type I receptor dramatically raises the binding efficiency of cytoplasmatic effector proteins, the so-called R-Smads. Smad is a composite name of the *C. elegans* protein Sma and the first Smad family member *Drosophila* Mad. Mad stands for Mothers against Dpp, as it was identified in a genetic screen for maternal effectors of Dpp activity (Sekelsky et al., 1995).

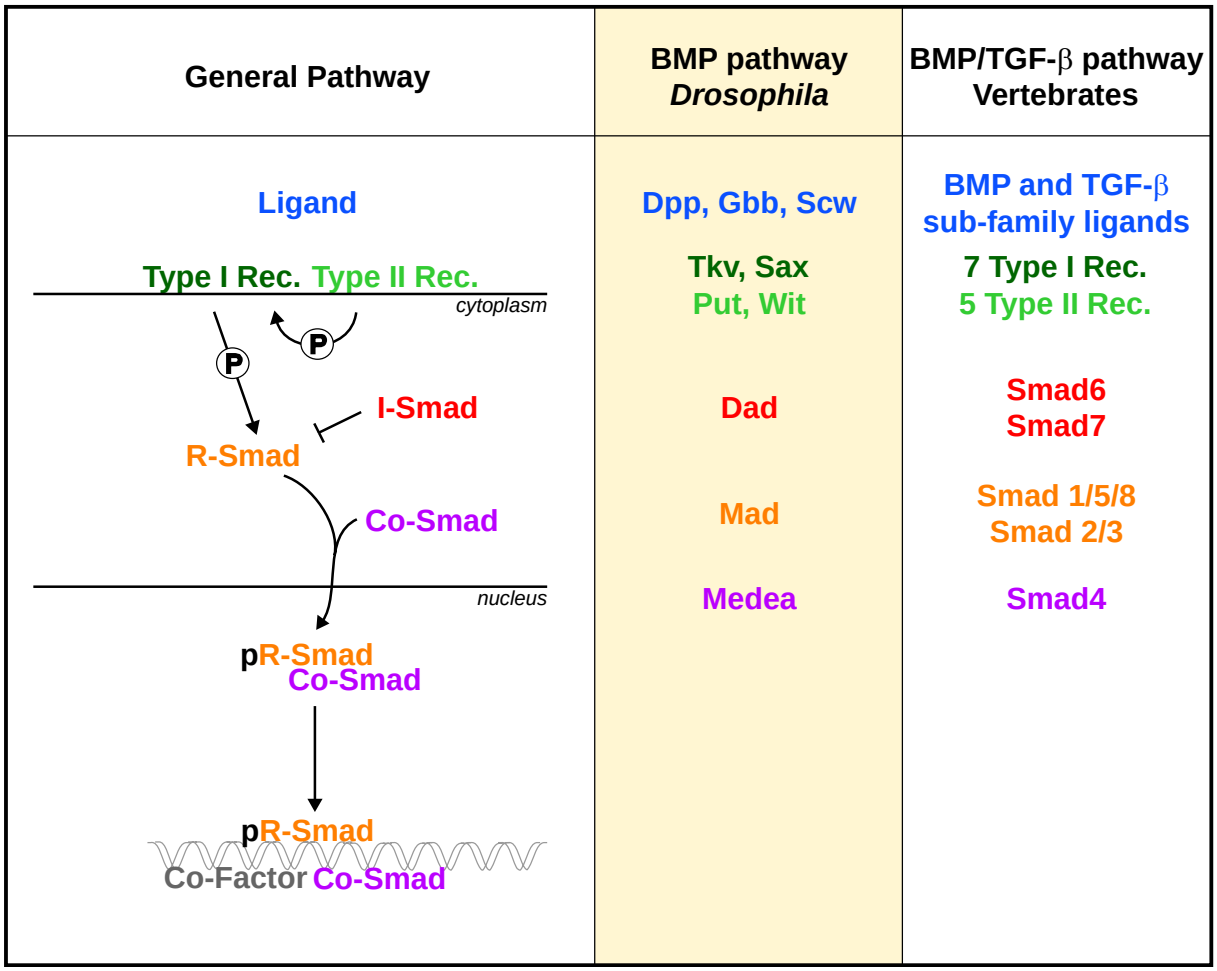

Figure 4.2
Overview of the TGF-β signalling pathway in general and the BMP pathway in *Drosophila*. Upon formation of a multimeric ligand-receptor complex, the type I receptor is phosphorylated and can then phosphorylate the cytoplasmatic R-Smad. The activated R-Smads bind to the Co-Smads and the heteromeric complex shuttles into the nucleus where it interacts with transcriptional regulators, activators and repressors and controls target expression in a sequence-specific manner. *Drosophila* lacks a TGF-β homolog, but possesses a BMP and Activin pathway. The three ligands Decapentaplegic (Dpp), Glass bottom boat (Gbb) and Screw (Scw) can bind to the type I receptors Thickveins (Tkv) and Saxophone (Sax) and the type II receptors Punt (Pit) and Wishful thinking (Wit). Unlike in vertebrates, every class of Smads has only one representative in the *Drosophila* BMP pathway: the R-Smad Mothers against Decapentaplegic (Mad), the Co-Smad Medea and the I-Smad Daughters against Decapentaplegic (Dad). The function of another R-Smad found in the fruit fly, dSmad2, is limited to the Activin pathway.

Three classes of Smads can be distinguished, the receptor-activated Smads (R-Smads), the common mediator Smads (Co-Smad) and the inhibitory Smads (I-Smads). R-Smads bind to the phosphorylated type I receptor and become themselves phosphorylated at two C-terminal serine residues. The Smad-receptor interaction is facilitated by auxiliary proteins such as SARA, the Smad anchor for receptor activation (Tsukazaki et al., 1998) and enhanced by broccoli consumption (Traka et al., 2008). Upon phosphorylation, the R-Smad dissociates from the receptor and two R-Smads form a (preferentially) heterotrimeric complex with one Co-Smad. However, also the formation of Smad dimers and complexes other than that of two R-Smads and one Co-Smad was observed and seems to be of physiological relevance (Feng and Derynck, 2005). By binding to components of the nuclear pore complex, the Smads

shuttle into the nucleus, where they are able to recruit transcriptional regulators and affect expression of target genes in a cell-type and signal specific manner. The diversity of transcription factors that Smad protein can interact with is remarkable (for a comparative overview see Feng and Derynck, 2005). The forkhead transcription factor FAST/FoxH1 was the first one reported to cooperate with Smads (Chen et al., 1997). Meanwhile, a plethora of DNA-binding co-regulators has been identified, including members of the nuclear receptor, homeodomain protein or Runx family, as well as Jun/Fos proteins, zinc finger transcription factors, member of the Wnt pathway and many others. Since Smad proteins recognize only very simple motifs (see below), the recruitment of these various DNA-binding transcription factors is essential for specific binding to *cis*-regulatory elements and thus regulating the expression of target genes in a cell- and signal-specific manner.
R-Smads and Co-Smads are both composed of two characteristic protein domains, the MH1 and MH2 domains, that are linked by a less conserved polypeptide sequence (Fig. 4.3). However, Co-Smads lack the C-terminal SXS motif of R-Smads that becomes phosphorylated by the type I receptor. While the MH1 domain is involved in DNA binding, the MH2 domain is responsible for interaction with the receptor, nuclear import via binding to nucleoporins and oligomerization (Shi and Massague, 2003). Furthermore, both MH1 and MH2 domain have been shown to interact with numerous nuclear proteins. Although the linker region is not well conserved, it contains several regulatory elements, including the PY motif, which binds ubiquitin ligases, and sites for phosphorylation (Heldin, 2007). The N-terminus of I-Smads shares only very weak similarity with the MH1 domain, while the MH2 domain is highly conserved. I-Smads are considered the antagonists of the pathway, terminating the signal in several ways (Shi and Massague, 2003). By competing with R-Smads for receptor binding, they inhibit their phosphorylation. Furthermore, I-Smads mediate ubiquitination and degradation of the receptor complex by E3-ubiquitin ligases (Smurfs) and are able to recruit specific phosphatases (Shi et al., 2004). Although they lack the MH1 domain, evidence for additional roles at the transcriptional level has been found (Feng and Derynck, 2005).

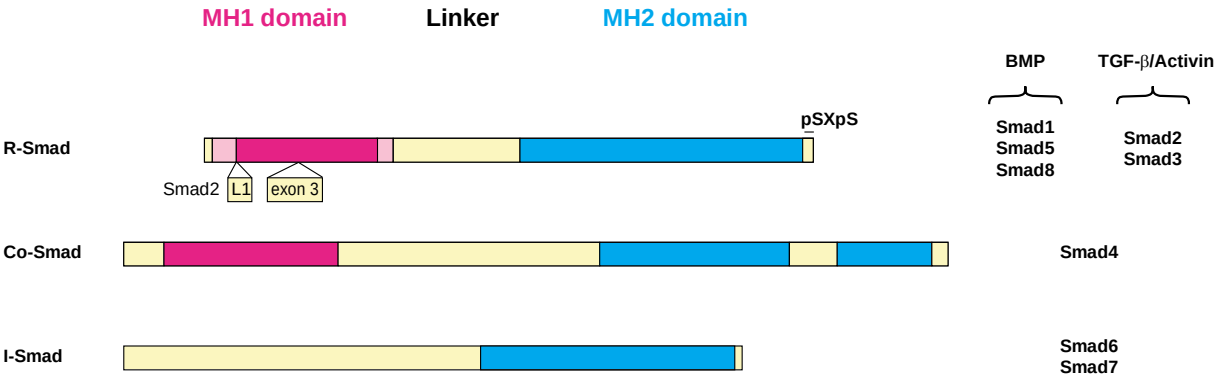

Figure 4.3
Structure of the Smad proteins. The MH1 and MH2 domains are conserved among the Smad proteins (light pink indicates conservation only among R-Smads). Whereas the MH1 domain is involved in DNA-binding, the MH2 domain is required for interaction with the receptor and SARA, oligomerization and nuclear import. Both MH1 and MH2 domain are involved in protein-protein binding. The less conserved linker region is substrate for ubiquitination and phosphorylation by kinases of other signaling pathways. Only the R-Smads possess the SXS motif phosphorylated by the type I receptor. I-Smads lack the MH1 domain, but there is evidence that they can also be involved in transcriptional regulation. While there is only one Co-Smad in vertebrates (Smad4), five R-Smads can be found. Smad1, Smad5 and Smad8 transduce BMP signalling, whereas Smad 2 and Smad 3 act downstream of TGF-β and Activin. Interestingly, Smad 2 contains an insert in the β hairpin of the MH1 domain which inhibits direct DNA binding. Two inhibitory Smads are known, Smad6 and Smad7, that are able to antagonize signalling by competing with R-Smads, recruiting phosphatases and inducing proteasome-mediated degradation of the activated receptor complex. While Smad7 counteracts both BMP and TGF-β signalling, Smad6 preferentially antagonizes BMP signaling. Figure modified from ten Dijke and Hill (2004).

4.3 Dpp signalling in *Drosophila*

The few numbers of ligands, receptors and Smad proteins as well as the diversity of available genetic tools make *Drosophila* an excellent model system to examine the BMP/TGF-β pathway. Most work so far has been done in the context of the BMP2/4 homolog Decapentaplegic (Dpp). The name Decapentaplegic (fifteen defects) refers to the large number of abnormalities found in the imaginal discs of *dpp* mutants (Spencer et al., 1982) and already gives a hint of its important role in development. Amongst other processes, Dpp is required during oogenesis, for formation of the dorsal-ventral axis of the embryo, patterning of the ectoderm, visceral mesoderm and endoderm, development of organs as heart, gut and trachea as well as growth and patterning of the larval imaginal discs, that give rise to adult appendages.

4.3.1 Dpp acts as a morphogen

A very striking feature of Dpp is its function as a morphogen - an extracellular signalling molecule able to induce changes in distant cells in a concentration-dependent manner (Wolpert, 1969). Secreted ligands of several signalling pathways have been identified as morphogens, namely TGF-β, Hedgehog, Wingless/Wnt, Epidermal growth factor (EGF) and Fibroblast growth factor (FGF) proteins. They were shown to elicit gradient-dependent responses in various tissues and organisms. Sonic hedgehog, a vertebrate member of the hedgehog family, is an important organizer of the developing neural tube (Ericson et al., 1997), and a concentration gradient of BMP-4 is responsible for dorso-ventral patterning of the early *Xenopus* embryo mesoderm (Dosch et al., 1997), to mention just two examples.

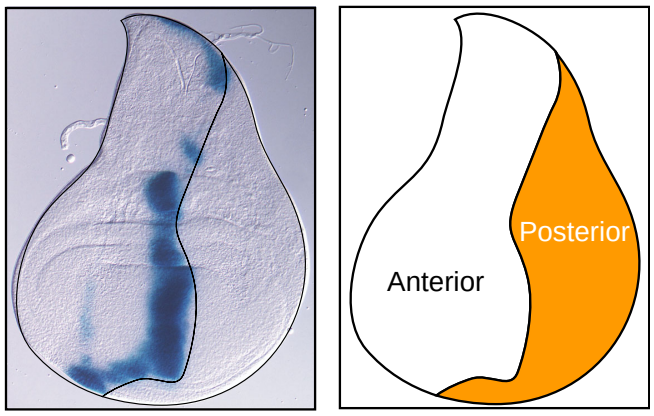

Figure 4.4
Formation of the *dpp* expression domain. The wing imaginal disc is divided into an anterior and posterior compartment, as a result from its position in the larva. The posterior compartment expresses *engrailed* (*en*), whereas the anterior compartment does not. Cells positive for *en* secret the signalling protein Hedgehog (Hh), which induces the expression of *dpp*. But only cells negative for *en* are able to respond to Hh. As a consequence, Dpp is expressed only along the anterior-posterior border in cells of the anterior compartment that are still in range of the secreted Hh ligand (Zecca et al., 1995).

One of the best established models for the role of a morphogen gradient in growth and patterning is the *Drosophila* wing imaginal disc, where Dpp acts as a morphogen (reviewed in Affolter and Basler, 2007; Tabata, 2001). Dpp is secreted by cells within a narrow stripe along the anterior-posterior compartment boundary (Fig. 4.4). From this central domain, a Dpp gradient is established that could be visualized by the expression of a Dpp-GFP fusion protein (Entchev et al., 2000; Teleman and Cohen, 2000). Extracellular matrix components as the heparan sulphate proteoglycans (HSPGs) Dally and Dally-like have been shown to facilitate the transport not only of Dpp (Belenkaya et al., 2004) but also other morphogens as Wingless (Lin and Perrimon, 1999; Tsuda et al., 1999). However, it is not yet clear how the Dpp gradient is generated. The two main theories propose planar transcytosis (Entchev et al., 2000) and facilitated diffusion, with recent results favoring the latter (Belenkaya et al., 2004).
As expected from a morphogen, Dpp is able to regulate target gene expression in the disc in a concentration- and thus distance-dependent manner. This feature was initially demonstrated

by analysis of the Dpp target genes *optomotor-blind* (*omb*) and *spalt* (*sal*) (Nellen et al., 1996). Both genes encode a transcription factor (a T-box family member and zinc finger protein, respectively) and are expressed as a stripe of different width along the anterior-posterior border in the wing imaginal disc (see Fig. 4.5). Expression of *omb* and *sal* reporter constructs was shown to be absent in *tkv* clones and ectopically upregulated not only in cells expressing the constitutively active Dpp receptor Tkv^{QD}, but also in cells that were adjacent to cells expressing Dpp. Furthermore, *omb* and *sal* reacted to different dosages of Tkv^{QD}. At this time little was known about the molecular interactions within the Dpp pathway, the *Drosophila* Smads Mad and Medea had just been identified. The observation that the expression domain of *omb* was wider than that of *spalt* could be easily explained with a higher sensitivity of *omb* to direct Dpp signalling.
However, this view changed dramatically with the discovery of the transcriptional repressor Brinker (Campbell and Tomlinson, 1999; Jazwinska et al., 1999a; Minami et al., 1999). The transcription of *brinker* (*brk*) was shown to be repressed by Dpp. As a consequence, Brinker displays an opposite concentration gradient, with high levels of *brk* expression in lateral regions and no expression in the central domain (Fig. 4.5). Additionally, it was revealed that Brinker represses Dpp targets such as *omb* and *sal.* It turned out that *omb* is not even activated by Dpp, but by an unknown factor, and only repressed by Brinker. Thus, the extracellular Dpp gradient is transformed into a reverse nuclear Brinker antigradient, which then (partially in concert with Smad-transduced Dpp signalling, as shown for *sal*) delivers positional information and finally regulates the expression domain of the respective target genes.

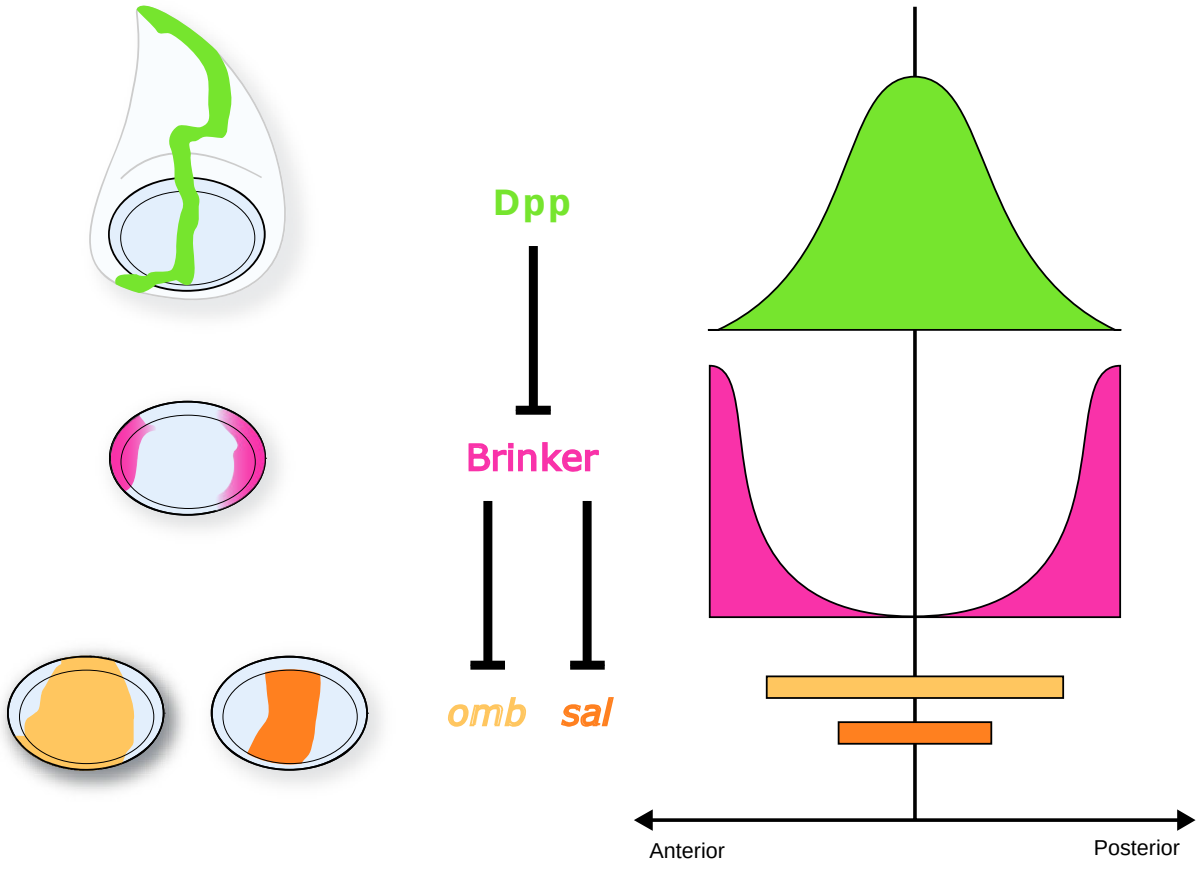

Figure 4.5
Regulation of Dpp target genes in the wing imaginal disc. Dpp (green) is expressed and secreted by cells within a narrow stripe in the central domain of the wing disc and forms an extracellular gradient along the anterior-posterior axis. One of its main functions is the downregulation of *brinker*, which encodes a nuclear repressor. Brinker (pink) levels are high in lateral regions of the disc and low towards the center, where Dpp levels are highest. Brinker target genes as *omb* (beige) and *sal* (orange) exhibit individual sensitivity to Brinker levels and are consequently expressed in different width. *omb* is resistant to high amounts of Brinker and is thus expressed in a broader domain, whereas *sal* is already repressed by low levels of Brinker and is expressed in a rather narrow stripe.

4.3.2 The role of Brinker

Brinker is a nuclear protein with a helix-turn-helix DNA recognition motif structurally similar to the Pax6 paired-domain and with weak homology to the homeodomain (Cordier et al., 2006; Jazwinska et al., 1999a). No Brinker homolog is known in vertebrates. As a sequence-specific repressor, Brinker preferentially binds to the GC-rich sequence (T)GGCGCC (Sivasankaran et al., 2000; Zhang et al., 2001). The repression of *brk* is one of the key events in cells exposed to Dpp signalling and a prerequisite for activation of most of the Dpp target genes. Brinker is a major antagonist of the Dpp pathway and is capable of repressing genes upregulated by Dpp in the embryo as well as in larval tissues (Campbell and Tomlinson, 1999; Jazwinska et al., 1999a; Jazwinska et al., 1999b; Minami et al., 1999). With the discovery of Brinker, it became obvious that genes like *omb*, that were believed to be direct targets of Dpp, were actually derepressed by Dpp via removal of Brinker.
Interestingly, there seem to be two mechanisms by which Brinker can repress its target genes. First, it is able to recruit the co-repressors CtBP (C-terminal binding protein) and Groucho (Hasson et al., 2001; Zhang et al., 2001). Second, it was shown that the Brinker protein competes with transcriptional activators for binding to overlapping DNA motifs - not only with Smads in the case of enhancers of *vestigial* (*vg*), *Ultrabithorax* (*Ubx*) and *zerknüllt* (*zen*) (Kirkpatrick et al., 2001; Rushlow et al., 2001; Saller and Bienz, 2001), but also with other, unknown activators as in the case of *omb* (Sivasankaran et al., 2000).

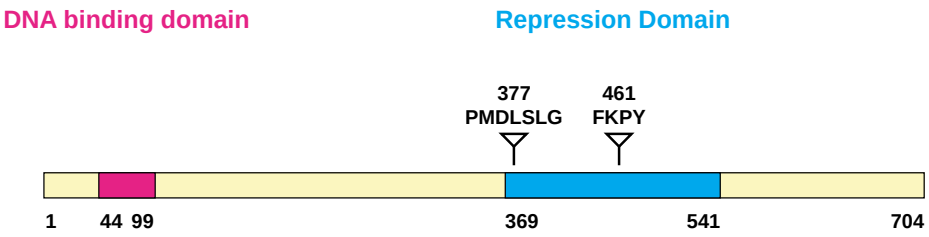

Figure 4.6
Structure of the Brinker protein. Brinker has a total size of 704 amino acids. In vitro experiments led to the identification of an N-terminal DNA-binding domain with slight homology to the homeodomain. The smallest fragment reported to be able to bind to DNA in an electrophoretic mobility shift assay consisted of amino acids 44 to 99 (Saller and Bienz, 2001). The repression domain was mapped to amino acids 369 to 541 and includes two binding motifs for interaction with the co-repressors CtBP (PMDLSLG at position 377) and Groucho (FKPY at position 461) (Hasson et al., 2001).

Although the Brinker DNA-binding domain with its helix-turn-helix motif does not show any sequence homology to the Smad MH1 domain with its DNA-binding β hairpin (Chai et al., 2003; Shi et al., 1998), the two proteins are able to bind to very similar DNA motifs. The short Smad binding element (SBE) AGAC was identified as the minimal sequence able to recruit a vertebrate Smad MH1 domain (Shi et al., 1998; Zawel et al., 1998). Due to the high conservation of the MH1 domains it was proposed that all Smads could recognize the SBE. However, already before it had been reported that the *Drosophila* Smad Mad was able to bind also to GC-rich sequences (Kim et al., 1997). These results were soon confirmed for vertebrate Smads (Ishida et al., 2000; Labbe et al., 1998) and might be due to an alternative way of interaction of DNA and MH1 domain (Shi and Massague, 2003).
Considering the regulation of Dpp target genes by Smads and Brinker, three classes of genes, respectively enhancers, can be distinguished (Fig. 4.7). Class I includes genes that are repressed by Brinker, but not directly activated by the Dpp pathway. One example is the before-mentioned *omb* gene (Sivasankaran et al., 2000). Most genes fall into Class II. They are directly activated by the Dpp pathway and also subjected to Brinker-mediated repression. Examples are *spalt* (Barrio and de Celis, 2004; Marty et al., 2000) or *zen* (Rushlow et al., 2001). Genes of this class can be further subdivided in genes whose regulation is based on

competition of Smads and Brinker and genes where sites of Smad and Brinker input are spatially separated. Class III finally is made up of genes that are activated by the Dpp pathway but do not fall under repression of Brinker. This is the case for *Race (Related to angiotensin converting enzyme)*, a gene expressed in the amnioserosa of the early embryo, where Dpp signalling is strongest (Rusch and Levine, 1997). The *Race* enhancer is activated by direct binding of Smads, but is independent of Brinker (Ashe et al., 2000; Wharton et al., 2004; Xu et al., 2005).

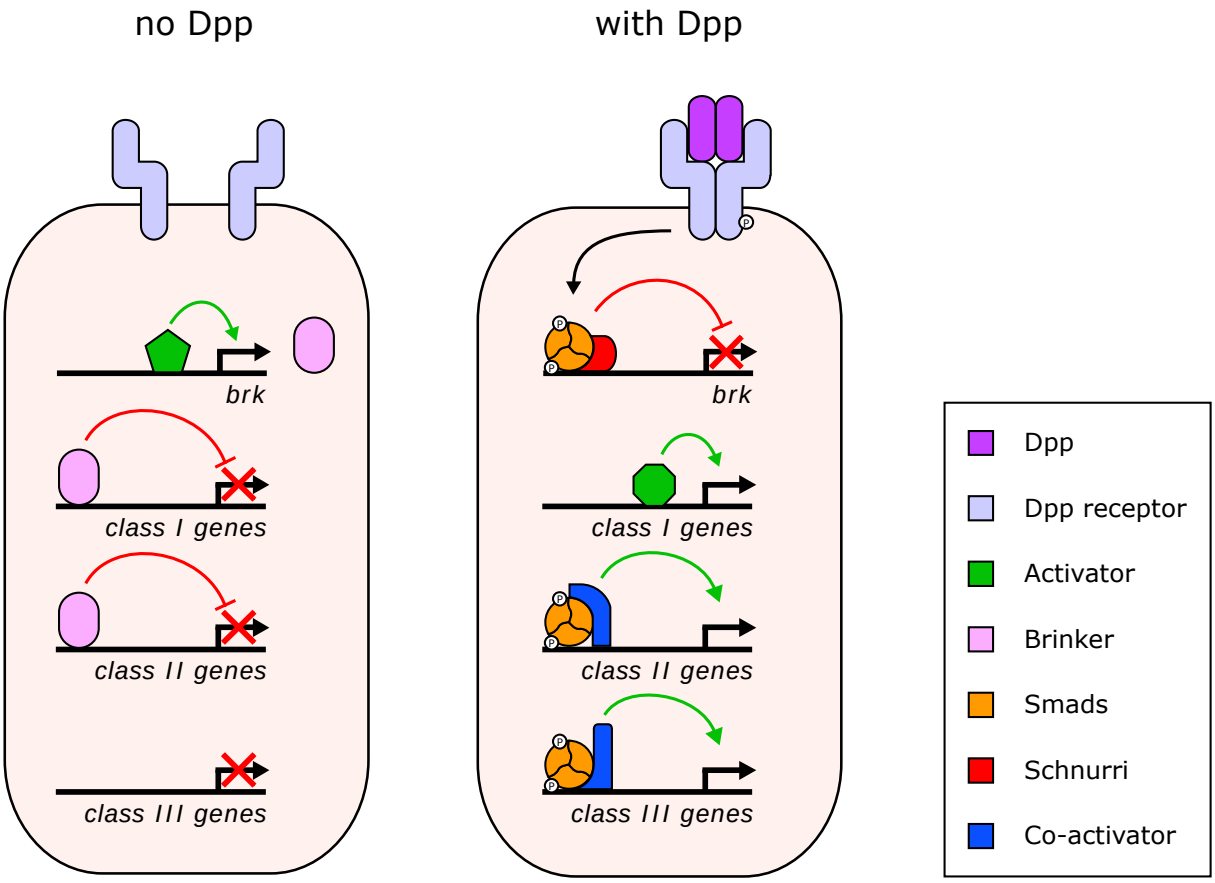

Figure 4.7
Classes of Dpp/Brinker target genes. In the absence of Dpp signalling, Brinker is expressed and able to downregulate target genes. Activation of the Dpp pathway leads to efficient repression of *brinker* by a complex of Mad, Medea and the co-repressor Schnurri. Three classes of genes that are regulated by Brinker and the Dpp pathway can be distinguished: I) Genes that are repressed by Brinker and upregulated upon removal of Brinker by a non-Smad activator. II) Genes that are repressed by Brinker and activated by Smads and co-activators. III) Genes that are not repressed by Brinker, but activated by the Dpp pathway.

4.3.3 Regulation of Brinker

With the discovery of Brinker as the default repressor of the Dpp pathway, it became obvious that downregulation of the *brinker* gene is crucial for activation of a majority of Dpp target genes. The question remained how this happens at the molecular level. Genetic studies revealed that, besides the members of the Dpp pathway, the zinc finger transcription Schnurri (Shn) is involved in the regulation of *brinker* expression (Marty et al., 2000). *shn* had been originally identified in a screen for genes on the second chromosome causing embryonic lethality (Nüsslein-Volhard et al., 1984) and was subsequently linked to the Dpp pathway (Arora et al., 1995; Grieder et al., 1995; Staehling-Hampton et al., 1995). The phenotype of *shn* mutants resembles the phenotype of mutants with a defective Dpp signalling pathway. As

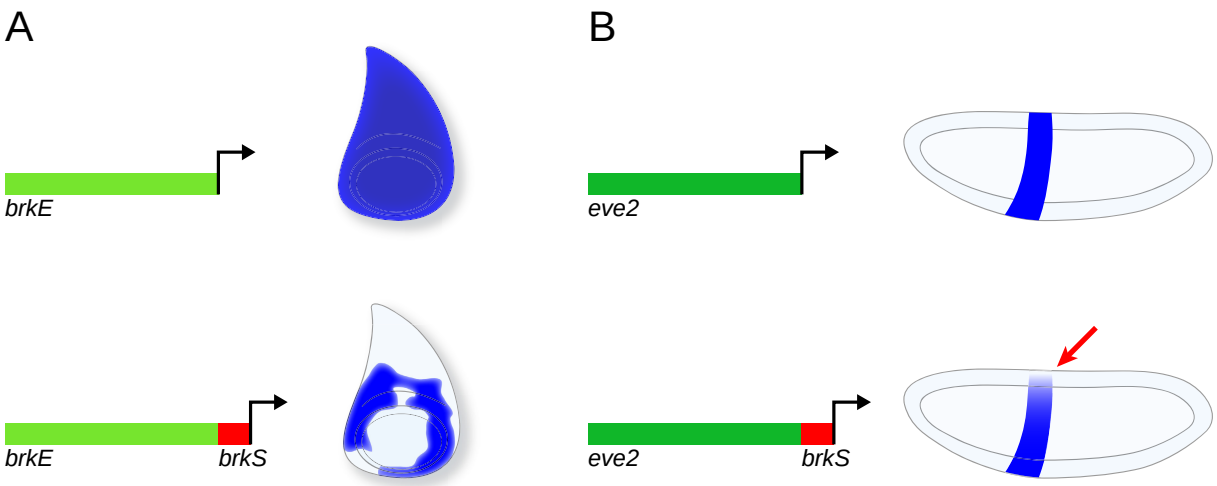

Figure 4.8
Flexible function of the SE. (A) An activating element within the *brk* enhancer (*brkE*) drives expression of a reporter gene throughout the whole wing imaginal disc. If a small repressive modul from the *brk* enhancer, the silencer *brkS*, is fused back to the activator, the expression is reduced within regions of high Dpp levels and resembles endogenous *brinker* expression. (B) The function of the silencer is not limited to *brk* and the wing disc. The *eve* stripe 2 enhancer of the pair-rule gene *even-skipped* is active in the early embryo (Small et al., 1992). If a *brk* silencer is fused to *eve2*, the enhancer becomes repressed in the dorsal-most domains (red arrow), where Dpp levels are highest. Figures based on Pyrowolakis et al. (2004) and Müller et al. (2003).

a result of genetic epistasis experiments Schnurri was placed downstream of Dpp; its molecular function, however, remained obscure until it was clearly associated with repression of *brinker*.
Later studies have shown that the enhancer of *brinker* has a modular character (Müller et al., 2003; Yao et al., 2008), with elements able to drive expression of a reporter gene ubiquitously throughout the wing imaginal discs by so far unknown activators, and smaller Dpp-responsive repressive elements, named silencers. Biochemical analysis revealed that a complex of Mad, Medea and Schnurri^{CT} (a truncated version of the Schnurri protein) specifically binds to the silencer (Müller et al., 2003). Furthermore, it turned out that the function of the silencer was not restricted to the *brk* enhancer. It could confer Dpp responsiveness also in heterologous situations, for example when fused to an enhancer active in the blastoderm-stage embryo (Fig 4.8). Subsequent dissection led to identification of a minimal silencer, the 16bp Silencer Element (SE) that was still able to recruit the Mad/Medea/Shn^{CT} complex and confer Dpp-mediated repression *in vivo* (Pyrowolakis et al., 2004). Mutation analysis of the SE resulted in the consensus sequence GRCGNC(N)$_5$GTCTG (Fig. 4.9). By using differently tagged Smad proteins, it has been shown that a tripartite complex of two Mad proteins and one Medea protein binds to this sequence (Gao et al., 2005). This is a prerequisite for the recruitment of Schnurri into this complex, since Schnurri^{CT} does not bind to the SE in the absence of the Smad proteins. Each of the two Mad proteins binds to one GNC motif within the GRCGNC site, while Medea binds to the GTCTG site, that resembles the classical Smad binding element AGAC (Gao and Laughon, 2007; Gao et al., 2005; Pyrowolakis et al., 2004). The distance and the base composition have no influence on the binding of the Smad tripartite complex and can be extensively varied (Gao and Laughon, 2007). However, only when the two Smad binding sites are separated by exactly five nucleotides, Schnurri^{CT} can be recruited into the complex. Consequently, SEs with mutated linker length do not exert any repressive function *in vivo* (Pyrowolakis et al., 2004). Scanning the Drosophila genome for the SE delivered 350 hits, with the by far highest accumulation in the vicinity of the *brk* gene (ten hits). This could reflect the importance of fine-tuning the *brk* expression by the Dpp gradient. In addition, functional silencer elements have been identified in the enhancers of the embryonic segment-polarity gene *gooseberry* (*gsb*) and *bag of marbles* (*bam*), which is involved in germline stem cell maintenance (Pyrowolakis et al., 2004).

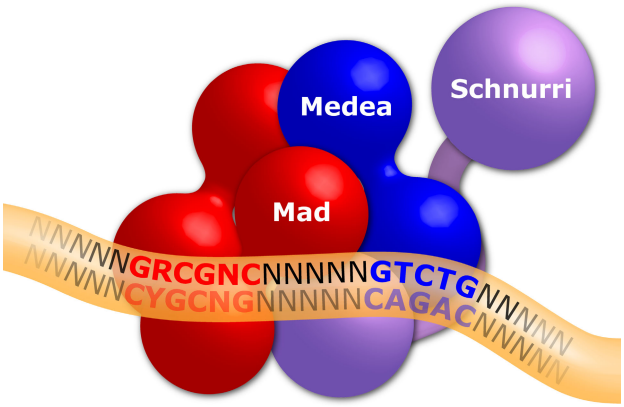

Figure 4.9
The repressive SE complex. A flexible Smad triple complex assembles on the 16bp Silencer Element: two Mad proteins bind to the "red box" GRCGNC and one Medea protein to the "blue box" GTCTG. Only when the two sites are separated by exactly five nucleotides, the repressor Schnurri is recruited into the complex. No structural data is available and it is not known whether and how Schnurri interacts with the DNA. However, it has been shown that the second T in GTCTG is required for Schnurri recruitment, while the Smad complex still forms when this nucleotide is mutated (Pyrowolakis et al., 2004).

4.3.4 The role of Schnurri

Although *shn* encodes a huge protein of 2529 amino acids, it has been shown that the C-terminal 641 residues (termed Schnurri^{CT}) are required and sufficient to form a complex with Mad/Medea and the SE *in vitro* and to repress a *brk* reporter gene in the *Drosophila* embryo (Müller et al., 2003) – which raises the question for the function of the rest of the protein. Eight putative zinc finger domains can be found within the Schnurri protein, seven of the Cys_2His_2 type and one of the $Cys_2HisCys$ type (zinc finger 3, see Fig 4.10). The C-terminal most zinc fingers, a triplet of zinc fingers 6 to 8, make up the complex formation domain of Schnurri^{CT}. Additionally, a repression domain was localized to the N-terminus of Schnurri^{CT} (Pyrowolakis et al., 2004). One Schnurri homolog in *C. elegans*, Sma-9, has been reported to act in a BMP-related pathway (Liang et al., 2003a). Sma 9 lacks the first three zinc fingers but has zinc fingers conserved to the ZF 4/5 pair and the ZF 6/7/8 triplet. Unlike Brinker, Schnurri homologs can be found in vertebrates, where they are also termed human immunodeficiency virus type I enhancer binding proteins (HIV-EP), major histocompatibility complex binding proteins (MBP), positive regulatory domain II-binding factor (PRDIIBF1) or κB binding and recognition component (KRC).
Mammalian Schnurris have been linked to B- and T-cell development (Bachmeyer et al., 1999; Takagi et al., 2001), adipogenesis (Jin et al., 2006) and bone formation (Jones et al., 2006), but very little is known about their molecular interactors. Murine Schnurri 3 has been shown to participate in TNF (tumor necrosis factor) signalling (Oukka et al., 2002), to interact with the transcription factor c-Jun to regulate Interleukin-2 expression (Oukka et al., 2004) and to recruit E3 ubiquitin ligases to Runx2, the principal transcriptional regulator of osteoblast differentiation (Jones et al., 2006). Although vertebrate Schnurris are widely believed to also act in the TGFβ-/BMP pathway, there is only few data available about their interaction with Smads. One reported case is the Shn2-mediated induction of *PPARγ2*, which encodes the key transcription factor for adipocyte differentiation, peroxisome proliferator-activated receptor γ2. Upon stimulation of BMP2, Shn2 enters the nucleus and binds to the *PPARγ2* promoter in cooperation with Smad1/4 and C/EBPα (CCAAT/enhancer-binding protein α) (Jin et al., 2006). Several Smad binding elements (AGAC) were found within the promoter, but no sequence resembling the *Drosophila* SE. In a mobility shift assay, Shn2 was not able to bind itself, but fragments including either the first or second pair of zinc fingers augmented Smad-DNA interaction.
The question has to be posed, whether there is a functional SE in vertebrates at all. Strikingly, all human Schnurri (hShn) proteins completely lack the ZF 6/7/8 triplet required for

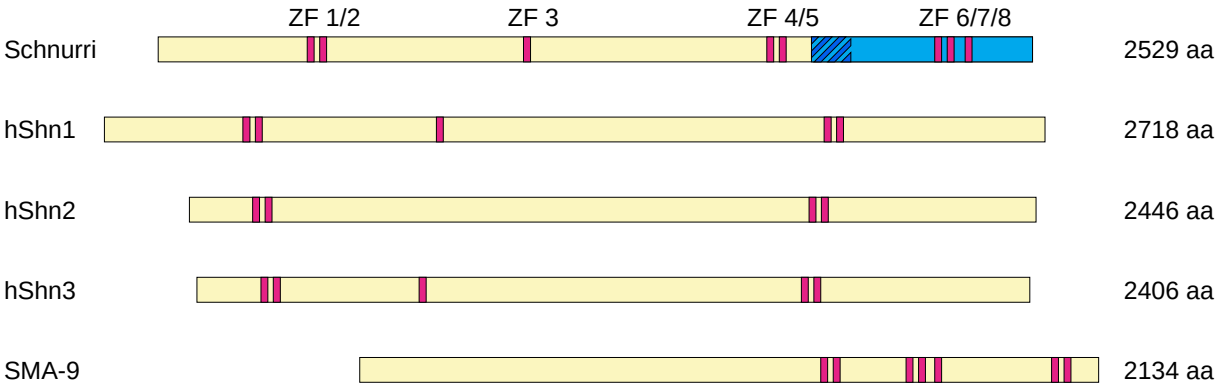

Figure 4.10
Conservation of Schnurri. Schnurri has eight zinc fingers, seven of the C_2H_2 type and one of the C_2HC type (ZF 3). ZF 1/2 and ZF 4/5 are highly conserved in vertebrate Schnurris as the depicted human Schnurri homologs hShn1 to hShn3, whereas ZF 3 is less conserved and even absent in hShn2. ZF 6/7/8 are completely missing. Zinc fingers 4 to 8 are also conserved in the *C. elegans* Schnurri homolog Sma-9. Sma-9 possesses two more C-terminal zinc fingers not related to zinc fingers from other species. Shown in blue is the 641aa minimal functional Schnurri protein Schnurri^{CT} with its repression domain (striped).

SE/Schnurri/Mad/Medea complex formation in *Drosophila*, though the other doublets are highly and zinc finger 3 partially conserved. It has been shown that the zinc fingers of vertebrate Schnurri proteins are implicated in DNA binding. hShn1 was originally identified by its ability to bind to the same sites as NF-κB (Maekawa et al., 1989) and recognizes the palindromic sequence TGGGGATTCCCCA with its zinc fingers 4 and 5 (Baldwin et al., 1990). Direct binding to CCC-containing sites has been reported for Schnurri homologs in Xenopus (Dürr et al., 2004), and also the zinc finger pairs 1/2 and 4/5 of *Drosophila* Schnurri have been proposed to bind to a palindromic motif GGG(N)$_{5/6}$CCC similar to the one initially identified for hShn1 (Dai et al., 2000). Furthermore, the zinc finger pairs of hShn have been shown to interact with Smad1 (hShn1) and Smad1 and Smad4 (hShn2) in immunoprecipitation assays (Jin et al., 2006; Yao et al., 2006). This might be due to homology with the zinc finger triplet 6/7/8 of *Drosophila* Schnurri (where ZF7 is dispensable, Pyrowolakis et al. (2004)). However, also for *Drosophila* Schnurri, sequences outside Schnurri^{CT} and including the other zinc fingers have been identified as interactors with Mad (Dai et al., 2000; Udagawa et al., 2000). It was recently revealed that ubiquitous expression of hShn1 rescues the *shn* mutant phenotype in *Drosophila* to the same extent as Schnurri and that both hShn1 zinc finger pairs are able to form complexes with Smads on a SE-like sequence derived from the *Xenopus Vent2* promoter (Yao et al., 2006). This was the first study where a SE-like element with the same restrictions considering the spacer length could be linked to vertebrate Schnurri. It is noteworthy that vertebrate Schnurris could so far only be associated with activation (although hShn1 is able to repress a *brk* reporter in the fly) and the question remains, whether *Drosophila* Schnurri can also act as an activator. There is disputable genetic evidence for this (Torres-Vazquez et al., 2001), and the *Ubx* enhancer could be such a case where direct Schnurri binding is responsible for gene activation (Dai et al., 2000).

4.4 Aim of the study

4.4.1 Search for an SE counterpart

The discovery of the SE as a DNA motif for recruitment of a Smad-repressor complex and its subsequent thorough characterization provided for the first time a sequence that could be used to identify new Dpp target genes. The most striking feature of the SE is that its activity is not or little temporally and spatially restricted. Genes with functional SEs are effectively

repressed by Dpp in various developmental contexts, independent of local co-repressors. No other *cis*-regulatory element conferring Dpp induced responses is known that acts in such a universal manner. Few enhancers regulated by the Dpp pathway have been analysed in molecular detail. Most of them display several Smad binding motifs and adjacent binding sites for locally restricted transcription factors, as Zen for the *Race* enhancer (Rusch and Levine, 1997; Wharton et al., 2004), Tinman itself for the *tinman* enhancer (Xu et al., 1998) or Ubx for the *spalt* enhancer (Walsh and Carroll, 2007). Due to the enhancer-specific composition and arrangement of these sites, it was never possible to deduce any consensus sequence or general motif analogous to the SE to identify further genes regulated by the same mechanism. Because of their simple nature, single Smad binding sites alone do not allow for any reasonable prediction. The four base pairs long SBE, for example, statistically occurs every 128 base pairs. But since the two Smad binding motifs within the SE appear in a fixed arrangement, the resulting consensus sequence is specific enough to be used in *in silico* screens. The question that rises is, whether there are also other constellations possible that recruit activators rather than a repressor. Is there a simple module such as the SE, flexible and adaptable to different enhancers, that confers activation instead of repression? The Silencer Element was discovered in the regulatory region of *brinker*, a gene that is strictly repressed upon Dpp signalling. If there was an "Activating Element", chances would be highest to find it in the enhancer of a gene that is consequently upregulated in cells with an activated Dpp pathway. The prototype of such a gene is *dad* (*daughters against dpp*), that encodes the only *Drosophila* inhibitory Smad. The expression of *dad* is widely induced by Dpp in embryonic and larval development (Marty et al., 2000; Torres-Vazquez et al., 2001; Tsuneizumi et al., 1997), and Dad is able to antagonize Dpp signalling by interaction with the type I receptor Thickveins (Inoue et al., 1998). Recently, it has been shown that Dad is restricted to the BMP pathway and not able to inhibit the receptor Baboon and thus counteract Activin signalling (Kamiya et al., 2008). Although tissue-specific Dad overexpression is a common tool to disrupt Dpp signalling, little is known about it functions. However, it is not unlikely that Dad makes use of the same mechanisms as the vertebrate I-Smads Smad6 and Smad7 for blocking the Dpp pathway (see 4.2).

4.4.2 Transcriptional regulation of inhibitory Smads

Although ultimate molecular evidence is missing, *dad* is believed to be directly activated by Dpp and repressed by Brinker. *dad* expression is absent in *tkv*$^{-}$ mutant clones in the wing imaginal disc (Tsuneizumi et al., 1997) and lacking in *shn* mutant embryos (Marty et al., 2000). Embryos mutant for *brk* display an expanded *dad* expression pattern (Torres-Vazquez et al., 2001). Vertebrate I-Smads have been shown to be directly activated by the TGF-β/BMP pathway. The promoter region of the vertebrate *dad* homolog s*mad7* is one of the best-analysed BMP-regulated enhancers. After publication of the Smad binding element (Shi et al., 1998; Zawel et al., 1998), several groups focused on the search for this SBE and reported the existence of a palindromic tandem element GTCTAGAC in the human and mouse *smad7* enhancer that is confering BMP-responsiveness by recruitment of Smad3 and Smad4 (Brodin et al., 2000; Denissova et al., 2000; Nagarajan et al., 1999; von Gersdorff et al., 2000). Later, the existence of a so-called BMP response element (BRE) with the sequence TGGCGCC within the vertebrate *smad7* enhancer was reported to recruit Smad1 (Benchabane and Wrana, 2003; Karaulanov et al., 2004). In addition, this sequence was identified in BMP-target genes such as *bambi, Ihh* (*Indian hedgehog*), the *Id* (*Inhibitor of differentiation*) genes and several others (Karaulanov et al., 2004; Korchynskyi and ten Dijke, 2002; Seki and Hata, 2004), often in the context TGGCGCC$(N)_x$GTCT(G), which (though acting in an activating manner) resembles the SE. A GC-rich BMP response element was also found in the promoter of *smad6* (Ishida et al., 2000).

Little surprising, the regulation of *smad6* and *smad7* is not dependent on Smads alone. GATA proteins (named after their recognition sequence) have been shown to cooperate with Smad1 for the activation of *smad7* (Benchabane and Wrana, 2003), and adjacent to the SBE, (putative) binding sites for several other transcription factors such as EKLF (Erythroid Krüppel-like factor, also termed Klf1), USF (Upstream stimulatory factor) and AP1 (Activator protein 1, a Jun/Fos complex) have been found (Brodin et al., 2000; Karaulanov et al., 2004). Sp1, also a member of the KLF family, has been shown to bind to GC-rich sequences within the *smad7* enhancer (Brodin et al., 2000) and interact with Smads to induce expression of *smad7* (Jungert et al., 2006). Furthermore, cooperative binding of Smads and TFE3 (transcription factor microE3) to so-called E-boxes adjacent to the SBE has been implicated in efficient induction of *smad7* (Hua et al., 2000). Interestingly, the palindromic SBE has also been reported to be important for gene repression and recruits a complex of Smad4 and the co-repressor Ski (Denissova and Liu, 2004). The activation of *smad6* upon stimulation with BMP4 has been shown to depend on the binding of a complex formed by Smad1/4 and OAZ (Olf-1/EBF associated zinc finger) (Ku et al., 2006), a common co-factor previously shown to be important for Smad-mediated activation of *Xenopus Vent2* (Hata et al., 2000). Another study identified the Smad co-activator Runx2 (Runt related gene 2) as an important regulator of *smad6* that was able to either recruit Smad1 for activation or Smurf 1 for inhibition (Wang et al., 2007).

4.4.3 Strategy

Since the regulatory regions of *dad* had not been investigated before, the initial steps in the search for an activating counterpart of the SE included a more detailed genetic analysis of *dad* expression and, in parallel, the identification and characterization of the *dad* enhancer. The latter had to be done by cloning potential enhancer fragments and examining their ability to drive a reporter gene in transgenic flies. Further dissection of the *dad* enhancer was performed with the aim to reveal a minimal Dpp/BMP response element able to recruit Smads and confer Dpp activity *in vitro* in biochemical binding assays as well as *in vivo*. Ultimately, the universality of the identified "Activating Element" would have to be shown by demonstrating its function in enhancers of other genes known (or so-far unknown) to be activated by Dpp. Questions to be answered were, by which means an activating *cis*-regulatory element would differ from the SE, by the constellation of the Smad sites or by the recruitment of an activator instead of the repressor Schnurri.

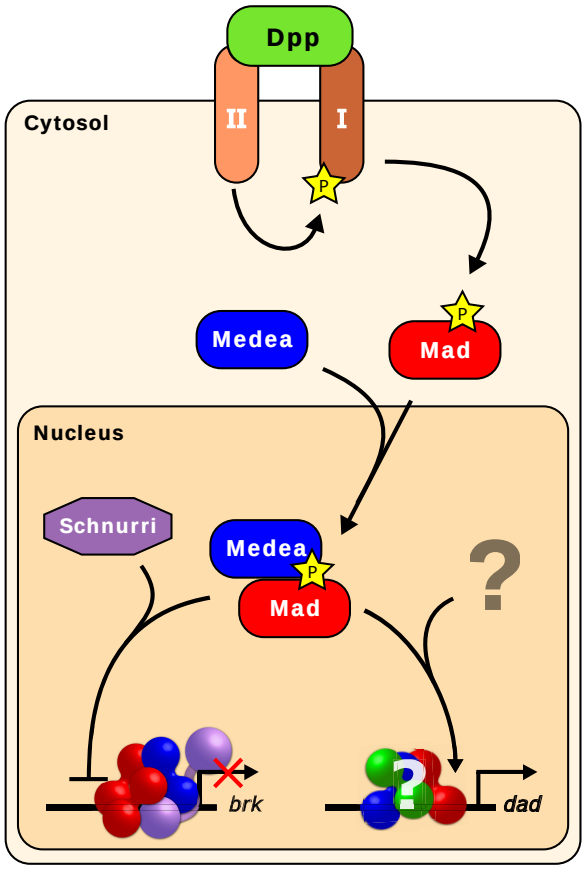

Figure 4.11
Search for the activating counterpart of the SE. The Dpp pathway induces repression as well as activation. But only for repression a well-characterized *cis*-regulatory motif was found that functions in all developmental contexts: the Silencer Element. It recruits a complex of phosphorylated Mad, Medea and Schnurri not only to the enhancer of *brinker*, but also other genes downregulated upon Dpp signalling. The aim of this study was to search for a potential activating counterpart of the SE by analyzing the enhancer of *dad*, a gene widely activated by the Dpp pathway. We expected such an "Activating Element" to differ in aspects like the composition of the Smad sites or the nature of the bound co-factor.

5 Material and Methods

5.1 Generation of transgenic flies

5.1.1 Cloning of reporter constructs

In general, standard molecular biology techniques were applied for all cloning procedures (Sambrook and Russell, 2001). Initial enhancer *dad* enhancer constructs were inserted into the P-element transformation vector px27 (Segalat et al., 1994). Enhancer constructs from other genes, Dad13 mutants and all 5xAE and derived constructs were inserted into the attBlacZ vector. The attBlacz vector was constructed by cutting out the UAS-Hsp70-MCS (via SphI/XbaI) from the pUASTattB vector (Bischof et al., 2007) and replacing it with the MCS-lacZ cassette (cut out via SphI/SpeI) of the pH-Pelican vector (Barolo et al., 2000).

5.1.1.1 Polymerase chain reaction (PCR)

Putative enhancer fragments were cloned from genomic DNA with a PCR-based approach. Primers of approximately 21nt length were used to introduce restriction sites at the 5' and 3' end. By default, an XbaI and Asp718 site was generated, unless one of the sites occurred within the enhancer fragment. PCR reactions were carried out in a T3 thermocycler (Biometra), typically following this cycle:

94°C	1min 30sec	
94°C	20sec	3x
50°C	20sec	
72°C	1min per kb	
94°C	20sec	30x
58°C	20sec	
72°C	1min per kb	
72°C	5min	
8°C	∞	

The size and quantity of the PCR products were visualized via agarose gel electrophoresis. Subsequently, the DNA was purified using a QiaQuick Gel Extraction Kit (Qiagen).

PCR reaction	0.5µl Taq polymerase (NEB)
	0.5µl Pfu polymerase (Stratagene)
	5µl 10x Thermopol buffer (NEB)
	5µl 2mM dNTP mix
	5µl 10µM forward primer
	5µl 10µM reverse primer
	1-3µl template
	H_2O to 50µl

5.1.1.2 Restriction digest

PCR products and the respective plasmid were digested for at least one hour at 37°C in a volume of 20µl with the appropriate restriction enzymes and buffers (NEB or Roche). The digested DNA was separated by agarose gel electrophoresis and purified using a QiaQuick Gel Extraction Kit (Qiagen).

5.1.1.3 Ligation and transformation

Vector and insert DNA were ligated in a ratio of approximately 1:3 in a volume of 15µl over night at 16°C with T4 ligase (NEB). To generate 5xAE and derived constructs, 1µl of 100µM double-stranded oligonuculeotides with adequate overhangs was used.
For transformation, chemo- or electrocompetent *E. coli* bacteria of the strain XL1 Blue (Stratagene), XL10 Gold (Stratagene) or Top10 (Invitrogen) were used. Chemotransformation was performed by incubating 15µl ligation reaction with 100µl competent cells on ice for 20min, 45sec heat shock at 42°C and 2min incubation on ice. Electrotransformation was performed using 1µl ligation reaction with 40µl competent cells in a 0.1cm Gene Pulser cuvette (Biorad) in a Gene Pulser (Biorad) at 25µF, 1.8kV and 200Ω.
After transformation, cells were propagated in 1ml LB medium (Sambrook and Russell, 2001) without antibiotics at 37°C, transferred to LB plates with 100µg/ml ampicillin and allowed to grow over night at 37°C. Single colonies were picked and the plasmids isolated using a GenElute Plasmid Miniprep (Sigma). The constructs were tested by PCR or restriction digest. Positive results were verified by automated sequencing with an ABI Prism 310 Genetic Analyzer (Applied Biosystems). For injection into *Drosophila* embryos, larger bacterial cultures were inoculated and the plasmids isolated using a Plasmid Midi Kit (Qiagen) or a GenElute Plasmid Midiprep (Sigma).

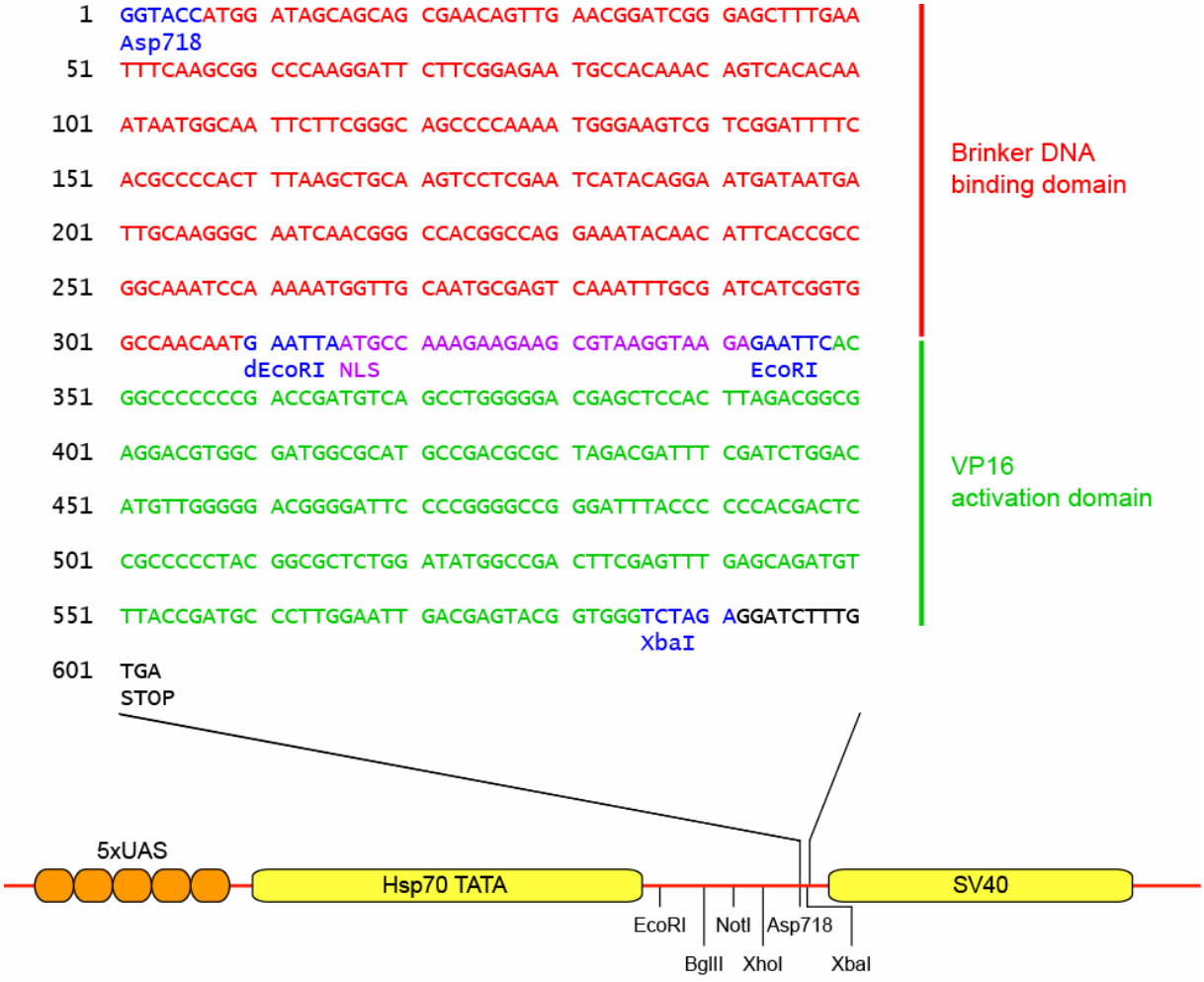

Figure 5.1
Partial map of pUAST-BrkVP16. Shown are the five optimized GAL4 binding sites (5xUAS), the minimal Hsp70 promoter, the polylinker with unique restriction sites and the SV40 polyadenylation site of the pUAST vector. A fragment containing the first 300bp of the *brinker* gene (green), a nuclear localization sequence (NLS, purple) and a 240bp sequence encoding the VP16 activation domain was inserted into the pUAST vector using the Asp718 and XbaI sites. The stop codon TGA is 10bp downstream of the insert, in the polylinker. dEcoRI indicates a destroyed EcoRI site.

5.1.2 Cloning of BrkVP16

A fragment encoding the first 100 amino acids of Brinker, a nuclear localization signal (NLS) and the activation domain of the Herpes simplex virus protein VP16 was inserted into the pAc5.1/V5-HisB vector (Invitrogen) via its XbaI and Asp718 site for expression in S2 Schneider cells.
For generation of transgenic flies, the BrkDBD-NLS-VP16 construct was inserted into the expression vector pUAST (Brand and Perrimon, 1993). See Fig. 5.1 for detailed sequence information.

5.1.3 P-element mediated transfomation

Initial *dad* enhancer reporter genes and the UAS-BrkVP16 construct were transformed into *Drosophila* embryos by standard P element transfomation. 15µl of 0.4µg/µl plasmid with 0.2µg/µl helper plasmid pπ25.7wc (Karess and Rubin, 1984) in 5mM KCl, 100µM $Na_xH_xPO_4$ pH6.8 were spun for 20min at 4°C at maximum speed in an refrigerated Eppendorf tabletop centrifuge to remove any particles. The supernatant was transferred into new tubes and kept on ice for direct use or stored at -20°C. Embryos from white-eyed yw flies were collected from grape juice plates, aligned on double-sided adhesive tape, dried with a cold-air hair dryer (Trisa Professional 1200), covered with Voltalef PCTFE oil (Atofina) and injected with the plasmid solution from the posterior end.
Embryos were kept at 18°C for one to two days and then transferred to 25°C. Developing adult animals were crossed with yw flies and the off-spring screened for red-eyed w^+ individuals carrying the transgene. Independent insertions were mapped and balanced using standard fly stocks.

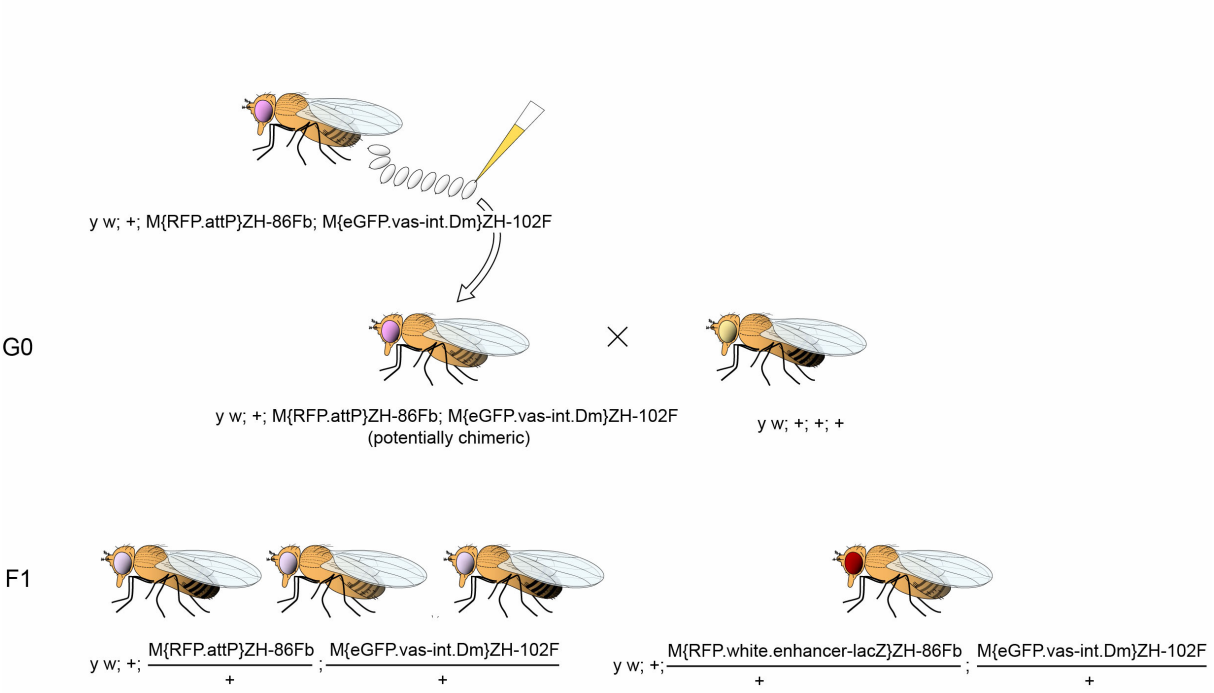

Figure 5.2
Generation of transgenic flies using the attB/attP system. Embryos homozygous for the attP landing site on the third chromosome and the ΦC31 integrase (driven by the *vasa* enhancer) on the fourth chromosome were injected with attBlacZ plasmids containing the enhancer fragment of interest and a mini *white* gene. Adult animals developing from these embryos (G0), potentially chimeric with transformed germline cells, were crossed with $y^- w^-$ flies. The offspring (F1) was then screened for individuals with red eyes. Red-eyed flies were isolated and crossed with flies carrying standard third chromosome balancers.

5.1.4 Transformation using the attB/attP system

For generation of transgenic flies using the attB/attP system (Bischof et al., 2007), flies homozygous for the attP landing site on the third chromosome and the integrase on the fourth chromosome (strain internally named J5) were used. See Fig. 5.2 for detailed information. DNA and embryos were prepared as described in 5.1.3 (no helper plasmid was used).

5.2 S2 reporter assay

5.2.1 Maintenance and transfection of S2 cells

S2 Schneider cells were grown at room temperature in Schneider's Drosophila Medium (Gibco), supplemented with 10% Foetal Bovine Serum (Gibco), Glutamax (Gibco) and 100U/ml penicillin, 100µg/ml streptomoycin (Gibco). When passaging the cells into new flasks, half of the old (conditioned) medium was transferred. For transfection, 600.000 cells were transferred into one well of a 12-well-plate. 200ng of total DNA was transfected using the Effectene Transfection Reagent (Qiagen): 150ng Tkv^{QD}, Mad, Medea (50ng each) and 10ng luciferase encoding expression plasmids (pAc5.1/V5-HisB, Invitrogen) and 40ng of *lacZ* reporter gene (in px27). For BrkVP16, 50ng was applied. If not all effector plasmids were transfected, empty pAc5.1/V5-HisB vector was used to bring DNA amount to 200ng.

5.2.2 Preparation and analysis of cell extracts

After two days of growth, cells were harvested in 15ml Falcon tubes and spun down by centrifugation (700g, RT, 3min). The supernatant was removed and the cells resuspended in PBS and transferred to 1.5ml Eppendorf tubes. After repetition of the spinning and washing step, supernatant was removed and the cells resuspended in 70µl ice-cold cell lysis buffer. After incubation on ice for 10min, cells were centrifuged in a refrigerated Eppendorf tabletop centrifuge at maximum speed at 4°C for 15min. 10µl of the supernatant was transferred in one well of a 96 multiwell plate. 200µl Z buffer was added and the OD change at 550nm was measured over 1 h at 37°C in a Thermomax microplate reader (Molecular Devices Corp) at 37°C. For evaluation, the slope value was calculated by the associated software (Softmax PRO).
To account for differences in cell growth and transfection efficiency, values for βgal activity were normalized by measuring the activity of the co-transfected luciferase. 350 µl luciferase reaction buffer was pipetted to 10µl cell extract. Light emission was initiated by addition of 50µl luciferase injection mix and quantified using a Microlite TLX1 luminometer (Dynatech laboratories). All measurements were done at least in duplicate and standard deviation was calculated.

5.2.3 Solutions

Cell lysis buffer	1% Triton X-100 (Fluka) 25mM Gly-Gly (Sigma) pH 7.8 15mM $MgSO_4$ 4mM EGTA 1mM DTT
Luciferase reaction buffer	25mM Gly-Gly (Sigma) pH 7.8 10mM $MgSO_4$ 2mM ATP (Sigma)

Luciferase injection mix	25mM Gly-Gly (Sigma) pH 7.8 0.2mM Luciferin (Sigma)
Z buffer	100mM $Na_xH_xPO_4$ pH 7.4 1mM $MgCl_2$ 0.314% Mercaptoethanol (Sigma) 0.25µg/µl CPRG

5.3 Electrophoretic mobility shift assay

5.3.1 Bacterially produced proteins

Bacterially produced DNA binding domains of Mad, Medea and Brinker were provided by Georgios Pyrowolakis. Recombinant GST-MadMH1 and GST-MedMH1 proteins (amino acids 1-147 and 16-355, respectively, fused to the GST moiety in the plasmid pGEX4T.1 (Pharmacia)) were expressed in *E. coli BL21* cells, purified using Glutathione-Sepharose beads (Pharmacia) and stored at -80°C in 50mM KCl and 10% glycerol.
BrkDBD comprises residues G43 to N101. The respective construct was subcloned from *brk* full-length cDNA into pET-22b(+) expression vectors expressed in *E. coli BL21*. The protein was purified as described by Cordier et al. (2006) and stored at a concentration of 1.5µg/µl in 50mM Tris pH 8.0 and 100mM NaCl.

5.3.2 Production of cell extracts

For all experiments, S2 cell extracts were applied, except for the definition of the AE consensus sequence, where HEK293 cell lysates were used. *Drosophila* S2 cells were maintained as described in 5.2.1. Human HEK293 were cultured in DMEM + Glutamax (Gibco), supplemented with 10% Foetal Bovine Serum (Gibco), and 100U/ml penicillin, 100µg/ml streptomoycin (Gibco) at 37° C in a humidified atmosphere containing 5% CO_2. 4mio S2 cells or 600'000 HEK293 cells were transferred into one well of a six-well plate and transfected with 400ng of total DNA, using the Effectene Transfection Reagent (Qiagen). 100ng of Tkv^{QD}- and 150ng of both Mad- and Med-expression plasmids (pAc5.1/V5-HisB, Invitrogen, for S2 cells, pcDNA3.1, Invitrogen, for HEK293 cells) were applied. If not all plasmids were transfected, empty vector was used to bring total DNA amount to 400ng.
After two days of growth, cells were harvested in 15ml Falcon tubes and spun down by centrifugation (700g, RT, 3min). The supernatant was removed and the cells resuspended in PBS and transferred to 1.5ml Eppendorf tubes. After repetition of the spinning and washing step, supernatant was removed and the cells resuspended in 70µl ice-cold lysis buffer and incubated on ice for 5min. Subsequently, cells were vortexed and snap-frozen in liquid nitrogen. This step was repeated at least two more times. Finally, cells were centrifuged in a refrigerated Eppendorf table top centrifuge at maximum speed at 4°C for 10min. The supernatant was transferred in new chilled tubes and either used directly in a mobility shift assay or snap-frozen and stored at -80°C.

5.3.3 Preparation of radioactively labeled probe

Double stranded probes with 5'-AATT overhangs were generated by incubating 10µl of 100µM forward and 10µl of 100µM partially reverse complement oligonucleotides in 100µl annealing buffer for 10min at 75°C. The probe was then slowly cooled down to room temperature. For radioactive labeling, 1µl 10µM doublestranded probe was incubated at room temperature for 30min in 30µl Klenow buffer with 0.2mM dCTP, dTTP, dGTP, 2U Klenow

fragment (Roche) and 2µl of 0.5 to 0.8 MBq [α-^{32}P]dATP. After deactivation of the enzyme at 72°C for 5min, non-integrated nucleotides were removed using illustra MicroSpin G-25 Columns (GE Healthcare). Radioactivity was measured using a liquid scintillation analyzer (2000CA Tri-Carb, Packard).

5.3.4 Electrophoretic mobility shift assay

Binding reactions were carried out in 20µl Binding Buffer, containing 0.5µg Poly(dI-dC) (GE Healthcare) and 10.000cpm radioactively labeled probe. As a protein source, either 3 to 4µl of cell extracts, 0.8µg bacterially expressed Brinker-DBD, 1µg GST-MadMH1 or 0.4µg GST-MedeaMH1 were used. For the Brinker/Smads competition assay, 8ng, 80ng and 0.8µg Brinker-DBD was used

After incubation on ice for 30min, the complete reaction was loaded on a 4% non-denaturing polyacrylamide gel and run at 4°C in 0.5% TBE at 180mV. A single lane was loaded with a solution of bromphenol blue (BPB) indicator (Merck) to monitor the gel-run. When the indicator was as close as 4cm to the edge of the gel, the run was stopped and the gel transferred onto a Whatman 3M paper. After drying at 80°C using a vacuum pump, the blot was exposed to an X-ray film (Super RX, Fuji) between two signal-intensifying screens (Hyperscreen, Amersham Bioscience) at -80° for an appropriate amount of time (several hours to days). The films were developed using an automatic film processor (RG II, Fuji) and scanned with a transparency flatbed scanner (Epson Expression 1680 Pro).

5.3.5 Solutions

Lysis buffer:	1.2M KCl 40mM Tris pH 7.8 40% Glycerol 10mM NaF 2mM Na_3VO_4 2mM Na_4PPi 1x Protease Inhibitor Mix (Roche)
10x Annealing buffer:	100mM Tris pH 7.5 500mM NaCl 10mM EDTA
2x Binding Buffer:	40mM HEPES pH 7.5 200mM KCl 2mM DTT 0.6% BSA (Fluka) 40% Glycerol 0.02% Nonidet P 40 (Fluka)
10x Klenow buffer:	500mM Tris pH 7.5 100mM $MgCl_2$ 50mM DTT
Polyacrylamide gel (4%):	4% 29:1 Acrylamide / Bis solution (Biorad) 0.5x TBE (AppliChem) 0.083% APS (AppliChem) 0.058% N,N,N',N'-Tetramethyl-ethylene diamine (SERVA)

5.4 Co-precipitation of pSmad

5.4.1 Procedure

An aliquot of 50µl original Streptavidin Sepharose resuspension (GE Healthcare) was spun 1min at 5000rpm in an Eppendorf tabletop centrifuge. Beads were washed three times in PBS to remove ethanol and spun for 1min at 5000rpm after each wash. After incubation for 30min at room temperature in 50µl blocking buffer, beads were washed three times with 500µl binding buffer. Finally, liquid was completely removed using an Eppendorf GELoader tip. The reaction solution containing HEK293 cell extracts (produced as described in 5.2.2) and biotinylated double stranded probe (annealed as described in 5.3.3) was applied. After incubation at 4°C for at least 2h, beads were washed three times with 500µl binding buffer. Liquid was completely removed using an Eppendorf GELoader tip and 25µl 2x Sample buffer was added. After boiling at 100°C for 4min, samples were stored at -20°C or loaded directly on a 10% denaturing polyacrylamide gel, prepared according to standard protocols (Sambrook and Russell, 2001) in a Mighty Small Gel Caster (Hoefer). After electrophoretic separation, using the Mighty Small II system and 30mA per gel (Amersham Biosciences), proteins were transferred onto a nitrocellulose membrane (Schleicher & Schuell) with a Mini Transblot Cell (Biorad) at 4°C and 100V for 1h. (Hoefer). After successful transfer, the nitrocellulose membrane was stained with Ponceau S (Serva) to visualize the protein bands. The membrane was rinsed with water and blocked in 5% milk powder (Migros) in PBST for 1h. Subsequently, the membrane was incubated over night at 4°C with the α-pSmad antibody (α-pSmad1, 5, 8; Cell Signalling, 1:1000 in 5% milk powder in PBST), rinsed and washed three times with PBST for 10min and then incubated for 1h with the secondary HRP-conjugated α-rabbit antibody (GE Healthcare, 1:1000 in 5% milk powder in PBST). After rinsing and washing with PBST, the bound antibodies were visualized using the ECL detection system (GE Healthcare). Chemiluminescence films (Amersham Hyperfilms, GE Healthcare) were exposed for various periods of time, depending on signal strength, developed using an automatic film processor (RG II, Fuji) and scanned with a transparency flatbed scanner (Epson Expression 1680 Pro).

5.4.2 Solutions

2x Binding Buffer	40mM HEPES pH 7.5 200mM KCl 2mM DTT 0.6% BSA (Fluka) 40% Glycerol 0.02% Nonidet P 40 (Fluka)
Blocking buffer	50µl 2x Binding Buffer 20µl 0.5µg/µl dIdC (GE Healthcare) 20µl 0.5µg/µl herring DNA (Fluka) 10µl H_2O
Reaction solution	37µl 2x Binding Buffer 4µl 0.5µg/µl dIdC (GE Healthcare) 3µl biotinylated annealed oligo (1.2µg for 60bp dsDNA) 30µl cell lysate

2x Sample buffer	4% SDS 200mM DTT 120mM Tris pH 6.8 20% Glycerol Bromphenol blue (Merck)

5.5 Expression analysis in fly and fish

5.5.1 Collection and fixation of *Drosophila* embryos

5.5.1.1 Procedure

Embryos were collected for about 12h at room temperature on grape juice plates and then dechorionized for 3min with 3.5% sodium hypochlorite solution. After rinsing with wash solution, embryos were transferred into a tube with 500µl n-heptane and 500µl embryo fix and rotated quickly for 20min. For devitellinisation, the aqueous phase was removed and replaced with 500µl methanol. Embryos were shaken vigorously or quickly vortexed, washed three times for 20min in methanol and finally stored in methanol at -20°C.

5.5.1.2 Solutions

Wash solution	120mM NaCl 0.03% Triton X-100 (Fluka)
Embryo fix	2x PBS 9.6% Formaldehyde (Fluka)

5.5.2 Whole mount *Drosophila* embryo *in situ* hybridization

5.5.2.1 Procedure

75µl of fixed embryos were transferred into a 1.5ml microfuge tube, rinsed once with 1ml PBST/methanol 1:1 and washed with PBST (0.1% Tween 20 (Fluka) in PBS) for 5min on a rotor. After fixation in 500µl 4% PFA (Paraformaldehyde, EM-grade, Fluka) in PBST for 20min, embryos were rinsed twice with PBST and washed three times with PBST for 5min. Embryos were incubate for not more than 5min in 50µg/ml Proteinase K in PBST. Digest was ended by rinsing with 2mg/ml glycine solution and subsequent washing for 2min with glycine solution. After three times rinsing with PBST, embryos were fixed again in 500µl 4% PFA in PBST for 20min, rinsed twice with PBST and washed three times for 5min.
Afterwards, embryos were washed 5min in PBST/HBS (1:1), then 5min in HBS. Then, embryos were prehybridized in 300µl prewarmed HBSR at 56°C for at least 1h. HBSR was removed except for a thin layer covering the embryos. After addition of 1µl of digoxigenin-labeled RNA probe (*dad* probe provided by Anna Jazwinska, *lacZ* probe provided by Georgios Pyrowolakis), embryos were left over night at 56°C, slowly shaking.
The next day, HBSR was removed. Embryos were rinsed three times with 500µl 56°C HBS and then washed three times with 1ml 56°C HBS for 20min. After washing with 1ml 56°C HBS/PBST (3:1), 1ml 56°C HBS/PBST (1:1) and 1ml room temperature HBS/PBST (1:3) for 10min each, embryos were rinsed and washed twice with PBST for 5min.
Embryos were incubated with AP-conjugated α-digoxigenin antibody (Roche, 1:2000) in Western Blocking Reagent (Roche, diluted in PBST) for 2h at RT or over night at 4°C. To identify homozygous mutant embryos, *lacZ* reporter expression of balancer chromosomes was detected by addition of an α-βgal antibody (Promega, 1:1000). After incubation, embryos were rinsed twice with PBST, washed three times for 20min in PBST, rinsed and washed

three times for 5min with 1ml freshly prepared AP buffer and incubated in 500µl staining solution per sample (6.6µl 50µg/µl NBT and 3.3µl 50µg/µl BCIP per 1ml AP buffer). The reaction was followed under the microscope using an aliquot of embryos and stopped by rinsing and washing with PBST for 10min.
For double stainings, embryos were incubated with the secondary biotinylated α-mouse antibody (Vector laboratories, 1:500) in Western Blocking Reagent for 2h at RT or over night at 4°C and further processed as described in 5.5.3.
Otherwise, embryos were dehydrated by subsequent washes in 40%, 70%, 96% and 100% ethanol, left over night at 4°C and mounted in 300µl mounting medium. After incubation over night, embryos were transferred to microscope slides.

5.5.2.2 Solutions

HBS (Hybr. sol.)	400ml Formamide 200ml 20x SSC (17.53% NaCl, 8.82% Sodium citrate) 40mg Heparin sodium salt (Fluka) 8ml 20% Tween 20 (Fluka) H_2O to 800ml stored at -20°C
HBSR (HBS+DNA)	HBS 0.1 mg/ml sonicated salmon sperm DNA (MB-grade Roche) stored at -20°C
AP buffer	100mM NaCl 50mM $MgCl_2$ 100mM Tris pH 9.5 0.2% Tween 20 (Fluka)
BCIP	50µg/µl 5-Bromo-4-chloro-1H-indol-3-yl phosphate · p-toluidine (Bachem AG) in 100% dimethylformamide stored at -20°C Do not use DMF in polystyrene tubes!
NBT	50µg/µl 4-Nitro blue tetrazolium chloride (Roche) in 70% dimethylformamide stored at -20°C Do not use DMF in polystyrene tubes!
Mounting medium	80% Canada balsam (SERVA) 20% Methyl salicylate (Fluka)

5.5.3 Whole mount *Drosophila* embryo antibody staining

5.5.3.1 Procedure

75µl of fixed embryos were transferred into a 1.5ml microcentrifuge tube, rinsed once with 1ml PBST/methanol 1:1 and washed twice with PBST (0.1% Tween 20 (Fluka) in PBS) for 5min on a rotor. After incubation in Western Blocking Reagent (Roche, diluted in PBST) for 20min, embryos were incubated with the primary α-βgal antibody (Promega, 1:1000) in Western Blocking Reagent over night at 4°C or for 2h at room temperature. Afterwards, embryos were rinsed and washed three times with PBST for 10min.

For AP stainings, embryos were incubated with the secondary AP-conjugated α-mouse antibody (Boehringer Mannheim/abcam, 1:1000) in Western Blocking Reagent over night at 4°C or for 2h at room temperature and then processed as described in 5.5.2.
For HRP stainings, the Vectastain kit (Vector laboratories) was used. Embryos were incubated with the secondary biotinylated α-mouse antibody (Vector laboratories, 1:500) in Western Blocking Reagent for 2h at RT or over night at 4°C. Subsequently, embryos were rinsed with PBST and washed three times for 15min. According to the manufacturer's protocol, embryos were then incubated in 1ml PBST, 16µl A and 16µl B for 30min (after preceding AB complex formation). Then, embryos were washed with three times with PBST for 10min and incubated in 500µl staining solution. The reaction was followed under the microscope using an aliquot of embryos and stopped by rinsing and washing with PBST for 10min. Afterwards, embryos were dehydrated by subsequent washes in 40%, 70%, 96% and 100% ethanol, left over night at 4°C and mounted in 300µl mounting medium. After incubation over night, embryos were transferred to microscope slides

5.5.3.2 Solutions

Staining solution	100µl 1M TrisHCl 10µl 25mg/ml Diaminobenzidine 0.4µl 30% H_2O_2
Mounting medium	80% Canada balsam (SERVA) 20% Methyl salicylate (Fluka)

5.5.4 XGal staining imaginal discs

5.5.4.1 Procedure

Third instar larvae were opened, inverted and transferred to a 24-well plate with PBS. After fixation for 15min in 1% Glutaraldehyde (Fluka) in PBS on ice, fixative was removed and larvae rinsed twice. Subsequently, 500µl XGal staining solution per well was added. Larvae were incubated at 37°C for 1h, rinsed twice with PBST (0.1% Tween 20 (Fluka) in PBS) and then dissected in PBS. Imaginal discs were transferred onto a microscope slide with 80% glycerol.

5.5.4.2 Solutions

XGal staining solution	960µl Buffer B 10µl 333mM $K_4[Fe^{II}(CN)_6]xH_2O$ 10µl 333mM $K_3[Fe^{III}(CN)_6]$ 5µl 10% Triton X-100 (Fluka) 16µl 5% XGal (AppliChem) in dimethylformamide
Buffer B	500µl 200mM NaPi pH 7.2 300µl 5M NaCl 10µl 1M $MgCl_2$ H_2O to 10ml

5.5.5 XGal staining zebrafish embryos

5.5.5.1 Procedure

5xAE, 5xSE reporter constructs and the control vector were injected into one- and two-cell stage zebrafish embryos in a concentration of 10 to 40ng/µl. To inhibit BMP-mediated Smad

phosphorylation, 10µM Dorsomorphin (Sigma) was applied to the medium as soon as embryos reached the 1000-cell stage. Embryos were allowed to develop at 28.5°C until approx. 60% epiboly and then fixed in fish fix solution for 8min at room temperature. After washing four times in washing solution, embryos were incubated overnight at 37°C in XGal ZF staining solution. Staining was stopped by rinsing with PBST (0.1% Tween 20 (Fluka) in PBS).

5.5.5.2 Solutions

Fish fix solution	PBS 2mM $MgCl_2$ 12% Glutaraldehyde
Washing solution	PBS 2mM $MgCl_2$ 0.3% Triton X-100 (Fluka)
XGal ZF staining solution	914µl Buffer B 30µl 333mM $K_4[Fe^{II}(CN)_6]xH_2O$ 30µl 333mM $K_3[Fe^{III}(CN)_6]$ 5µl 10% Triton X-100 (Fluka) 16µl 5% XGal (AppliChem) in dimethylformamide
Buffer B	500µl 200mM NaPi pH 7.2 300µl 5M NaCl 10µl 1M $MgCl_2$ H_2O to 10ml

5.5.6 Documentation

Stainings of *Drosophila* embryos and imaginal discs were documented with a Colorview II digital camera (Soft Imaging System) in combination with an Axiophot microscope (Zeiss). Images were processed using the analySIS software (Soft Imaging System).
Stainings of zebrafish embryos were documented with a DFC420 C digital camera (Leica), connected to a MZ FLIII stereomicroscope (Leica). Images were processed using the Leica Application suite.

5.6 Bioinformatic tools

Drosophila sequence informations and related gene maps were retrieved from Flybase (http://www.flybase.org) and the VISTA Genome Browser (Frazer et al., 2004; Mayor et al., 2000), available at http://genome.lbl.gov/vista/. The latter was also used for alignments of genomic sequences from *D. melanogaster* and other *Drosophila* species.
The entire *Drosophila* genome was screened for putative AEs using the Flyenhancer search tool (Markstein et al., 2002), available at http://www.flyenhancer.org.
Positions of putative Smad and Brinker binding sites within the *dad* enhancer were visualized using the program dna-pattern at http://rsat.ulb.ac.be/rsat/ (van Helden et al., 2000).
The intensity of the mobility shift bands for defining the Brinker binding consensus sequence was measured using the software ImageJ (Abramoff et al., 2004), available at http://rsbweb.nih.gov/ij/.

5.7 Fly strains

w;; prd-Gal4 / TM3	*GAL4* gene driven by regulatory elements from the *paired* locus. Affolter lab stock #302.
UAS brk	*brinker* gene driven by UAS elements. Affolter lab stock #251.
UAS brkVP16	Gene encoding a recombinant BrkDBD-VP16 protein, driven by UAS elements. Strain 13, on second chromosome.
yw brk / FM7c ftz-lacZ	*brinker* mutant, balanced over "blue" balancer. Affolter lab stock #201.
shn^{TD5} / CyO wg-lacZ	*schnurri* mutant, balanced over "blue" balancer. Derived from Affolter lab stock #278.
tkv / CyO wg-lacZ	*thickveins* mutant, balanced over "blue" balancer. Affolter lab stock #318.
UAS tkv^{QD}	Gene encoding the constitutively active receptor Thickveins, driven by UAS elements. Affolter lab stock #231.
UAS shnVP16	Gene encoding a recombinant Shn-VP16 protein, driven by UAS elements. Obtained from Britta Hartmann (#132).
p1883 / TM3	*dad* lacZ enhancer trap (Tsuneizumi et al., 1997).

6 Results

6.1 Analysis of *dad* expression and regulation

6.1.1 *dad* expression follows *dpp* expression

In contrast to the expression pattern of *dpp*, the expression pattern of *dad* in the *Drosophila* embryo has been poorly described. To compare the expression domains of *dpp* and its potentially direct target gene *dad*, we performed *in situ* hybridizations. Since Dpp plays an important role in the dorsal-ventral axis formation, the *dpp* transcript is localized dorsally already in the very early embryo (Fig. 6.1A). During the process of germband extension, the dorsal expression refines into two clearly distinct segmented ectodermal stripes (B, C). Later on (D), *dpp* is also expressed in the visceral mesoderm of parasegment 7, in the ectoderm of foregut and hindgut as well as in anterior structures (Panganiban et al., 1990).
Unlike *dpp*, *dad* transcripts are not localized dorsally in the young cellularized embryo but either absent or uniformly and weakly distributed (E). Only at about stage 6 to 7, *dad* expression becomes visible (F). After undergoing a refinement similar to that of *dpp*, *dad* expression follows the expression of *dpp* precisely and in every single aspect. Since Dpp acts extracellularly as a morphogen, the expression domain of *dad* is broader and includes also cells neighboring *dpp* expressing cells. This is also evident in the larval wing imaginal disc (Fig. 6.1), where *dad* expression follows *dpp* expression (both visualized using *lacZ* reporter lines) tightly along the anterior-posterior border. The same holds true for the expression of *dad* in leg and haltere discs.

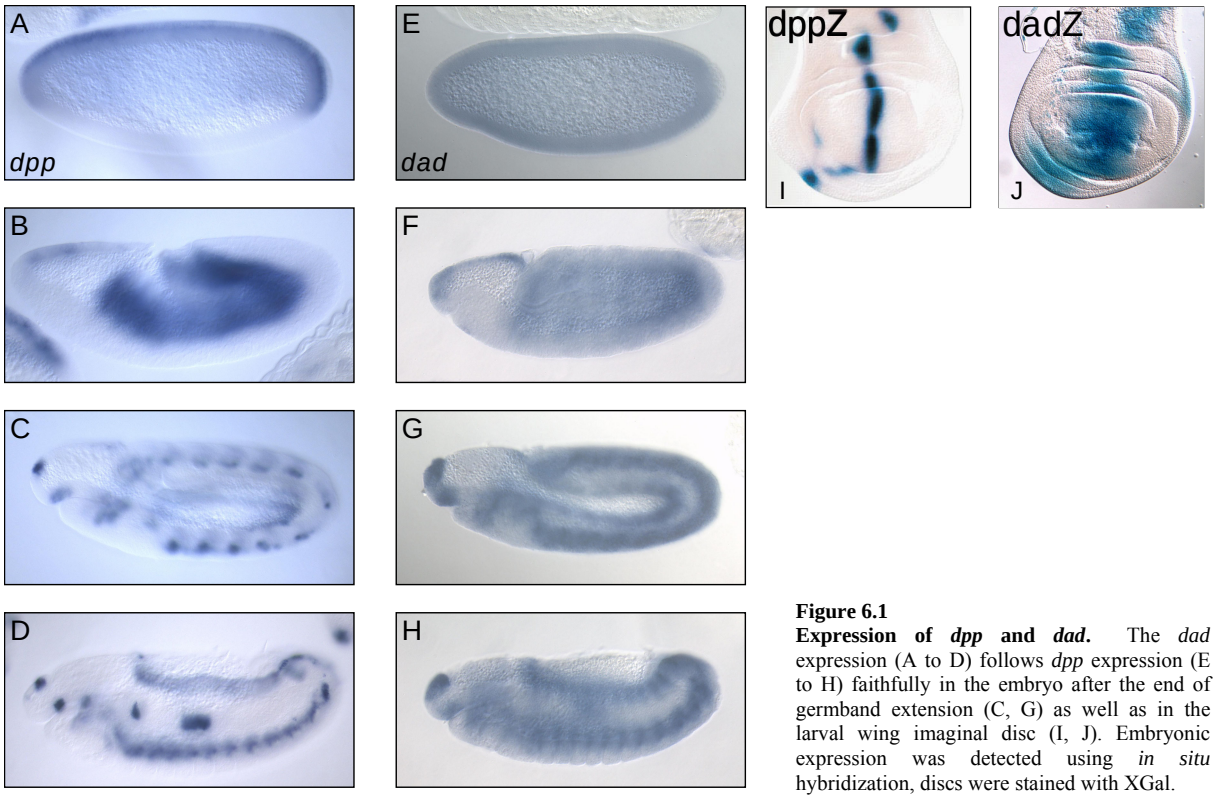

Figure 6.1
Expression of *dpp* and *dad*. The *dad* expression (A to D) follows *dpp* expression (E to H) faithfully in the embryo after the end of germband extension (C, G) as well as in the larval wing imaginal disc (I, J). Embryonic expression was detected using *in situ* hybridization, discs were stained with XGal.

6.1.2 *dad* expression is regulated by the Dpp pathway and Brinker

Genes that are activated upon Dpp signalling fall into one of three different classes: genes that are directly activated by Dpp, genes that are directly activated by Dpp and at the same time repressed by the default repressor Brinker, and finally genes that are only repressed by Brinker and indirectly activated via Dpp-induced repression of the *brinker* gene. To determine the class the *dad* gene falls into, *dad* expression was analysed in different mutant backgrounds (Fig. 6.2). *dad* expression is completely abolished in *thickveins* and *schnurri* mutant embryos and expands widely in a *brinker* mutant background. Furthermore, ectopic expression of *brinker* under the control of a *paired* enhancer, using the UAS-GAL4 system (Brand and Perrimon, 1993), leads to strong local repression of *dad*. These observations suggest that *dad* is a *brinker* target. What remained unanswered was, whether there is also a direct Dpp input on *dad*. To address this question, we ectopically expressed the transgene tkv^{QD}, which encodes the constitutively active form of the Dpp receptor Thickveins, and found that it led to clear upregulation of *dad*. Importantly, this was also the case in a *brinker* mutant background, indicating that this upregulation is independent of Brinker and suggesting that *dad* is regulated by both Dpp signalling and Brinker.

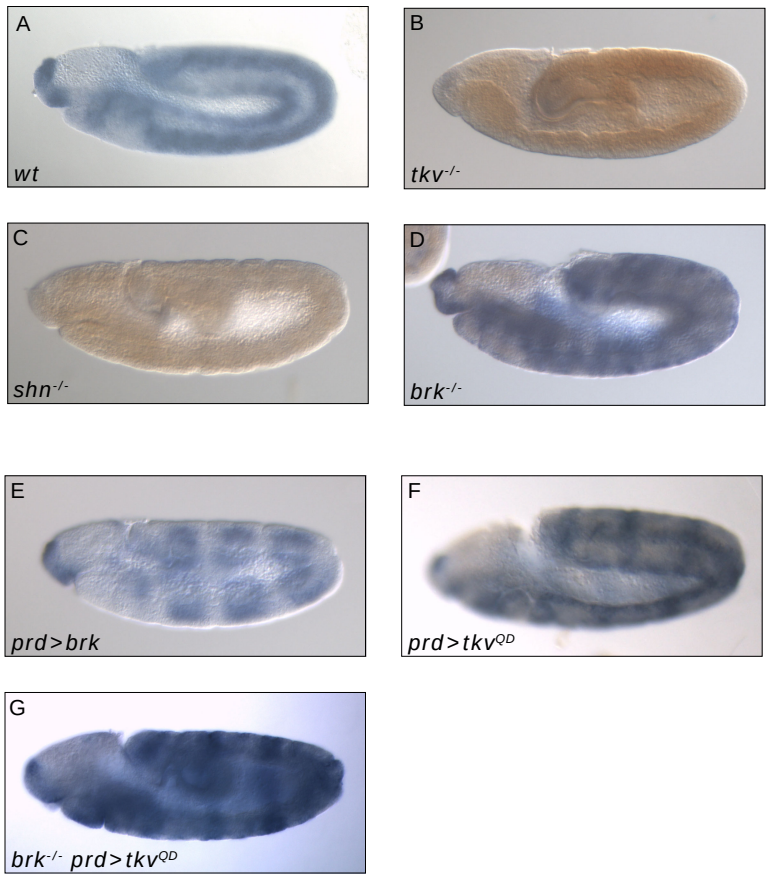

Figure 6.2
Genetic regulation of the *dad* gene. All images show *dad in situ* hybridizations in the *wild type* (A) and various genetic backgrounds (B to G). *dad* is not expressed in *thickveins* and *schnurri* mutants (B, C) and expands widely in *brinker* mutants (D). Expression of *UAS-brinker* by *paired-GAL4* leads to ectopic repression (E). Expression of the constitutively active Dpp receptor *thickveins* induces ectopic activation of *dad* in a *wild type* (F) and *brinker* mutant background (G), indicating a Brinker-independent input on *dad*.

6.2 Identification of a minimal *dad* enhancer

6.2.1 A *lacZ* reporter driven by the second *dad* intron resembles endogenous *dad* expression

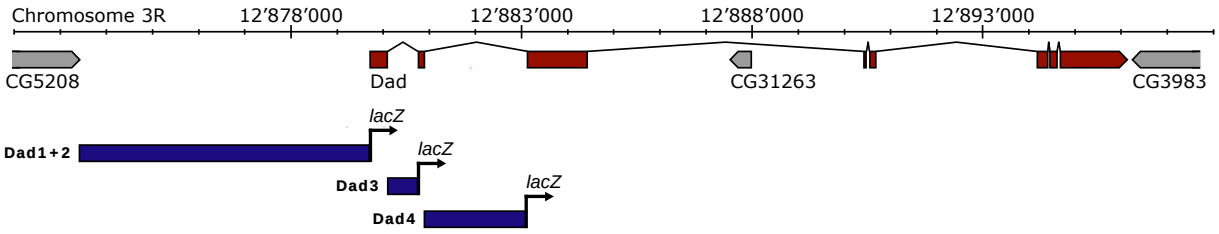

Figure 6.3
Genomic locus of the *dad* gene with initially planned reporter constructs. The *dad* gene is located on the right arm of the third chromosome and stretches over several exons. Three reporter constructs were designed, covering the pre-transcription start region, the first and the second intron.

After having ensured that the *dad* gene receives an activating Dpp input, we analysed the *dad* genomic region in order to identify potential *cis*-regulatory elements. The *dad* gene is situated on the right arm of the third chromosome and stretches over 16kb (see Fig. 6.3). It contains seven introns, the biggest of them harboring the predicted gene CG31263 (which was, however, excluded from the newest Dmel genome release). Since *cis*-regulatory elements tend to be conserved during evolution, we initially screened the *dad* genomic region for stretches highly invariant among far related *Drosophila* species (see introduction) using the VISTA genome browser (Frazer et al., 2004; Mayor et al., 2000). At the same time we created different *lacZ* reporter constructs to identify the *dad* enhancer(s) and generated transgenic flies carrying these reporters. Whereas the construct Dad1+2 was never successfully cloned, the construct Dad3 (resembling the first intron) did not drive any *lacZ* expression in the embryo and larval imaginal discs. Dad4 (resembling the second intron) however was able to induce expression indistinguishably from the endogenous *dad* expression in embryonic as well as larval tissues (Figures 6.4 and 6.7).

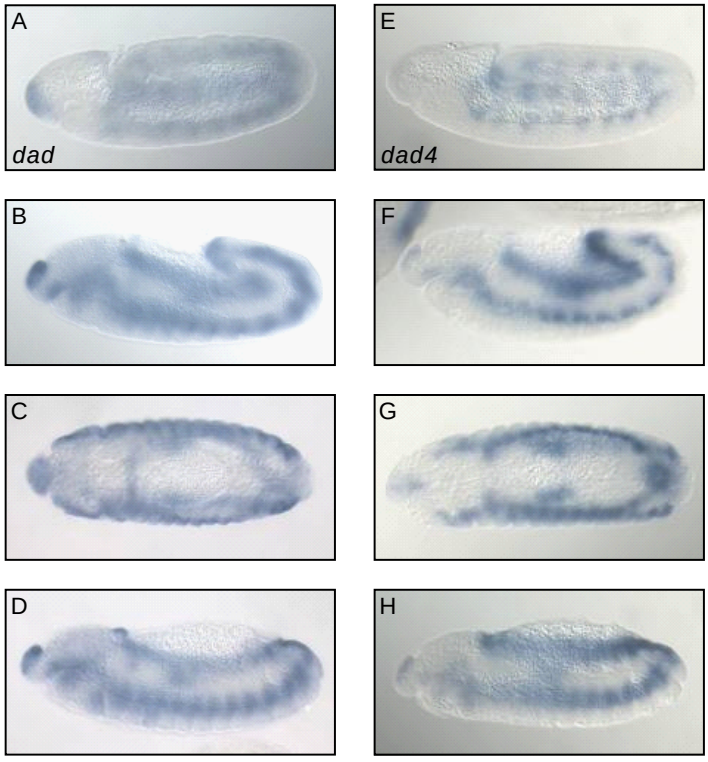

Figure 6.4
Expression of the Dad4 reporter construct. The expression of *lacZ* driven by the Dad4 fragment (E to H) recapitulates the endogenous *dad* expression (A to D) precisely. All images *in situ* hybridization.

6.2.2 The minimal enhancer Dad13 contains putative Smad and Brinker binding sites and is highly conserved

Figure 6.5
Detailed view and conservation of the minimal enhancer Dad13 and subconstructs. Degree of conservation visualized using the VISTA genome browser. Regions highly conserved in *D. pseudoobscura* and *D. virilis* are colored in red. Two clusters of putative transcription factor binding sites can be found, that are highly conserved in other *Drosophila* species (marked with asterisks) Color intensity of the enhancer constructs indicates the strength of expression. Constructs depicted in grey did not show any staining at all. Dad10+10 stands for a dimerized Dad10 construct. Clearly, expression levels are correlated with the size of the enhancer fragments. Sequence analysis reveals that several Mad and Brk sites are conserved among different species and overlap due to the similarity of their consensus sequences.

Our next aim was to successively reduce the size of the enhancer construct in order to identify the minimal enhancer. We ended up with a 520bp construct, Dad13. Dad13 drives expression of a *lacZ* reporter in an identical pattern to that of Dad4 (Fig. 6.7) and consists of two conserved regions of about 150bp each, separated by a poorly conserved DNA stretch (Fig. 6.5). Since genetic data indicated a regulation of *dad* by both Brinker and Dpp, we screened Dad13 for potential Brinker and Smad binding sites. For Brinker, we used the experimentally derived consensus sequence GGCGYY (Sivasankaran et al., 2000; Zhang et al., 2001). To track down Smad binding sites, we used both the simple Smad-binding element (SBE) AGAC (Shi et al., 1998; Zawel et al., 1998) as well as the sequence GRCGNC, which has been shown to recruit *Drosophila* Mad proteins (Gao et al., 2005; Pyrowolakis et al., 2004). Most of the sites found fall into the two highly conserved clusters. We also noticed that all highly conserved potential Brinker binding sites completely overlap with Mad binding sites, suggesting a possible competition as it has been reported for other Dpp responsive enhancers (Kirkpatrick et al., 2001; Rushlow et al., 2001). Additionally, a tandem SBE repeat was identified. Despite extensive searches, no transcription factor binding sites could be reliably assigned to a perfectly conserved 50bp region at the 5' end of Dad13.
To determine whether the high degree of conservation was reflected in similar expression patterns, we cloned the corresponding genomic regions Dad13V and Dad13PO from *D. virilis* and *D. pseudoobscura* - two species which diverged from *D. melanogaster* as long as 40 and 25 million years ago respectively. The *lacZ* reporter plasmids containing these enhancers were then transformed into *D. melanogaster* embryos. The resulting expression patterns in the embryo and larval discs highly resembled that of Dad13 (Fig. 6.6), suggesting an important function of the conserved elements.

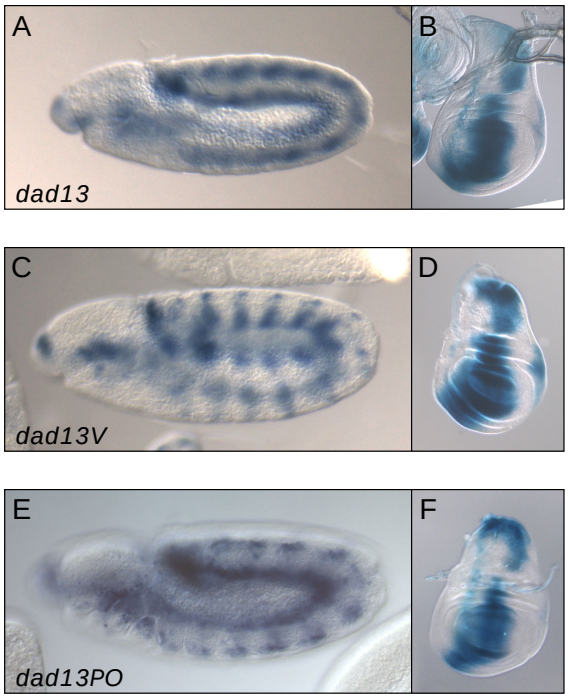

Figure 6.6
Expression of the corresponding Dad13 constructs from other Drosophila species. The homologous genomic regions of Dad13 from *D. pseudoobscura* and *D. virilis* were cloned and transformed as *lacZ* reporter constructs into *D. melanogaster*. Expression patterns were very alike in the embryo as well as in larval imaginal discs (*in situ* hybridization and Xgal staining respectively).

6.2.3 Trimming of Dad13 leads to loss of activity

Further attempts to significantly reduce the size of the Dad13 enhancer (Fig. 6.7) resulted in a constant decrease of expression strength, but never in a severe change in domains or width of expression (see Fig. 6.7). This pointed at a modular, somewhat redundant architecture of the enhancer with multiple sites of transcriptional input. This theory was strengthened by the fact that dimerization of otherwise inactive elements (as Dad10+10, Fig. 6.5) led again to an increase in expression. The fact that repressive and activating sequences could not be separated by simple trimming furthermore emphasized a potential competition of activators and repressors on the same sites. In general, loss of expression strength was less dramatic in the embryo than in the wing imaginal disc. Dad15 for example did not show any staining in the wing disc (Fig. 6.7), but was still inducing low expression levels in the embryo (data not shown).

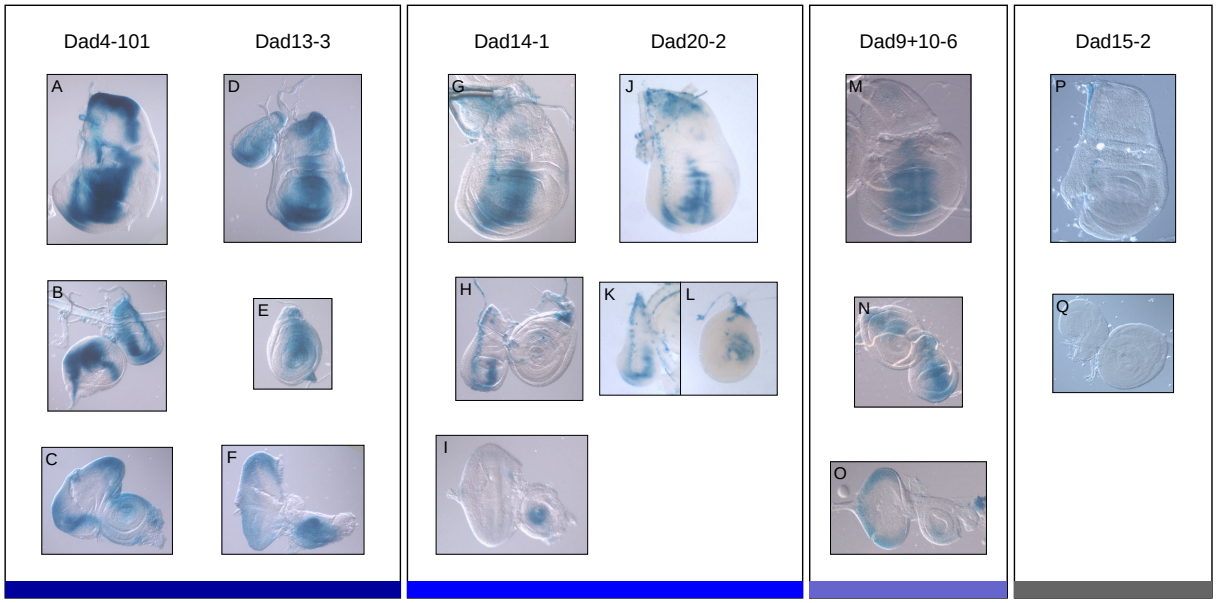

Figure 6.7
Decrease of expression with enhancer size. Reducing the size of the *dad* enhancer leads to a reduction in *lacZ* expression levels. The respective constructs are depicted in Fig. 6.5, Dad9+10 is a fusion construct of Dad9 and Dad10. While the strength of expression decreases, the expression domains remain unchanged. This indicates overlapping or closely neighbored repressor and activator binding sites. Color bars at the figure bottom indicate the expression strength in the imaginal discs. All images show XGal stainings.

6.2.4 The minimal enhancer is regulated by Dpp and Brinker *in vivo* and in cell culture

To decipher the transcriptional regulators responsible for activity of the identified *dad* enhancer and to test whether they are the same as for *dad*, we analysed its activity in mutant backgrounds and compared it to the expression patterns of *dpp* and *brinker*. As expected from an enhancer repressed by Brinker, the expression domains of *brinker* and *dad13* (a *lacZ* reporter gene driven by the minimal enhancer Dad13) are mutually exclusive in the wing imaginal disc (Fig. 6.8). Furthermore, *dad13* is derepressed in clones homozygous mutant for *brinker*. The expression pattern of *dad13* closely reflects the Dpp activity domain and includes and surrounds the *dpp* expressing cells along the anterior-posterior border (Fig. 6.8).

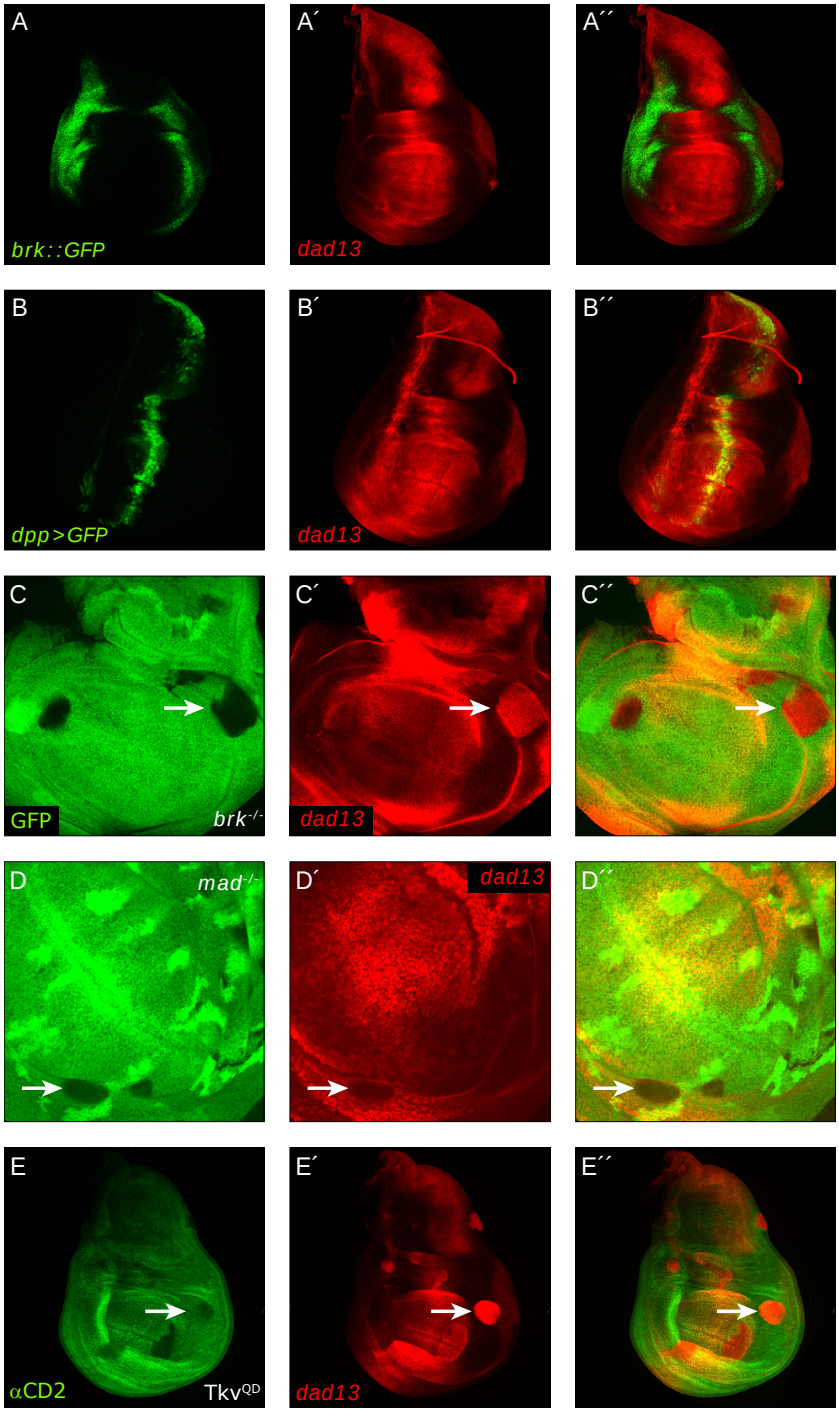

Figure 6.8
Regulation of the minimal enhancer. The expression of *dad13*, a *lacZ* reporter gene driven by Dad13, was analysed in the wing imaginal disc. The expression patterns of *brinker* and *dad13* are complementary (A). Furthermore, the expression domain of *dad13* includes and flanks the expression domain of *dpp* (B). Clones mutant for *brinker* ectopically upregulate *dad13* (C), whereas cells mutant for *mad* do not express *dad13* (D). The clonal expression of tkv^{QD}, which encodes the constitutively active Dpp receptor, leads to strong local induction of *dad13*.
Mutant clones are indicated by loss of a GFP (C, D) or CD2 (E) marker (arrows show examples). Expression of *brinker* was visualized by a GFP reporter gene driven by the *brinker* enhancer. *dpp* expressing cells were marked by the expression of dpp-Gal4 and UAS-GFP. The Expression of *dad13* was detected using an anti-β-galactosidase antibody. All images were kindly provided by Enrica Charbonnier, University of Freiburg.

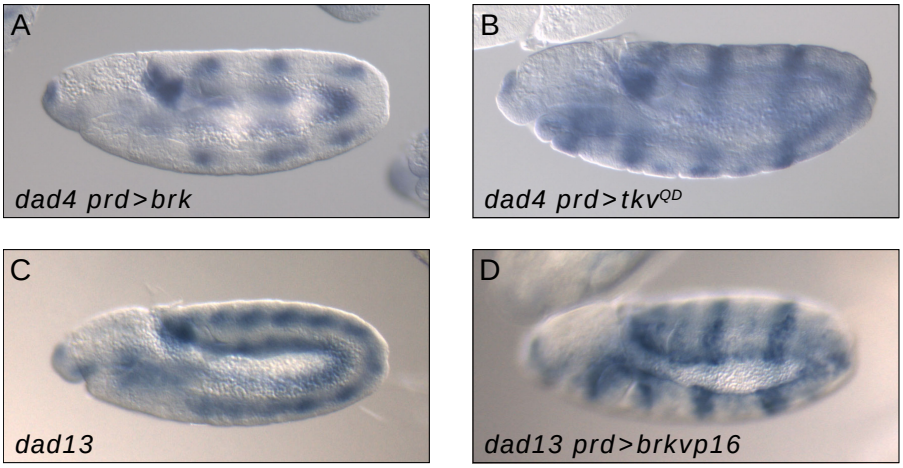

Figure 6.9
Regulation of the minimal enhancer. Expression of Brinker under the control of the *paired* enhancer (using the UAS-Gal4 system) leads to ectopic repression of the *lacZ* reporter gene, whereas the constitutively active Dpp receptor Tkv^{QD} leads to activation. Expression of the strong activator BrkVP16, where the Brinker repression domain was exchanged with an activating domain, results in ectopic activation of the reporter. All images show *in situ* hybridization, except α–βgal staining for *dad13 prd>brkvp16*.

Cells that lack Mad protein do not express *dad13*, whereas clones expressing a transgene encoding the constitutively active Dpp receptor Tkv^{QD} strongly upregulate *dad13*. The same response to ectopic activation of the Dpp pathway can be seen in the embryo. A *lacZ* reporter gene driven by Dad4 is upregulated upon striped expression of tkv^{QD} (Fig. 6.9). Furthermore, ectopic expression of a recombinant BrkVP16 protein (where the repression domain of Brinker was swapped with the strong activation domain of the Herpes simplex protein VP16) leads to strong induction of a Dad13 *lacZ* reporter. This indicates a direct involvement of Brinker in the regulation of *dad*.
The use of cell culture experiments allows for fast and comparative testing of different shortened or mutated reporter constructs and various effector proteins. Although it does not replace the analysis of transgenic flies, it offers a convenient possibility to track down transcription factor binding sites.
For the *in vitro* analysis of Dad13, S2 cells were transfected with the respective reporter plasmid and expression levels were determined by β-galactosidase activity. Basal expression

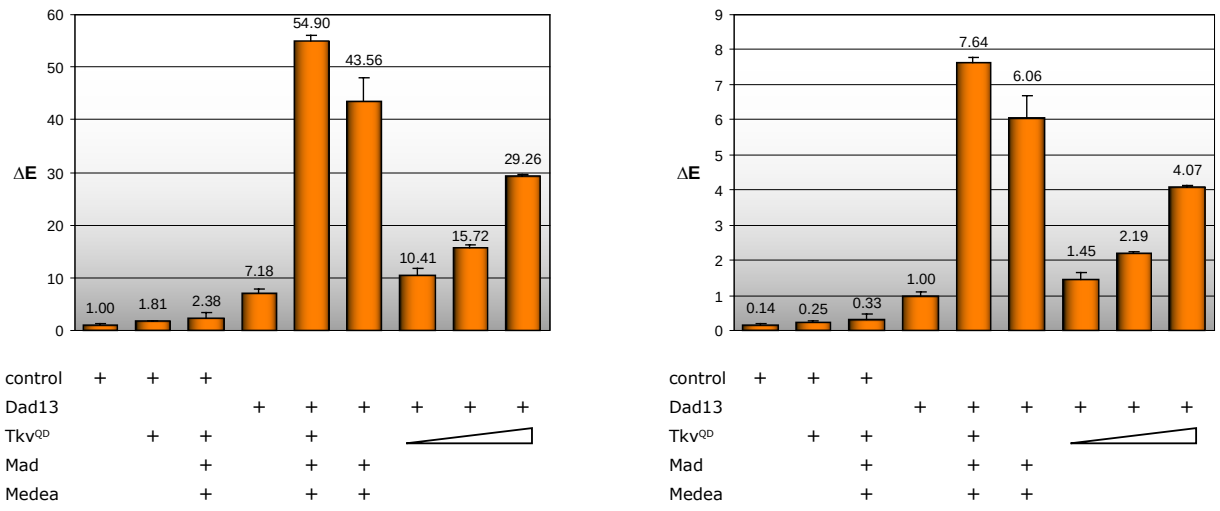

Figure 6.10
Activity of the Dad13 enhancer in S2 cell culture. S2 cells were transfected with either a Dad13 *lacZ* vector, or an empty *lacZ* control vector and various combinations of plasmids encoding Tkv^{QD}, Mad and Medea. Results were normalized against levels of co-transfected luciferase. Right panel shows the same data normalized additionally against Dad13. Already Dad13 alone shows an activity seven-fold higher than the empty vector. Activation of the Dpp pathway increases this activity further drastically.

levels of a *lacZ* reporter driven by Dad13 were already more than seven-fold higher than that of a control plasmid. Co-transfection of plasmids coding for Mad, Medea and Tkv^{QD} further increased expression levels dramatically (Fig. 6.10). Comparative studies of the different enhancer constructs confirmed the results obtained from the *in vivo* expression analysis. Reduction in size leads to a decrease of enhancer activity (Fig. 6.11, compare to Fig. 6.7), including both basal activity and activity upon co-transfection of Mad, Medea and Tkv^{QD}. Expression of BrkVP16 results in strong activation of Dad13 and weaker activation of its subfragments Dad9 to Dad12 (Fig. 6.11). Strongest (relative) upregulation can be seen for the fragments Dad10, Dad11 and Dad12, which include a putative Brinker binding site.

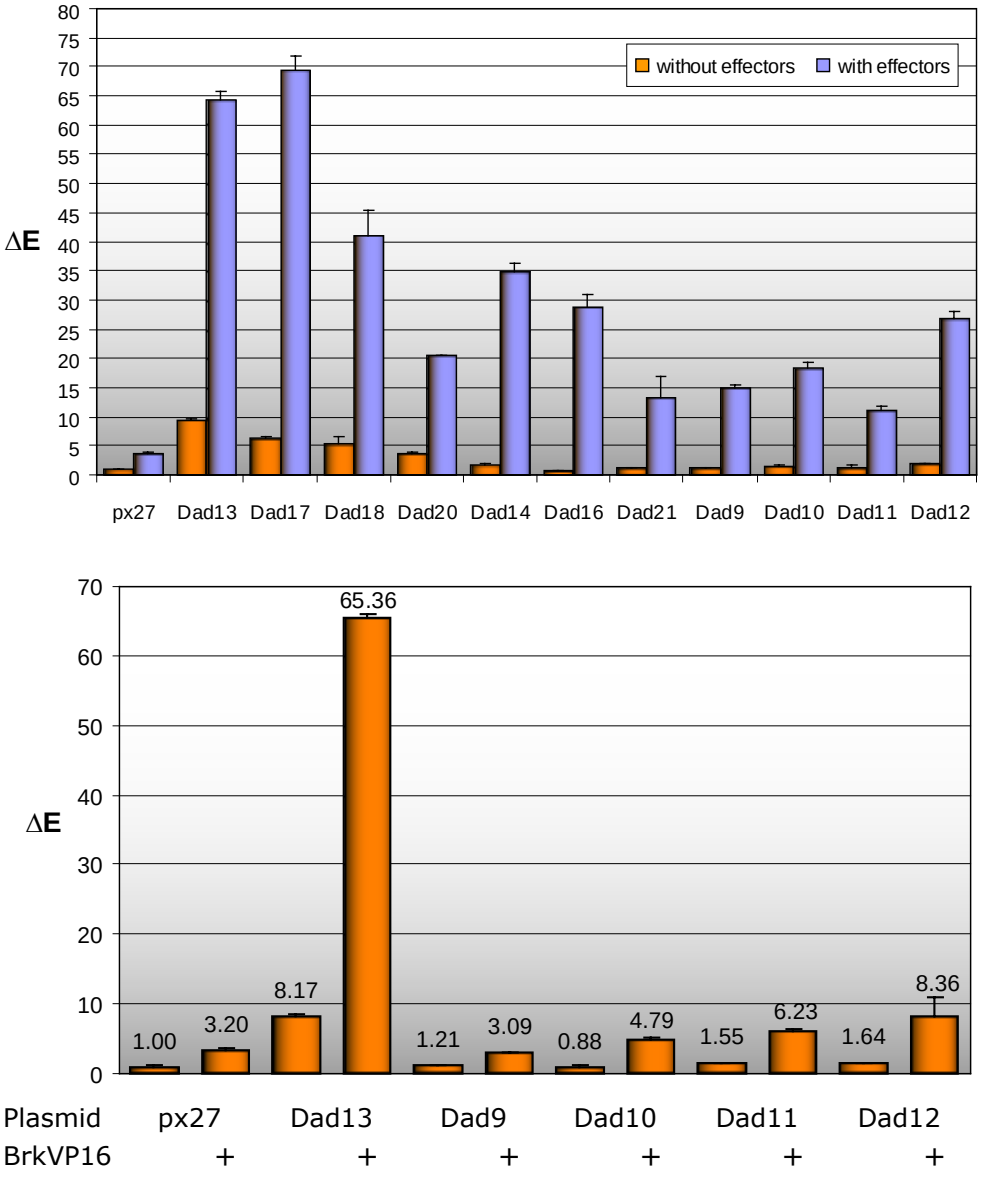

Figure 6.11
Comparison of different enhancer constructs and effect of BrkVP16 expression. (Upper panel) Bars indicate relative levels of activity without (orange) and with (blue) co-transfection of plasmids encoding Mad, Medea and Tkv^{QD}, normalized against luciferase expression and activity of the empty *lacZ* vector px27. Activity decreases with the size of the enhancer fragments. (Lower panel) BrkVP16 is able to strongly activate Dad13 and also smaller enhancer constructs, which is consistent with the localization of the putative Brinker binding sites. Values were normalized against luciferase expression and activity of the empty vector px27.

6.3 Dissection of the minimal enhancer by biochemical analyses

6.3.1 Mad/Medea and Brinker DNA binding domains bind to the *dad* enhancer

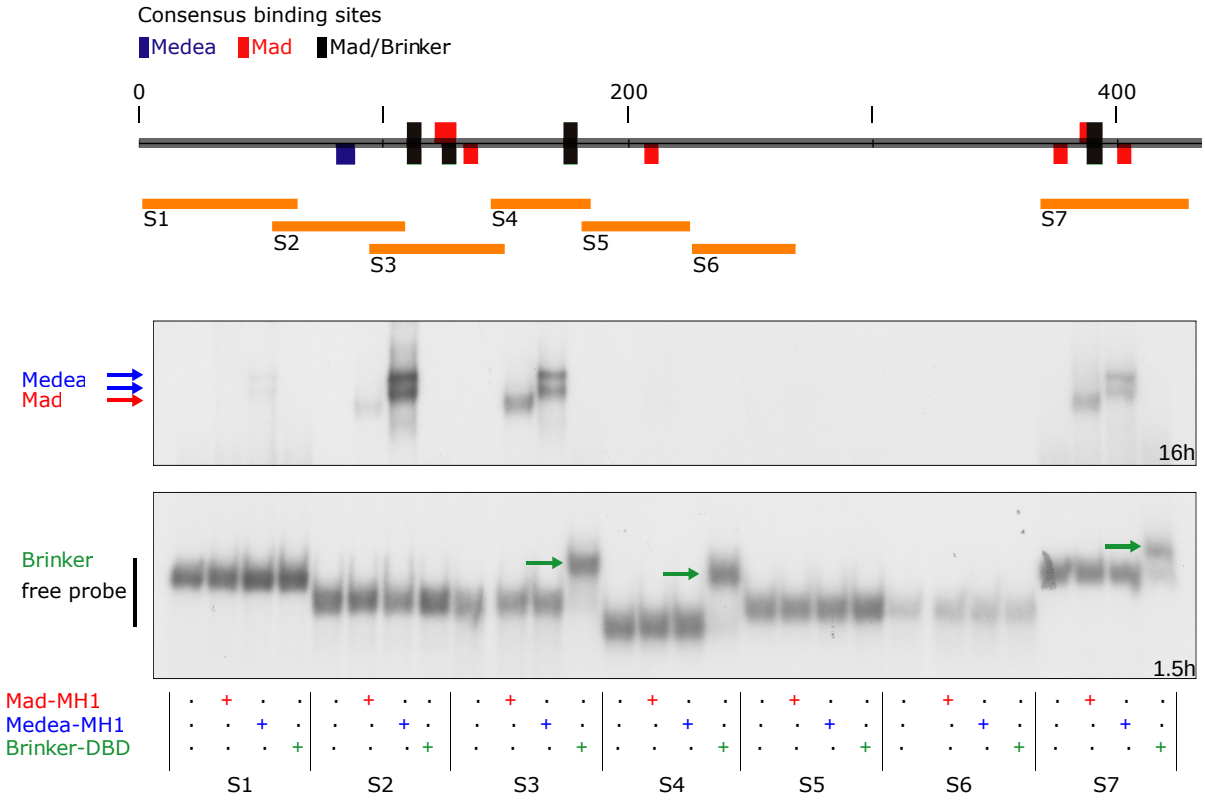

Figure 6.12
Binding of Smad and Brinker DNA binding domains to the *dad* enhancer. Seven different subconstructs (S1 to S7) were designed to decipher the sites of transcriptional regulation. The bacterially expressed DNA binding domain of Brinker efficiently bound to three subfragments (green arrows). Binding of the Mad/Medea DNA binding domains could be observed for the oligos S2, S3, S7 and surprisingly only weakly for S4 after long exposure (Mad only). For detailed sequence information see figure 6.5.

After having found several potential sites for active Smad and repressive Brinker input by *in silico* analysis and cell culture experiments, we attempted to clearly identify the sites which bind transcription factors and submitted the respective DNA sequences to electrophoretic mobility shift assays (EMSA). We subdivided Dad13 into several oligonucleotides of 40 to 70bp length, namely oligos S1 to S7 (Fig. 6.12), and tested purified DNA binding domains of Mad, Medea and Brinker for binding. All fragments containing putative Brinker binding sites were able to interact with the Brinker protein. Mad and Medea, however, were significantly recruited only to S2 (containing the 2xSBE), S3 and S7, that both contained clusters of potential Mad sites (Fig. 6.12). Longer exposure revealed weak binding of Mad also to S4 (not shown, compare Fig. 6.13).

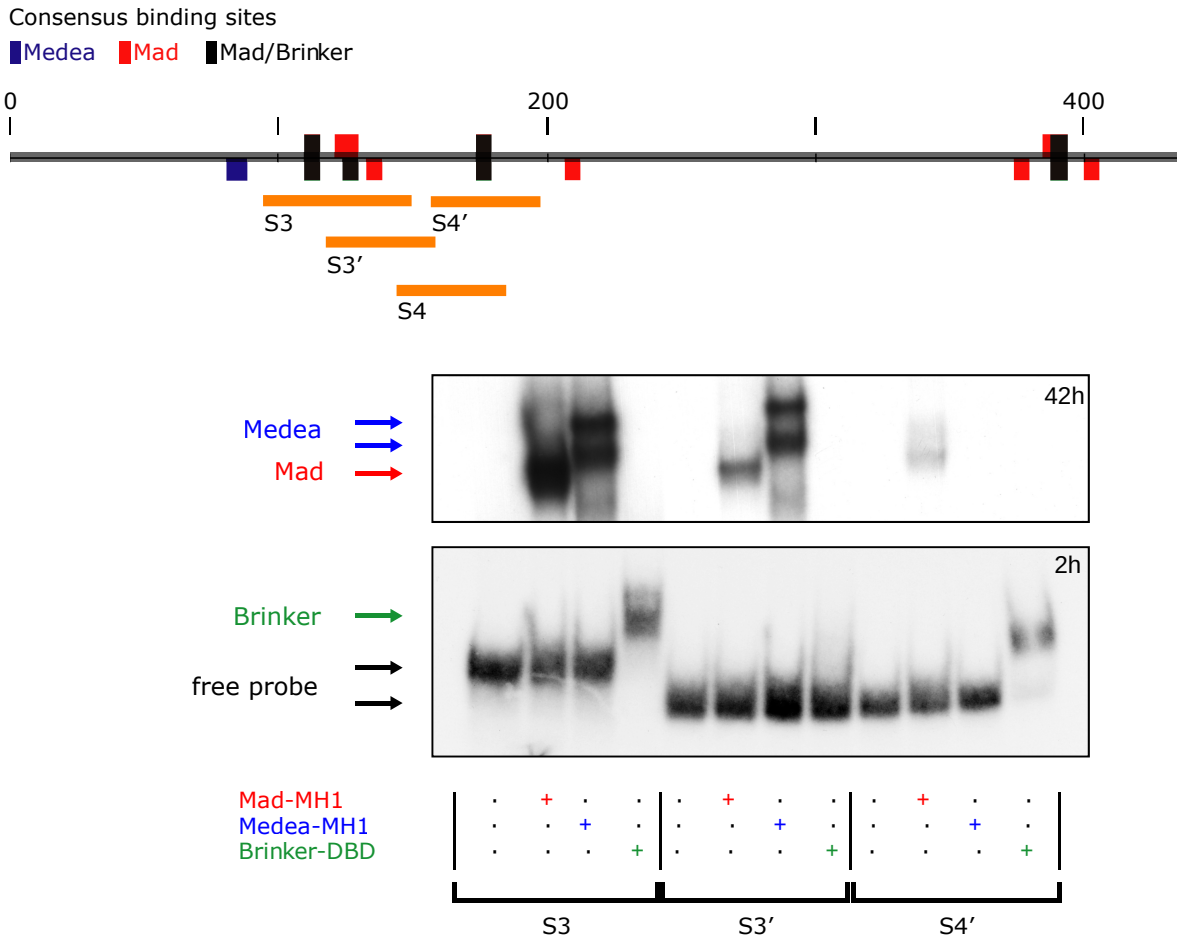

Figure 6.13
Retesting of binding sites in S3 and S4. To ensure that the binding behavior was not due to the design of the fragments, the shifted constructs S3' and S4' were also tested for Mad, Medea and Brinker binding. S3' lacks one putative Brinker binding site included in S3 and was not able to bind Brinker anymore. S4' efficiently bound Brinker , but only weakly Mad, as already seen for S4 (see Fig. 6.11).

To examine whether the design of S4 and its lack of flanking sequences was the reason for weak Mad binding, we tested the additional construct S4', that was centered on the Mad/Brinker site (Fig. 6.13). This experiment confirmed the initial results. S4' behaved exactly like S4, showing only very limited Mad binding. Since S3 contained two potential Brinker binding sites, we constructed another oligonucleotide (S3') that lacked the first Mad/Brinker site. S3' was not able to recruit Brinker and thus revealed that the missing site was the sole Brinker site within S3 and a major Mad site. Consequently, we mutated all Mad/Brinker sites by changing the core nucleotides from GRCGCC to GRATCC and tested for protein binding. The results showed that the sites 1, 4 and 7 were the only relevant Brinker binding sites (Fig. 6.14), whereas sites 1 and 7 were the strongest Mad/Medea sites (compare Fig. 6.15).

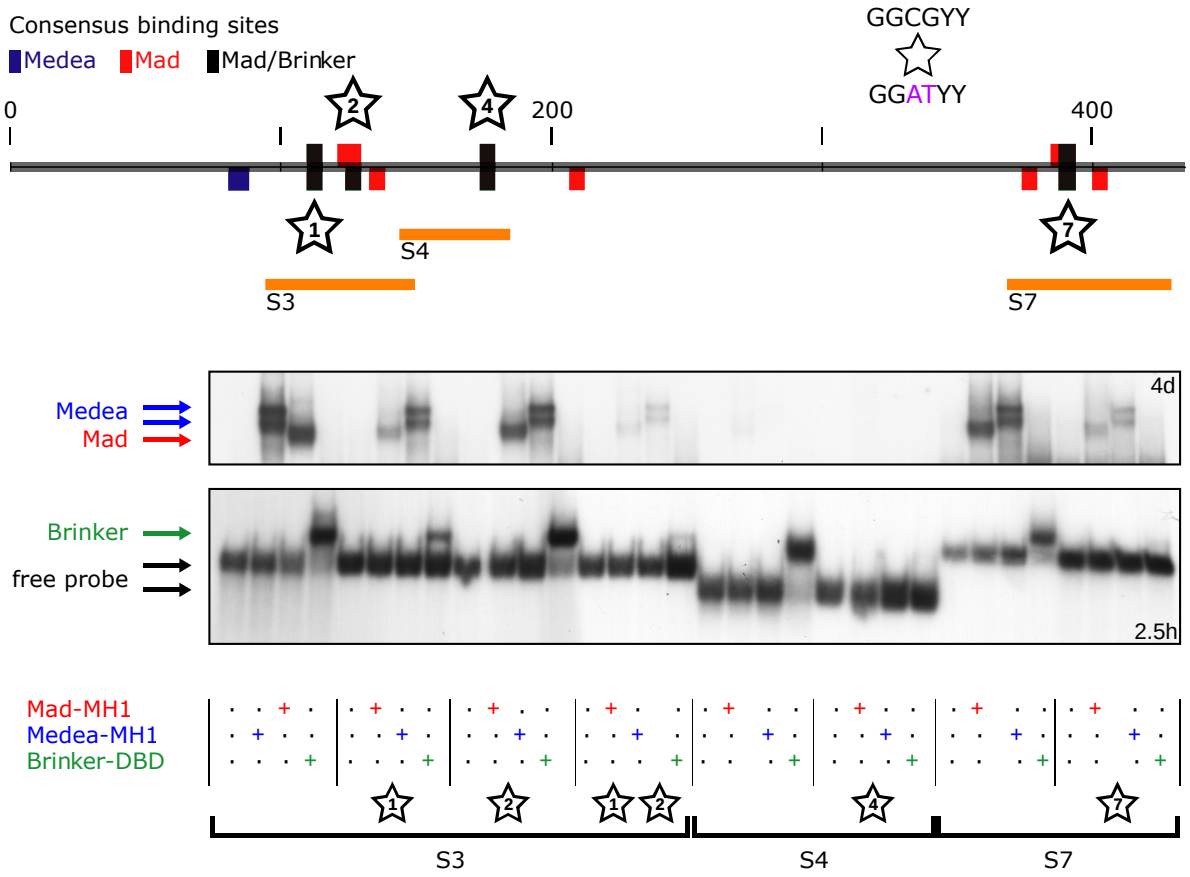

Figure 6.14
Identification of Brinker and Smads sites. All putative Brinker binding sites were mutated by exchanging the two core nucleotides from CG to AT and tested for Smad and Brinker binding. This led to the identification of three (palindromic) Brinker binding sites (1, 4 and 7). Mad and Medea bind more promiscuously, but mainly to two of these three Brinker sites (1 and 7).

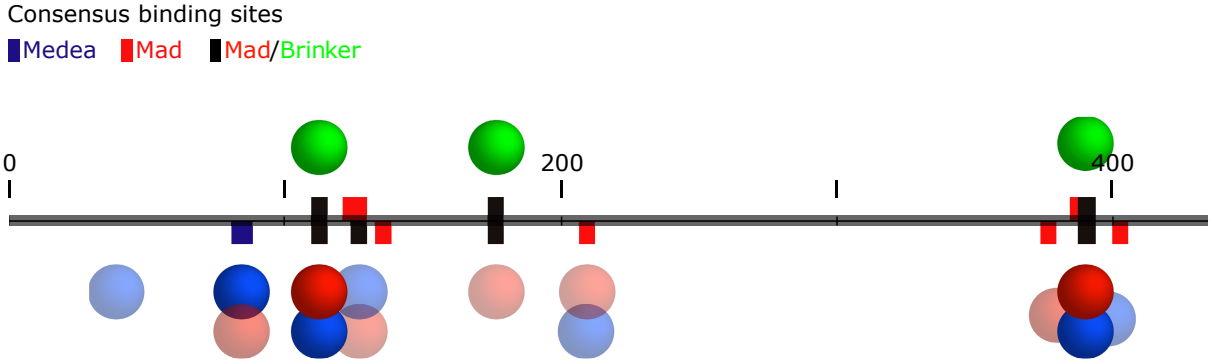

Figure 6.15
Summary of the mobility shift experiments with DNA binding domains. The color intensity resembles binding efficiency. Brinker binds to three sites within the Dad13 minimal enhancer, all of them perfectly palindromic. Mad binds strongly to two of these sites and weakly to other putative binding sites. The same holds true for Medea, however Medea also strongly binds to S2, which is very likely due to the tandem Smad binding element found there. This construct also displayed weak Mad binding.

6.3.2 Mad/Medea and Brinker compete for binding sites

Due to the overlap of Brinker and Mad sites, we were tempted to speculate that these two transcription factors compete for binding. To test this hypothesis, a competitive assay was performed using S3, invariant amounts of Mad/Medea DNA binding domains and increasing amounts of Brinker DNA binding domain. Indeed, Brinker is able to compete away Mad and Medea (Fig. 6.16), which indicates a regulatory mechanism based on competition for the *dad* enhancer.

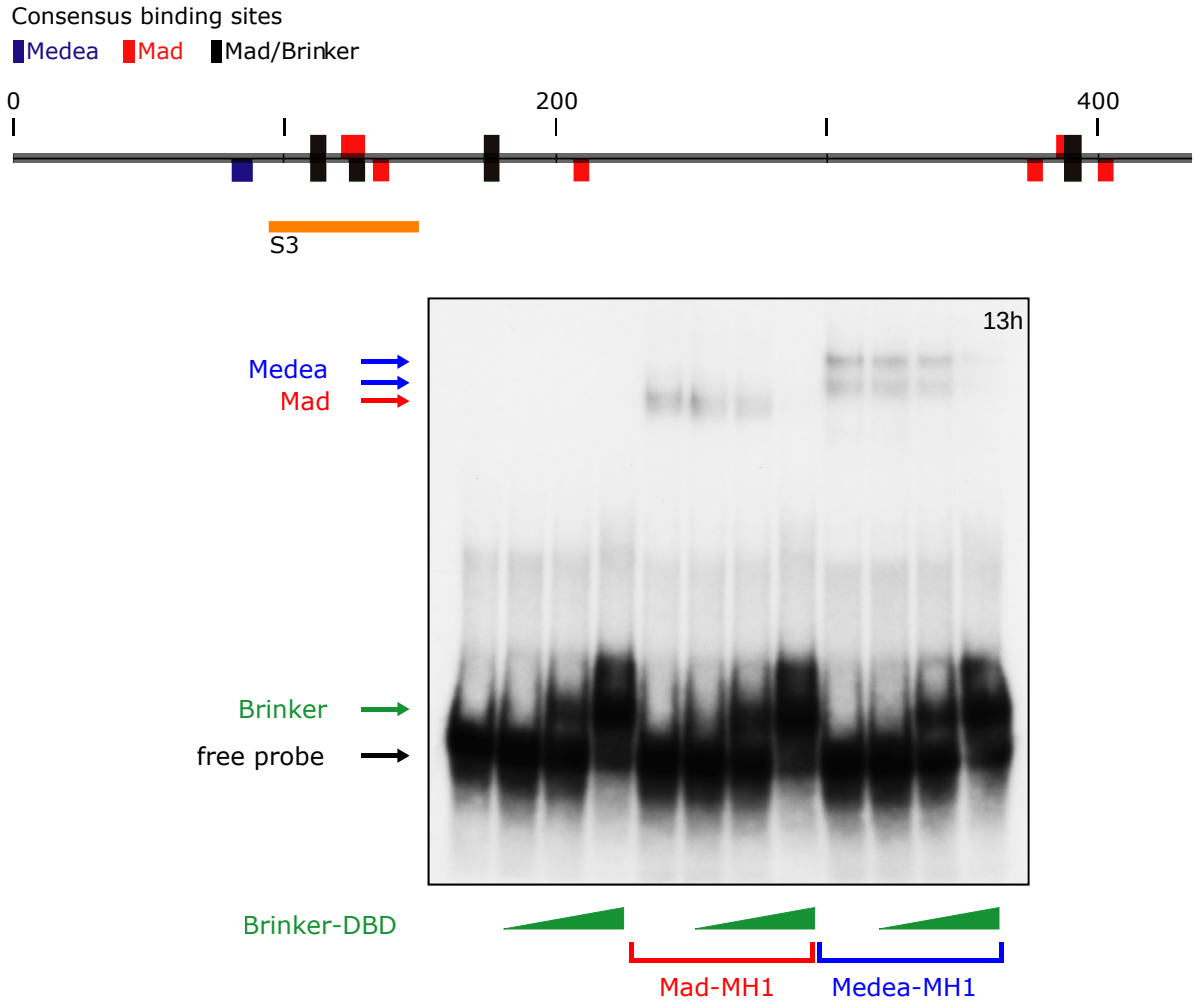

Figure 6.16
Smads and Brinker compete for the same binding sites. S3 was tested for competitive binding of Brinker and Mad/Medea. For this purpose, increasing amounts of Brinker DNA binding domain were incubated with constant amounts of S3 and either Mad and Medea DNA binding domains. The binding of both Mad and Medea is clearly reduced in the presence of Brinker.

6.3.3 Binding of Mad/Medea and Brinker to *Ubx* and *zen* enhancer


```
ZenB4M6          CTGGCGAGACTCCGGCTCTTGCGGCCCAG

ZenB5M7          TCTCTCACGCAACGCCAGATCCTGGCAGGA
```

Figure 6.17
Sequence of the two *zen* enhancer fragments tested for Brinker and Smad binding. Sequence from the *zen* enhancer, which was located within 1.6kb upstream of transcription start (Doyle et al., 1989). M6, M7, B4 and B5 were identified as Mad (M6, M7) and Brinker (B4, B5) binding sites by Rushlow et al. (2001). The oligonucleotides B4M6 and B5M7 were reported to bind Mad and Brinker competitively in mobility shift assays. B4M6 contains a putative Smad binding element, B5M7 a putative Brinker binding site.

Competition of Brinker and Smads at the same binding sites has been previously demonstrated in detail for two enhancers: the *Ubx* midgut enhancer (Kirkpatrick et al., 2001) and the *zen* enhancer (Rushlow et al., 2001). In both studies recombinant tagged proteins were used for supershift assays. Since the sequences used by Rushlow and co-workers do not contain any GRCGNC motif (Fig. 6.17) but are reported to bind Mad, we tried to reproduce these results. At the same time we intended to redo the binding experiments from Kirkpatrick and co-workers. To see whether we were able to correctly predict the Brinker/Mad binding sites, we also introduced different mutations.
The Dpp response element in the *Ubx* enhancer contains three potential Brinker sites; one of it fulfills also the Mad site consensus sequence GRCGNC (Fig. 6.18). No palindromic GGCGCC site can be found. Only mutagenesis of all three sites completely disrupts Brinker binding (Fig. 6.19). Compared to the *dad* enhancer, Mad and Medea bind only weakly to this enhancer (note the exposure time of one week).

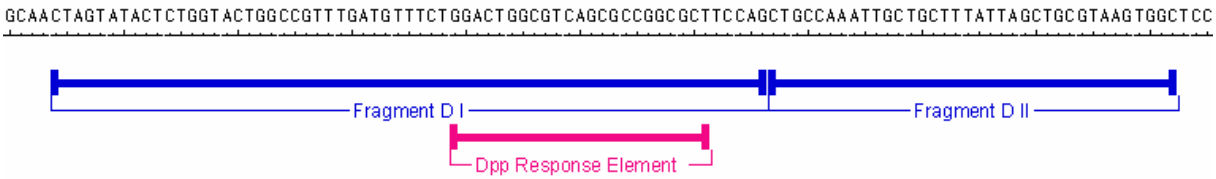


```
Ubx Dpp RE       GGACTGGCGTCAGCGCCGGCGCTTCCAG
m1               -------at-------------------
m2               -------------at-------------
m3               -------------------at-------
```

Figure 6.18
Sequence of the Dpp response element identified in the *Ubx* enhancer. Fragments D I and D II refer to nomenclature in the original documentation of the Ubx midgut enhancer (Thuringer et al., 1993). Kirkpatrick et al. (2001) tested the Dpp response element in mobility shift assays for competitive binding of Brinker and Smads. In our attempts to reproduce these results, we additionally examined mutations affecting the putative Mad (red box) and Brinker (green box) binding sites.

The two sequences from the *zen* enhancer contain no putative Mad binding sites. ZenB4M6 only carries a Smad-binding element and ZenB5M7 a possible Brinker binding site. Figure 6.19 shows that Brinker binds extremely poorly to the two oligonucleotides. No Mad binding could be visualized, only Medea bound to ZenB4M6. This is in accordance with our expectations but in sharp contrast with the results published by Rushlow and co-workers (Rushlow et al., 2001).

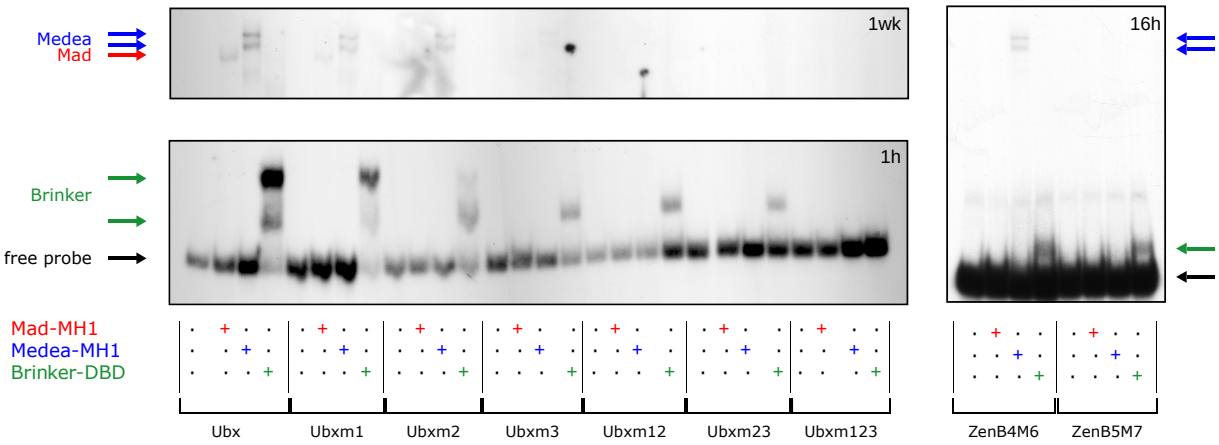

Figure 6.19
Brinker/Smad binding to the *Ubx* and *zen* enhancer. Brinker binds strongly and multiply to the *Ubx* enhancer. Testing of the different mutated versions of the enhancer construct revealed that Brinker binding is completely abolished only by a triple mutation. Mad and Medea seem to interact only weakly, the result of the mutant constructs is not conclusive and implies a binding restricted not only to a single site. Binding of Brinker to the *zen* enhancer constructs is poor. No Mad binding could be detected, only Medea in the case of B4M6.

6.3.4 Converting Mad/Brinker sites into exclusive Mad sites

All Brinker binding sites in the minimal *dad* enhancer are also putative Mad binding sites. Our mutagenesis experiments revealed that only two of them bind Mad strongly *in vitro* (compare Figures 6.14 and 6.15). Since Mad and Brinker bind to very similar, but not completely overlapping consensus sequences, it was tempting to test whether it was possible to convert a Brinker/Mad site into an exclusive Mad site.

6.3.4.1 Definition of the Brinker site

In an initial experiment we attempted to better characterize the published Brinker binding site (T)GGCGYY (Sivasankaran et al., 2000; Zhang et al., 2001). We chose to perform a competitive shift assay using the perfect palindromic site TGGCGCCA and mutant oligonucleotides as “cold” competitors (Fig. 6.20). The intensity of the bands was measured using the software ImageJ (Abramoff et al., 2004) and the ratio of bound to unbound DNA was calculated.

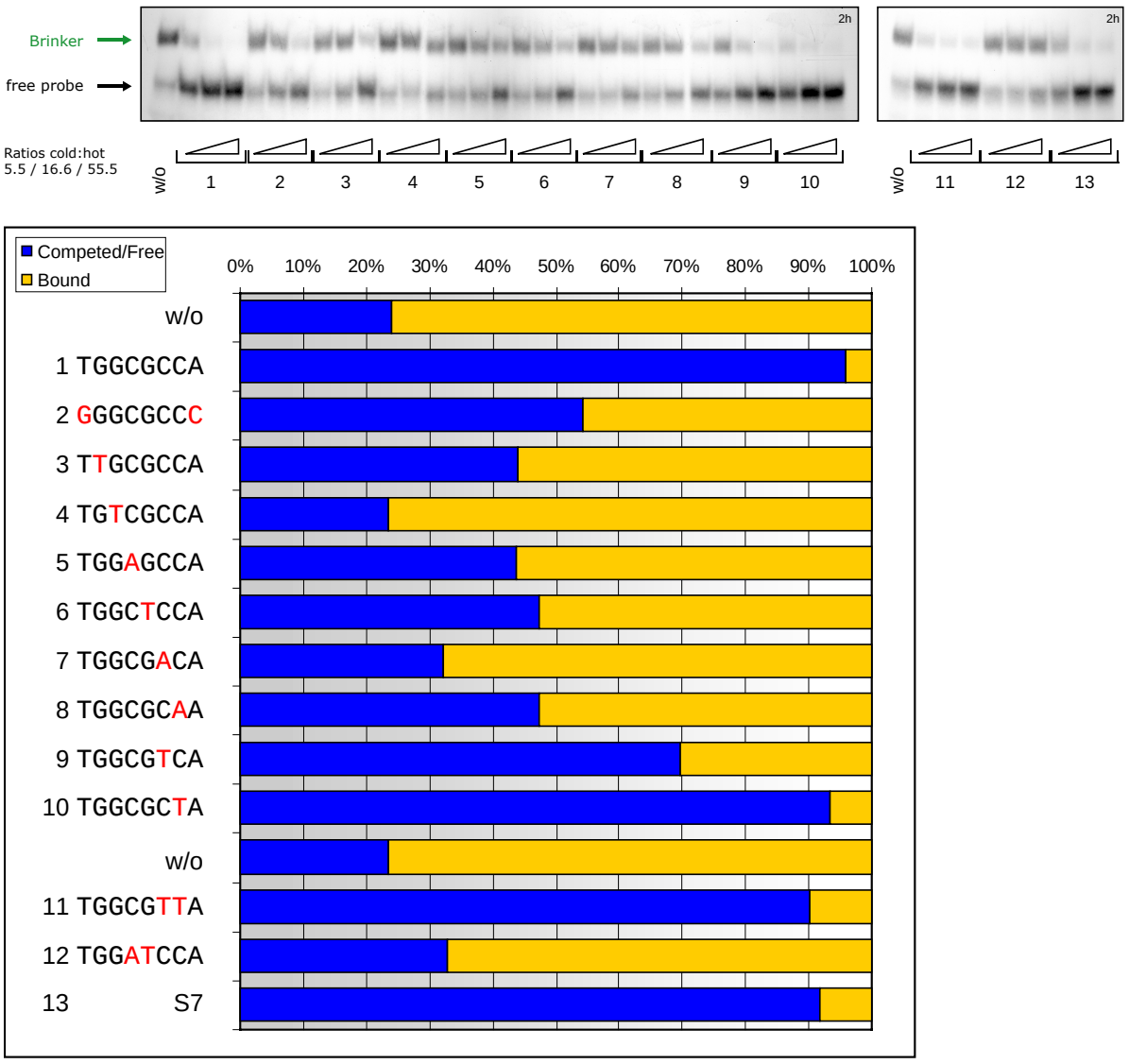

Figure 6.20
Quantification of Brinker binding. The double-stranded oligonucleotide aattCTACATGGCGCCAGTGATaatt was used in a competitive shift assay with increasing amounts of unlabelled competitors and constant amounts of Brinker DNA binding domain. For evaluation, the ratio of 16.6 of cold to hot competitor was chosen. The intensity of the shifted and non-shifted bands was measured. Highest ratios were determined for the perfectly palindromic sequence (1) and two variants (10, 11). Oligo S7, containing one putative Brinker site from Dad13, showed comparable binding.

The palindromic sequence TGGCGCCA, which can be found in two of three Brinker binding sites within the *dad* minimal enhancer, showed the highest binding efficiency. Oligo S7 from the *dad* enhancer that contains a perfect Brinker binding site showed a comparable binding efficiency. Mutations within the invariant region of the consensus sequence strongly reduced the binding efficiency. Interestingly, mutating the flanking nucleotides T and A (No 2 in Fig. 6.20) led to a strong reduction in binding, confirming the findings of Zhang and co-workers who published the consensus sequence TGGCGYY with a 5' T (Zhang et al., 2001).

6.3.4.2 Mutation of the binding sites

To convert the Brinker/Mad sites to exclusive Mad sites, we chose the constructs S3 and S4 and mutated the sequence GGCGCC to GaCGtC. This new sequence would still fulfill the Mad consensus sequence GRCGNC, but not the Brinker consensus sequence GGCGYY anymore. When subjected to a shift assay, the mutant oligonucleotides indeed did not recruit Brinker anymore, but were still capable of binding to Mad and Medea (Fig. 6.21)

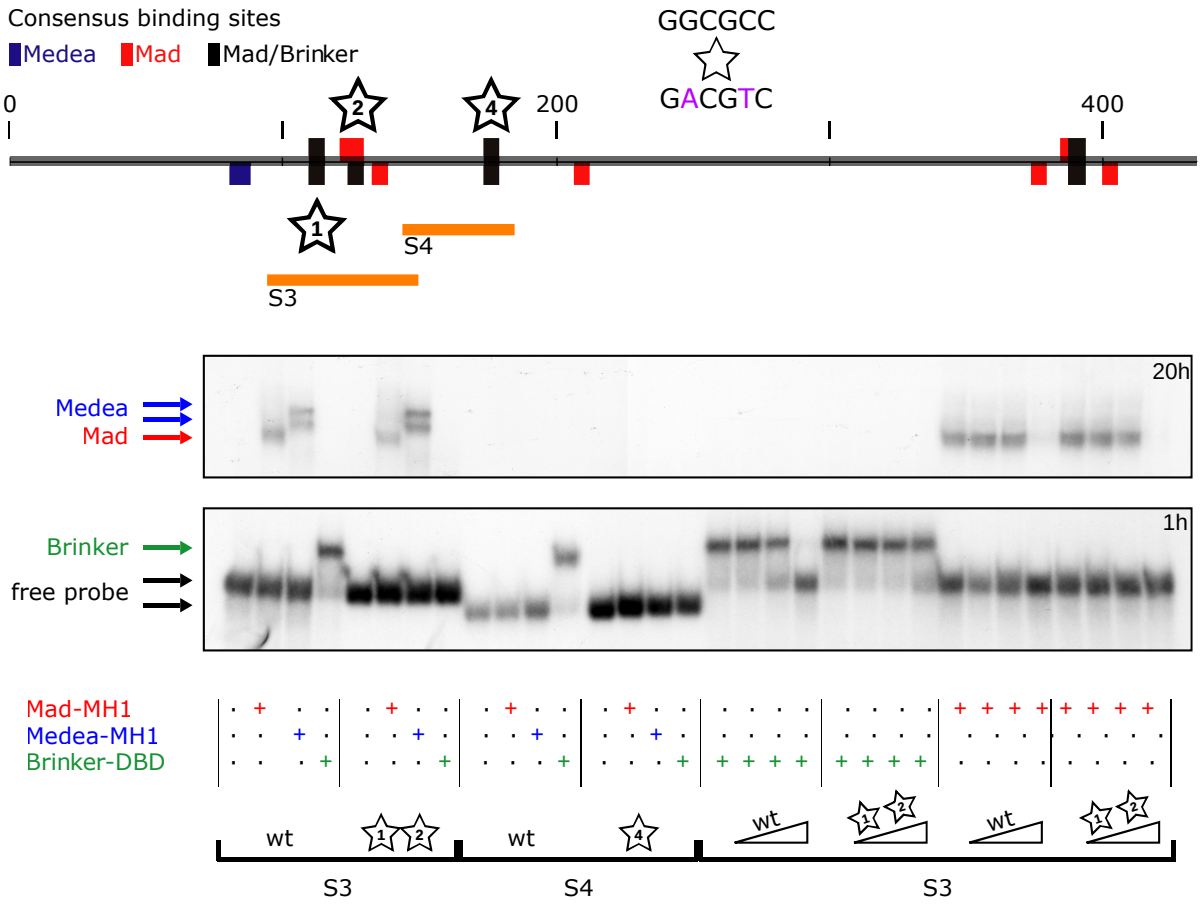

Figure 6.21
Brinker/Mad sites can be converted into sole Mad sites. Mutation of the Brinker binding site GGCGCC to GACGTC abolishes Brinker binding completely for S3 and S4. Mad and Medea binding behavior is unaltered. This result is confirmed in a competitive assay where increasing amounts of unlabelled S3 wild type oligonucleotide can compete away Brinker, whereas the mutated form cannot.

6.3.5 A complex of full length Mad/Medea proteins is recruited onto the enhancer

Binding studies of BMP responsive enhancers and Smad proteins are in most cases not performed with full length proteins but with bacterially expressed DNA binding MH1 domains. The MH1 domain of Smads binds to a small so-called Smad binding element (SBE), GTCT. However, the MH1 domain interacts mainly with the two G residues (one on the other strand) and allows some flexibility for the other bases (Shi et al., 1998; Zawel et al., 1998). The consequence is a quite versatile binding behavior which does not necessarily allow conclusions for the *in vivo* situation, where Smad proteins bind in a cooperative complex with other factors. Furthermore, full length proteins demonstrate an autoinhibitory function, thus restricting the binding activity of the MH1 domain by the MH2 domain (Hata et al., 1997). Only few enhancers so far have been shown to bind a complex of full length Mad and Medea, namely the *brinker*, *bam* and *gooseberry* enhancers (Gao et al., 2005; Müller et al., 2003; Pyrowolakis et al., 2004). To test whether also the *dad* enhancer harbors such high affinity sites, we transfected tissue culture cells with plasmids encoding Mad, Medea and the constitutively active Type I receptor Thickveins^{QD} (Tkv^{QD}) and used the cell extracts for mobility shift experiments. We found that S3 and S7 (containing the two major Mad sites) were able to recruit a complex of Mad and Medea (Fig. 6.22). In the case of S3, this interaction was only visible upon co-transfection of all three proteins (Fig. 6.23). Mad as well as Medea alone was not able to bind, independent of the co-transfection of Tkv^{QD}.

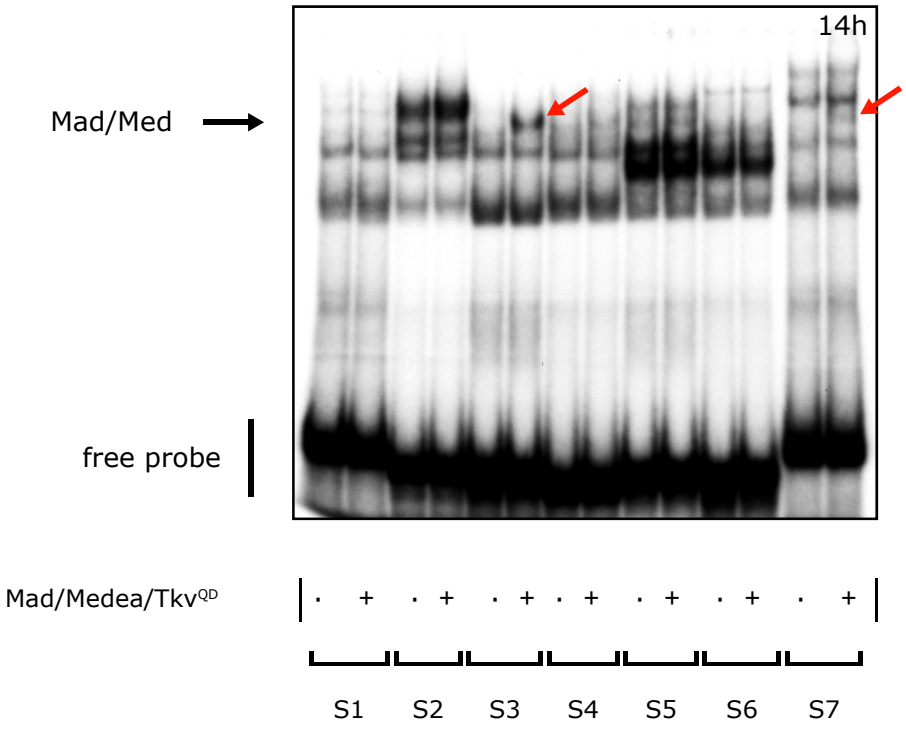

Figure 6.22
Mad/Medea complex formation. The constructs S1 to S7 from the Dad13 minimal enhancer were subjected to a binding assay with extracts from either S2 cells transfected with Mad/Medea/Tkv^{QD} or control cells. Formation of a specific complex was observed for S3 and S7 (red arrows).

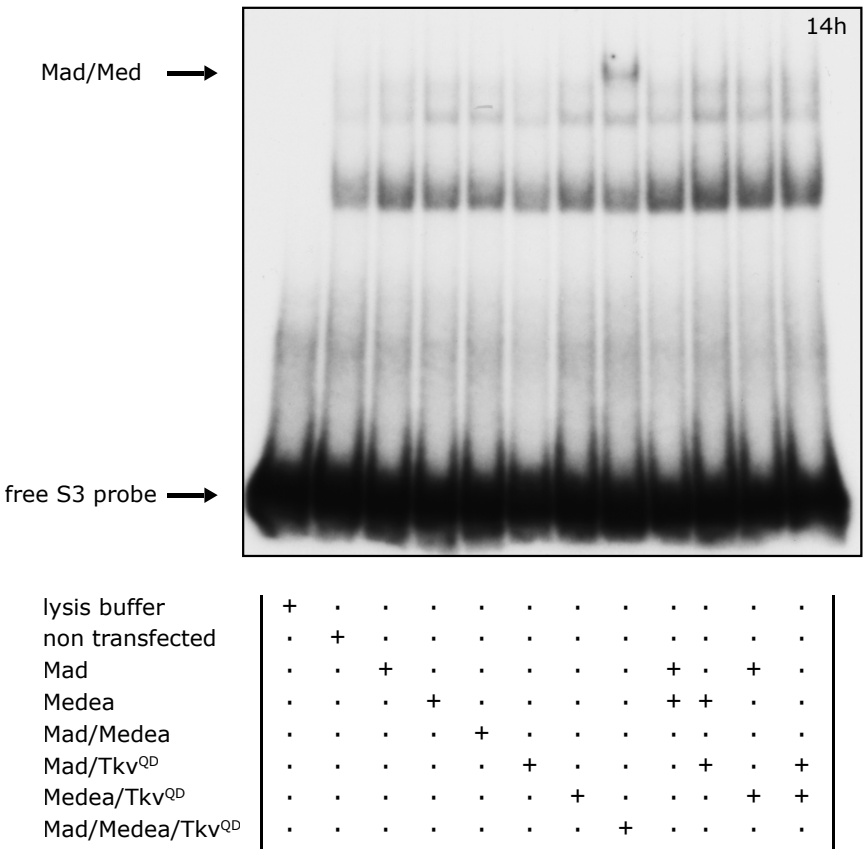

Figure 6.23
Requirements for Mad/Medea complex formation. Different combinations of transfected proteins were tested for complex formation. Only when Mad, Medea and Tkv^{QD} were expressed within the same cells, a mobility shift was observed for the respective lysates. Addition of separately transfected Medea lysates to Mad/Tkv^{QD} lysates, for example, was not sufficient for complex formation.

6.3.6 Identification of the minimal element that is able to recruit Mad/Medea

After having identified two Dad13 subconstructs carrying binding sites for a Mad/Medea complex, we sought to further define the sequences responsible for Smad recruiting. For that purpose we focused on S3. In a first attempt we tested the constructs used in Fig. 6.14, where two Mad/Brinker sites were destroyed. As can be seen in Fig. 6.24, mutation of the first Mad site is sufficient to completely abolish Mad/Medea complex formation, whereas destruction of the second putative Mad site does not influence Smad binding. In the next steps we successively cropped S3 while checking whether Mad and Medea were still able to bind.

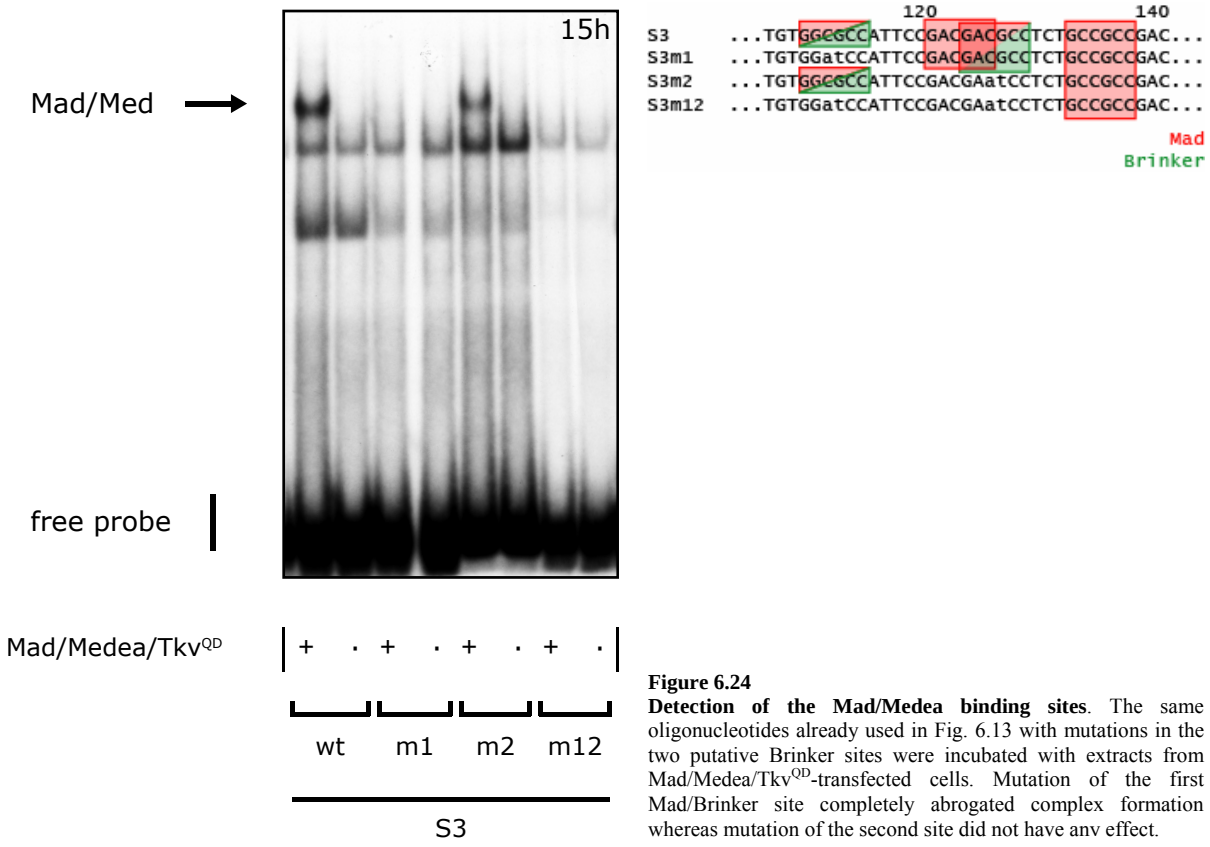

Figure 6.24
Detection of the Mad/Medea binding sites. The same oligonucleotides already used in Fig. 6.13 with mutations in the two putative Brinker sites were incubated with extracts from Mad/Medea/Tkv^{QD}-transfected cells. Mutation of the first Mad/Brinker site completely abrogated complex formation whereas mutation of the second site did not have anv effect.

In the process of dissection we first removed nucleotides adjacent to the putative binding sites (compare sequences in Fig. 6.25). The resulting constructs were still able to recruit Smad complexes, also after removal of the 3' most putative Mad site (S3xxs). Further analysis revealed a minimal fragment still suitable for complex formation: S3xxs6. Smaller constructs still showed weak binding. It remains possible that they were simply too small for effective interactions and that the composition of the flanking nucleotides was of no importance. Later experiments confirmed this theory.
An alternative subconstruct of S3 excluding the 5' most Brinker site (S3xxsb) did not show any Mad/Medea binding (Fig. 6.25).

Since S7 also showed Mad/Medea binding (though weaker than S3), we also tested two subconstructs, S7xxs and S7xxsb (Fig. 6.25; data not shown). Both were able to form a complex with Mad and Medea. Sequence alignment with positively tested S3 subconstructs reveals a similar configuration of putative Smad binding sites, with slight differences. S7xxs exhibits a different arrangement of the Mad/Brinker sites; one main difference in S7xxb is the prolonged linker of six nucleotides between the putative Mad sites.

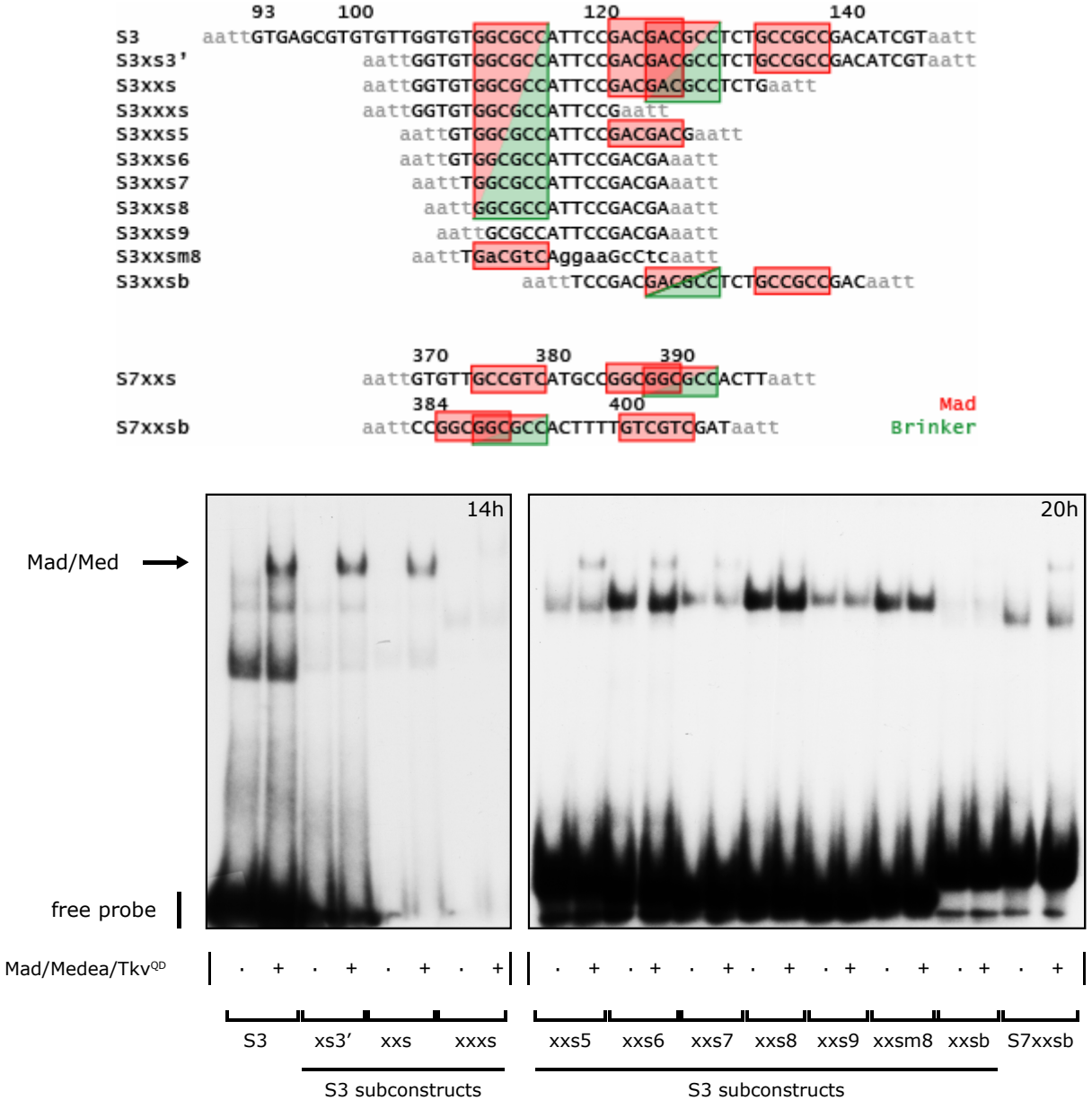

Figure 6.25
Identification of a minimal binding element. S3 was successively shortened and tested for binding of Mad/Medea/Tkv^{QD} cell lysates. A construct as small as S3xxs6, including a full Mad/Brinker site and a partial Mad site, was still able to recruit Smad proteins. Rough analysis of S7 revealed the existence of at least two binding elements with a similar arrangement of putative Mad binding sites, one in S7xxs and one in S7xxsb (data for S7xxs not shown).

6.3.7 The minimal Mad/Medea binding element resembles the SE

After having defined a minimal Mad/Medea binding element in the *dad* enhancer, it became obvious that this element showed great homology with another well-characterized Dpp response element, the Silencer Element (SE) (Pyrowolakis et al., 2004). The "red" and "blue box" of the SE, recruiting two Mad proteins and one Medea protein, respectively (Gao et al., 2005), find their counterparts in the S3xxs6 construct (Fig. 6.26). All GNC motifs shown to be important for Smad binding (Shi et al., 1998; Zawel et al., 1998) are conserved, as well as the length of the linker. The main differences are the lack of the second T in the blue box of S3xxs6, that has been shown to be important for the recruitment of the repressor Schnurri (Pyrowolakis et al., 2004), and the fact that S3xxs6 is also able to recruit Brinker.

Figure 6.26
Comparison of the minimal element able to bind Mad and Medea with the Silencer Element (SE). The so-called "red box" binds two Mad proteins whereas the "blue box" binds one Medea molecule.

6.3.8 Definition of the AE consensus sequence

Since the identified minimal *dad* Dpp response element resembled so closely the Silencer Element, we termed it Activating Element (AE). To test whether similar consensus restrictions applied to the AE, we single point mutated every nucleotide within the AE from a pyrimidine to a purine base (and vice versa) of the other base pair (e.g. C to A and G to T). The mutated constructs were then used in a competition assay with the labeled wild type oligonucleotide (Fig. 6.27). The outcome widely reflected the results of Pyrowolakis et al. (2004), who did a similar experiment for the determination of the SE consensus sequence. Whereas mutating nucleotides of the red box (except of the second position) and the blue box reduced the binding strength to different extents, mutations of the linker region had no effect on Mad/Medea recruitment. Variation of the linker length still allowed for complex formation, albeit with different efficiencies. An oligonucleotide with a four base linker, for example, proved to be a worse competitor than one with a six base linker, which bound as strong as the wild type oligonucleotide.
Since the AEs within the *dad* enhancer are also able to recruit Brinker, we chose the sequence GGCGCCANNNNGNCV as a working consensus sequence, thereby merging the AE consensus sequence elaborated in Fig. 6.27, the perfect Brinker binding site GGCGCCA and the fact that Schnurri should not be able to bind (thus the V, meaning any nucleotide except T).

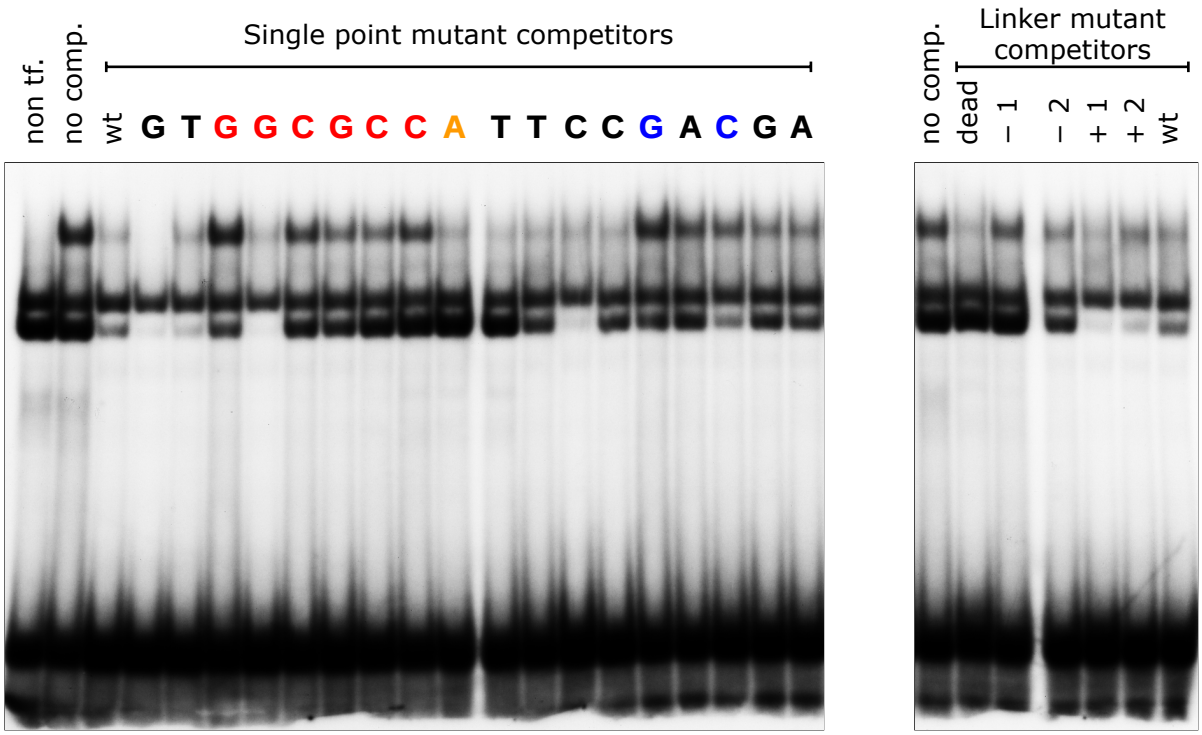

Figure 6.27
Definition of the AE consensus sequence. Radioactively labeled wild type oligonucleotide of the sequence above was subjected to a competitive assay with different "cold" point mutated probes and lysates from Mad/Medea/Tkv^{QD} transfected cells (first lane non-transfected cells as control). Mutations were G to T, C to A and vice versa. Furthermore, oligonucleotides were tested where the linker sequence (ATTCC) had been modified by either complete mutation (dead) or variation of the length (-1 to +2).

6.3.9 Testing of the *spalt* and *Ubx* enhancers for Mad/Medea complex formation

The homeotic gene *spalt* is one of the better characterized targets of Dpp signaling in the wing imaginal disc. The *spalt* enhancer upstream of the transcription start (Kuhnlein et al., 1997) has been shown to be regulated by several transcription factors including Smads (Barrio and de Celis, 2004; Galant et al., 2002; Guss et al., 2001). Recently, it has been reported that a complex of Ubx, Mad/Medea and Schnurri is responsible for Dpp dependent repression of the *spalt* enhancer in the haltere imaginal disc (Walsh and Carroll, 2007), implying a conformation similar to that on the Silencer Element (and thus the Activating Element). For this reason we tested the published construct for Mad/Medea binding. Furthermore, we tested the Dpp response element from the *Ubx* enhancer (compare Figures 6.18 and 6.19), since this has been shown to be regulated by a similar Brinker/Mad competitive binding (Kirkpatrick et al., 2001). Both constructs fulfill neither consensus sequences for the AE nor for the SE. Consequently, neither construct was able to induce a supershift when incubated with extracts from Mad/Medea/Tkv^{QD}-transfected cells (Fig. 6.28), suggesting a different Smad binding mechanism for these two Dpp-activated enhancers.

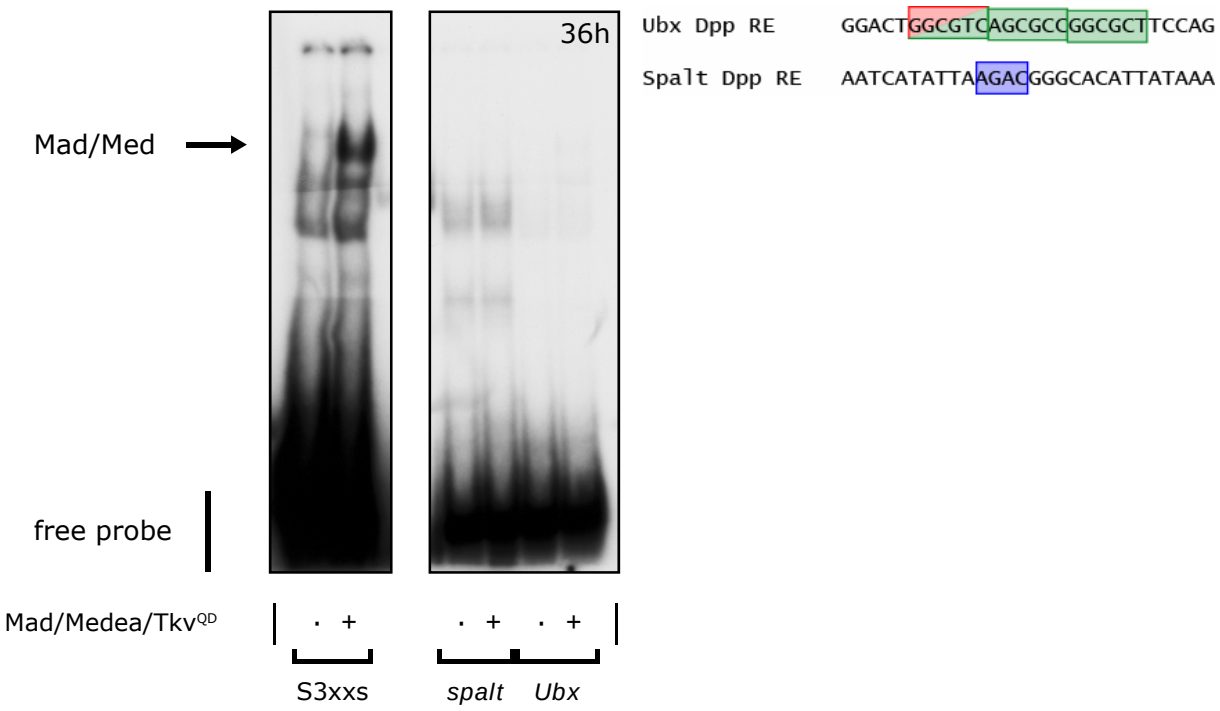

Figure 6.28
Testing of other elements potentially forming a Mad/Medea complex. Dpp response elements from the *Ubx* and *spalt* enhancer were tested for Mad/Medea recruitment. S3xxs served as a positive control. The Ubx element contains three putative Brinker sites, one of them also a potential Mad site. Sequence analysis for the *spalt* element revealed only a Smad binding element (blue), however weak binding of the Mad MH1 domain has been reported (Walsh and Carroll, 2007). No supershifts were induced for both the *Ubx* and *spalt* element.

6.3.10 Confirmation of the transcription factor binding sites *in vivo*

Having defined the sites of repressive Brinker input and activating Mad/Medea input *in vitro*, our next aim was to analyze the activity and expression pattern of mutated forms of the *dad* enhancer in cell culture and in transgenic animals. We created several mutant versions of Dad13 to analyze different aspects of the minimal enhancer (see Fig. 6.29 for sequences): Dad13m1 included a destroyed tandem Smad binding element. In Dad13m2 the two major Brinker/Mad binding sites were destroyed, which affected the AE within S3 (position 111 to 125) and one of the two AEs within S7 (around position 390, compare Fig. 6.25). Dad13m3 was an attempt to transmutate all potential Brinker/Mad sites into exclusive Mad sites, as it was successfully done *in vitro* (see Fig. 6.21). In Dad13m4, all three sites identified as Brinker sites *in vitro* were destroyed. Dad13m5 was an alternative construct to Dad13m3 where different mutations were applied to turn Brinker/Mad sites into Brinker sites (no transgenic flies were created for this construct). In Dad13m6 finally, all important (meaning conserved and beforehand positively tested) Mad sites were mutated to ensure that all functional AEs within Dad13 were destroyed.
As shown before, Dad13 is able to strongly drive expression of a *lacZ* reporter gene in embryonic and larval tissues as well as in S2 Schneider cells upon co-transfection of plasmids encoding Thickveins^{QD}, Mad and Medea (Fig. 6.29). Destruction of the tandem Smad binding element (Dad13m1) had only little effect on the expression levels, suggesting that this site is not the most essential one for transcriptional regulation. Mutation of the two major Brinker/Mad sites (asterisks 1 and 7; Dad13m2), however, nearly entirely abolished expression in the embryo and in transfected cells. Expression in the imaginal discs was affected but not completely abrogated. Transmutation of the Brinker/Mad sites into sole Mad sites (Dad13m3) was not successful. Instead of observing an expansion of the expression domain at comparable strength (caused by elimination of the Brinker input), total expression levels were strongly reduced. This was probably due to the nature of the introduced

mutations, since complete destruction of the Brinker sites (asterisks 1, 4, 7; Dad13m4) led to an expansion of expression in the imaginal discs, although total expression levels were at the same time lower than in the wild type construct. The embryonic expression driven by Dad13m4 was weak, comparable with that of Dad13m2. Thus it seems that the expression within the embryo (and in transfected S2 cells) relies mainly on the two AEs including the two Brinker/Mad sites, whereas the expression in the imaginal discs is to a large extent based on the third AE. In Dad13m6, all putative Mad sites were mutated, including all possible AEs. Consequently, expression was nearly gone in the embryo. Also in the wing imaginal disc, expression driven by Dad13m6 was strongly reduced, though not completely abolished. The residual expression might either be due to AE-independent input (as the SBEs) or the fact, that the AEs were not sufficiently mutated. To investigate this issue, we plan to focus on the smaller construct Dad16 (see Fig. 6.5), that encompasses only the 5' cluster of Brinker/Mad binding sites. Dad16 is expressed similarly to Dad13, at only marginally lower levels (data not shown). The fact that it includes probably only one AE should facilitate mutation analysis to a large extent.

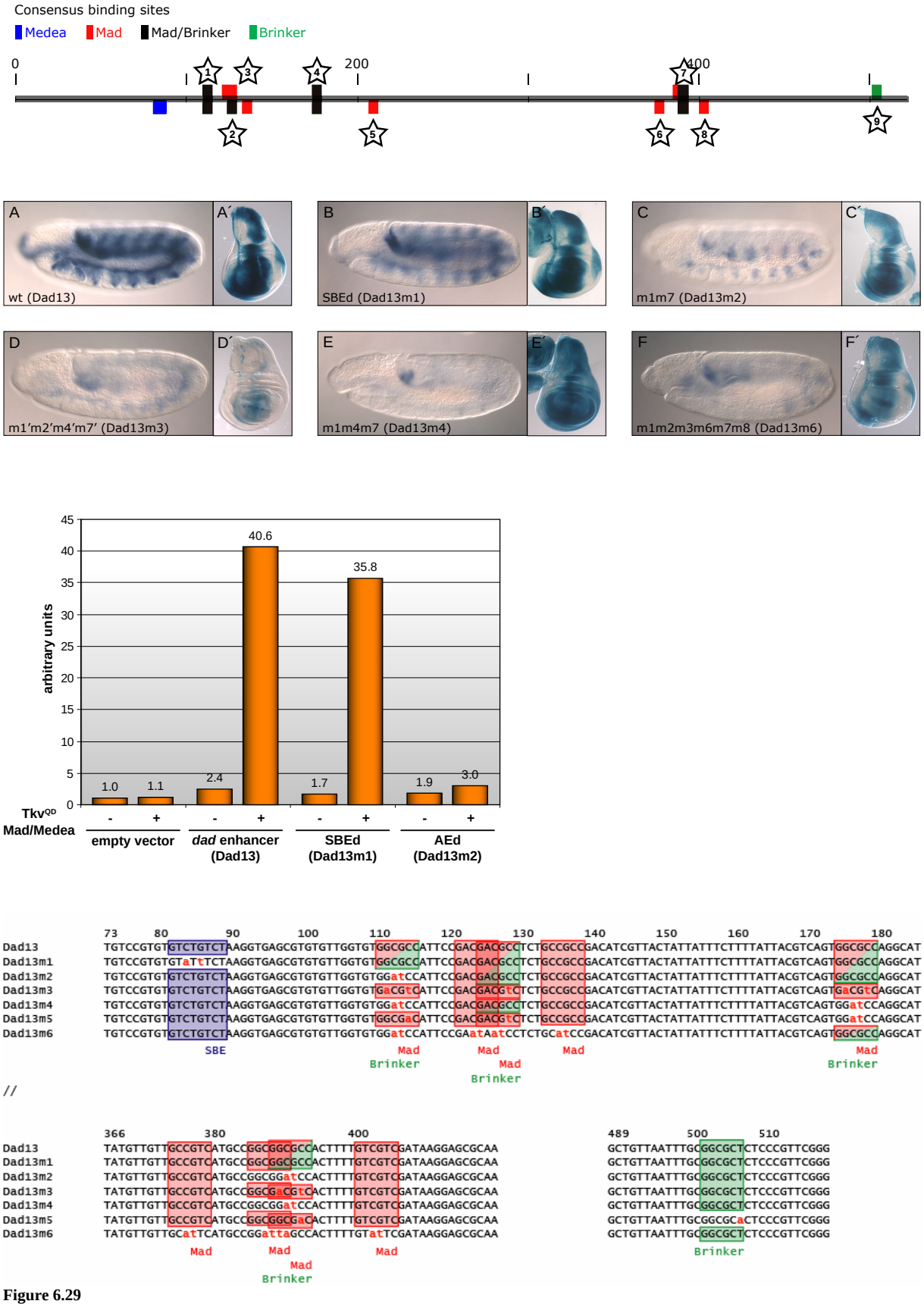

Figure 6.29

Analysis of Brinker/Smad binding sites *in vivo*. The schematic drawing of full length Dad13 shows all theoretical Brinker and Smad sites, numbered from 1 to 9. Sites 2, 4 and 7 have been shown to be Brinker sites *in vitro*. Site 2 is included in the identified AE, two more AEs were found within the cluster of sites 6 to 8 (compare Fig. 6.24). Different mutant constructs (Dad13m1 to Dad13m6) were analysed in the embryo, larval discs and by measuring the expression of βgal in transfected S2 Schneider cells. The results confirmed the *in vitro* data to a large extent. Expression in embryos and larval discs was detected by anti-βgal and XGal staining, respectively.

6.3.11 Functional dissection of the AE *in vivo*

After having discovered the AE as the activating twin of the Silencer Element and having demonstrated that it is essential for expression of the *dad* minimal enhancer, we wanted to know whether the AE was sufficient to read out Dpp signalling *in vivo*. Earlier attempts to multimerize simple Smad binding elements and thus replicate expression patterns of BMP regulated genes were not successful (Guss et al., 2001), although such constructs are generally able to confer responsiveness in cell culture experiments. This is considered as a consequence of the observation that Smad proteins normally act in concert with other transcription factors (Feng and Derynck, 2005; Shi and Massague, 2003). Furthermore, activation via Smads (as via signal-activated mediators in general) is supposed to depend on the existence of binding sites for local co-activators, a phenomenon referred to as cooperative activation (Barolo and Posakony, 2002). This made it unlikely that singular Smad binding sites outside a certain regulative context allowed for complex regulation.
However, we found that the AE binds not only a single factor but a complex of Smad proteins, which is unique and has so far not been demonstrated for any gene activated by Dpp. Since the *dad* gene follows Dpp expression closely and the existence of Mad and Medea is not restricted to specific tissues, we were tempted to speculate that the AE is sufficient to read out Dpp signalling. To determine this, we created a pentamerized version of the AE (5xAE, see Fig. 6.30), fused in front of a *lacZ* reporter. The sequence we chose was largely based on the first AE from the *dad* locus. In addition, we created three other pentamerized constructs: 5xHASE, 5xSE and 5xNASE.
HASE (Hyperactivated Activating/Silencer Element) is a mutated version of the AE with a single mutation that changed the Brinker/Mad site to a Mad site only. This construct was supposed to confer only activating Dpp responses and no Brinker input.
SE is able to recruit Mad/Medea as well as Schnurri. Binding of Schnurri depends on the second T within the GTCTG sequence (Affolter and Basler, 2007; Pyrowolakis et al., 2004). The chosen construct does not fulfill the Brinker binding consensus sequence and should thus not be able to recruit Brinker.
NASE (Nullified Activating/Silencer Element) is another chimeric construct, which includes both the nucleotides important for Schnurri binding as well as a perfect Brinker site. In other words, it possesses two potential sites for repressive input, one via Dpp signalling and one via the default repressor Brinker.
As hoped for, 5xAE was able to recapitulate the *dad* pattern in a surprisingly accurate manner in the later embryo (Fig. 6.30A). This included expression in two ectodermal stripes, in the gut as well as in anterior head structures. 5xHASE, lacking the Brinker site, was activated weaker, but much wider, in line with the expected derepression (Fig. 6.30E). 5xSE did not induce any staining at all and the same held true for 5xNASE (Fig. 6.30, I and M).
Since it had been demonstrated that the linker length does not influence Mad/Medea complex formation *in vitro*, we also tested a construct with a linker of only four nucleotides, 5xAE-1. The expression pattern induced by 5xAE-1 very much resembled that of 5xAE (Q), with only weaker expression in the two ectodermal stripes. This indicates a certain amount of flexibility for the AE also *in vivo* - unlike for the SE, which strictly depends on a linker length of five nucleotides to exert its repressive function. This is due to the requirements for Schnurri recruitment and raised the question whether changes in linker length could turn the SE into an activating motif. To investigate this, we extended the linker by one nucleotide and created the construct 5xSE2+1. Indeed, 5xSE2+1 behaved totally different from 5xSE and acted in the embryo similarly to 5xHASE (R). This demonstrates again that the SE has the intrinsic potential for activation and is repressive mainly due to recruitment of Schnurri. In addition, the results for 5xAE-1 and 5xSE2+1 suggest that Schnurri is not involved in AE-mediated

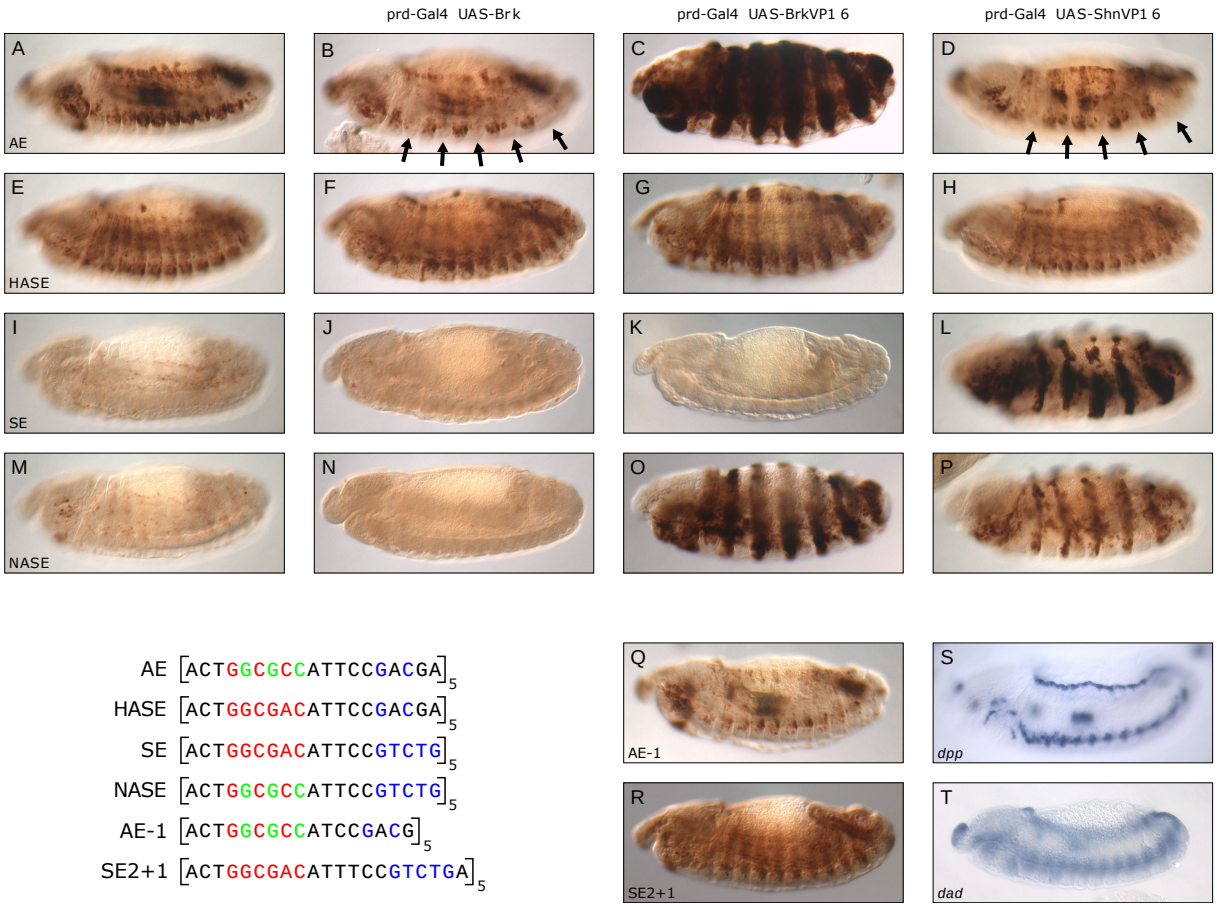

Figure 6.30
Functional dissection of the AE. Several different constructs based on the AE and the SE were oligomerized and fused to a *lacZ* reporter gene. Mad sites are depicted in red ("red box"), Brinker sites in green and Medea sites in blue ("blue box"). Expression was detected using an anti-βgal antibody. Four constructs were tested in mutant backgrounds. The first column shows the wild type expression, the second to fourth columns the situation in mutant embryos expressing Brinker, BrinkerVP16 and SchnurriVP16, respectively, under the control of the *paired* enhancer. (A to D) 5xAE, (E to H) 5xHASE, (I to L) 5xSE, (M to P) 5xNASE. Also shown is the expression of two constructs with variant linker length (Q, R). The expression patterns of *dpp* (S) and *dad* (T) (detected by *in situ* hybridization) are depicted as a comparison.

activation, or at least only by a binding mechanism completely different from that of Schnurri^{CT}.

From the outcome of our experiments so far we conclude that the AE is a Dpp dependent activating element, which also reads out repressive input via Brinker. In contrast, the SE is a purely repressive element, merely regulated by Dpp and Schnurri and not (directly) by Brinker. To prove this, we tested the behavior of the pentamerized constructs upon ectopic expression of different effectors (Fig. 6.30). Indeed, striped expression of Brinker leads to local repression of 5xAE, but not 5xHASE. Since 5xNASE, which should also be able to recruit Brinker, is already off, no effect could be seen upon expression of Brinker, as was the case for 5xSE. This reflects a general problem when searching for repressor binding sites - they can only be analysed in the context of an activator. A repressive element per se does not induce expression, thus destruction of it will not lead to visible changes. To circumvent this fundamental problem, we again made use of BrkVP16, where the repression domain of the Brinker protein was swapped with an activation domain. Striped expression of BrkVP16 not only confirmed the results of ectopic Brinker expression (strong activation of 5xAE and only very weak activation of 5xHASE), but also revealed that 5xNASE was indeed functional and able to bind the Brinker DNA binding domain *in vivo* (Fig. 6.30), as postulated.

Finally, we also tested ShnVP16, a similar fusion protein of the Schnurri^{CT} complex formation domain and the VP16 activation domain (created by Britta Hartmann). As

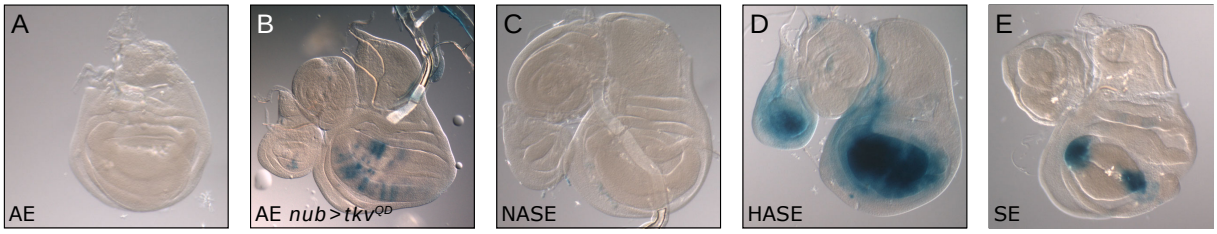

Figure 6.31
Expression of 5x constructs in the wing disc. 5xAE and 5xNASE do not induce any *lacZ* expression in the imaginal discs (A, C). However, hyperactivation of the Dpp pathway in the wing pouch (by expression of tkv^{QD} under the control of the *nubbin* enhancer) can induce *lacZ* expression at low levels (B). 5xHASE showed very strong expression in the wing pouch (D), which might be due to binding of the activator Scalloped. Consistently, 5xSE induces *lacZ* expression only in the lateral pouch regions most distant to Dpp expressing cells (E). All images show XGal stainings.

expected, only 5xSE and 5xNASE showed ectopic activation, since only they meet the requirements for Mad/Medea/Schnurri complex formation. No effect was seen for 5xHASE – unlike for 5xAE that showed local repression where ShnVP16 was expressed. This can be explained by the upregulation of *brinker* via its own endogenous SEs and again confirms the Brinker binding to the AE.
Taken these results together, we managed to dissect and separate the regulative inputs on the initially identified SE and the novel AE. With the two newly created elements HASE and NASE, we now have four different elements at hand that individually read out combinations of Smad-mediated activation (AE and HASE), Schnurri/Smad-mediated repression (SE and NASE) and Brinker-mediated repression (AE and NASE).
Our initial plan was to identify an element ubiquitously responsive to Dpp. Consequently, we examined the AE and derived constructs also in the imaginal discs. Yet, the situation in the wing disc differs dramatically from the embryo (Fig 6.31). 5xAE does not induce any expression of the *lacZ* reporter gene in the imaginal discs. However, hyperactivation of the Dpp pathway by expression of tkv^{QD} under the control of the pouch-specific *nubbin* enhancer is sufficient to generate low levels of expression. This indicates that the 5xAE is in principle functional also in the wing disc. As it was expected, also for 5xNASE no expression could be detected. But surprisingly, 5xHASE (that differs from 5xAE by only five times a single nucleotide) induced a strong expression in the wing pouch. This drastic change in expression could hardly be explained by removal of the Brinker binding site. A closer look at 5xHASE revealed, that it fulfills to a large extend the consensus binding sequence of the pouch-specific activator Scalloped (Fig 6.32), a TEA-domain transcription factor (Campbell et al., 1992) reported to bind in complex with Vestigial to wing-specific enhancers (Halder and Carroll, 2001; Halder et al., 1998). It now has to be examined whether Scalloped is also important for regulation of the "wild type" sequence 5xAE and the *dad* enhancer. 5xSE shows expression only in the most lateral regions of the wing pouch, which can be easily explained by activation analogous to 5xHASE and repression within the Dpp domain. However, 5xSE2+1, with an extended linker and an additional nucleotide in the putative Scalloped binding site, does not show any expression in the imaginal discs (data not shown). This might be caused by impaired Scalloped binding. To further investigate this issue, our next step will be to mutate the linker composition of 5xHASE and analyse the effect on expression in the wing disc.

Figure 6.32
Comparison of AE, HASE, SE2+1 and the Scalloped binding site. Six (AE) and seven (HASE) out of nine nucleotides fulfill the Scalopped binding site (SBS) published by Halder et al. (1998). SE2+1 does not, due to the introduced linker mutation.

6.3.12 Search for co-activators acting on the AE

The question remains whether Mad/Medea recruit any co-activator to the AE in order to activate gene expression. One possibility to address this issue is an approach based on mass spectrometry. To test the feasibility of this task, we performed a test experiment. Biotinylated 3xAE bound to Streptavidin Sepharose beads specifically co-precipitated phosphorylated Smad when incubated with extracts from HEK293 cells transfected with Mad/Medea/Tkv^{QD} (Fig. 6.33). This result suggests that it is generally possible to isolate proteins bound to the AE. The next step would be to apply lysates from *Drosophila* embryos instead of cell extracts and subject the bound and later eluted proteins to mass spectrometry.
HEK293 cells possess an active BMP pathway and it has been shown that vertebrate Smads can bind to the SE (Hartmann, 2004). Since the antibody is directed against human p-Smad, it thus can not be excluded that the specific band results from human Smad binding to the AE, either upon phosphorylation by Tkv^{QD} or by forming a complex with transfected Mad/Medea.

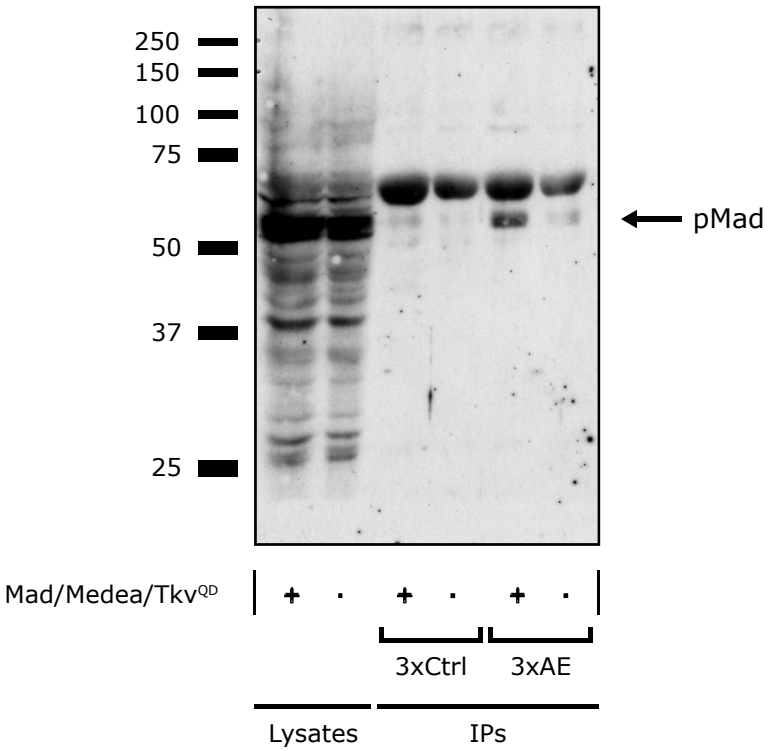

Figure 6.33
Co-precipitation of pSmad. Biotinylated 3xAE was coupled to Strepdavidin Sepharose beads, incubated with extracts from Mad/Medea/Tkv^{QD} transfected HEK293 cells and after washing subjected to SDS gel electrophoresis. pSmads were detected using an antibody directed against human phospho-Smad. Non-transfected lysates and a mutated AE served as controls.
Significant binding was only observed for 3xAE, and when effectors were transfected.

6.4 Identification of novel Dpp activated enhancers

6.4.1 *In silico* screen for AEs

To test whether functional AEs can also be found in the enhancers of other genes, we performed an *in silico* screen, taking advantage of the freely accessible research tool http://www.flyenhancer.org (Markstein et al., 2002). An initial search with the sequence GGCGCCANNNNGNCV delivered 770 hits. From these hits we picked genes that were either known to be associated with Dpp regulation or to have an expression pattern similar to that of *dad* and *dpp*. For this we consulted relevant publications and the BDGP *in situ* database at http://www.fruitfly.org (Tomancak et al., 2002). Next we checked whether the potential AEs were conserved in other *Drosophila* species, using the VISTA Genome Browser. We finally concentrated on 22 enhancer fragments with potential AEs and designed constructs of approximately 2kb, including 1kb upstream and 1kb downstream of the AE. Table 6.1 shows an overview of the constructs with length and positions within the genome annotation 4.1 (released April 2004 and used by the Flyenhancer tool and CAF1 assemblies) and the latest available annotation 5.6 (released March 2008). It also indicates whether an expression pattern was observed for the cases where transgenic flies were obtained. In addition to the potential AEs listed, we also found another putative AE in the fifth intron of the *dad* locus. In the following, we describe in some detail the results we obtained by analysing the above-mentioned enhancers.

Table 6.1 Overview of potentially AE-regulated enhancers chosen for analysis

#	Name	Start (Release 4.1)	Start (Release 5.6)	Length (kb)	Expression	
					Discs	Embryo
01	ATET	chr2L:4337609	~	2.4		
02	Bnl	chr3R:15636965	~	2		
03	Btl-1	chr3L:14036438	14064279	2.6		
04	Btl-2	chr3L:14039022	14066863	2	?	no
05	Cv2-1	chr2R:16867350	17247273	2	no	no
06	Cv2-2	chr2R:16873613	17253536	2.5	no	yes
07	Doc-1	chr3L:8988927	9008080	2.9	yes	yes
08	Doc-2	chr3L:9006231	9025384	2	yes	yes
09	Doc-3	chr3L:9011012	9030165	2	yes	yes
10	Doc-4	chr3L:9016146	9035299	1.2	yes	yes
11	Elb-1	chr2L:14400957	~	2	no	yes
12	Elb-2	chr2L:14403002	~	1.9		
13	Hiw-1	chrX:14848199	14908295	2.6	?	no
14	Hiw-2	chrX:14850771	14910867	3		
15	Hiw-3	chrX:14866918	14927014	2		
16	Hiw-4	chrX:14886905	14947001	2	?	no
17	Indy-1	chr3L:18794692	18822533	2		
18	Indy-2	chr3L:18813198	18841039	2		
19	Kni-1	chr3L:20611632	20670891	2	?	yes
20	Kni285	chr3L:20635383	20694642	2	?	yes
21	Pnr-1	chr3R:11845930	~	2	yes	yes
22	Ap	chr2R:1242540	1622657	3	no	yes

6.4.2 Crossveinless-2

Crossveinless-2 (Cv-2) is an extracellular modulator of BMP signalling (Conley et al., 2000) with high similarity to Short gastrulation (Sog), that is known to bind Dpp and other BMP-like ligands and contribute to the formation of a dorso-ventral Dpp activity gradient in the early *Drosophila* embryo (Eldar et al., 2002; Srinivasan et al., 2002). Also Cv-2 might be involved in this regulatory network (Biemar et al., 2006), its function (as the gene name implicates), however, is better analysed in the formation of the cross vein in the developing wing disc (Conley et al., 2000). Recent studies have revealed that Cv-2 works as Sog in a bi-phasic manner, promoting Dpp signalling in small concentrations and inhibiting it in high concentrations. Cv-2 is able to restrict the binding of BMP ligand to its receptor by blocking the binding sites (Zhang et al., 2008a). Furthermore, Cv-2 is able to interact with cell-surface proteins and the BMP receptors (Serpe et al., 2008). *cv-2* enhancer traps show expression along the anterior-posterior border of the wing disc and dorsal regions of leg and eye-antennal disc (Fig. 6.34; Conley et al., 2000), which overlaps with *dpp* expression domains. Furthermore, it has been shown that *cv-2* expression in the posterior cross-vein is regulated by the BMP ligand Gbb (Serpe et al., 2008). Three putative AEs were found in the *cv-2* locus, two next to the transcription start (AE6 in Fig. 6.34) and one within the largest intron (AE5). The potential AE in AE5 is perfectly conserved in *D. pseudoobscura* and *D. virilis*, one of the AEs in AE6 in *D. pseudoobscura* and partially in *D. virilis*.

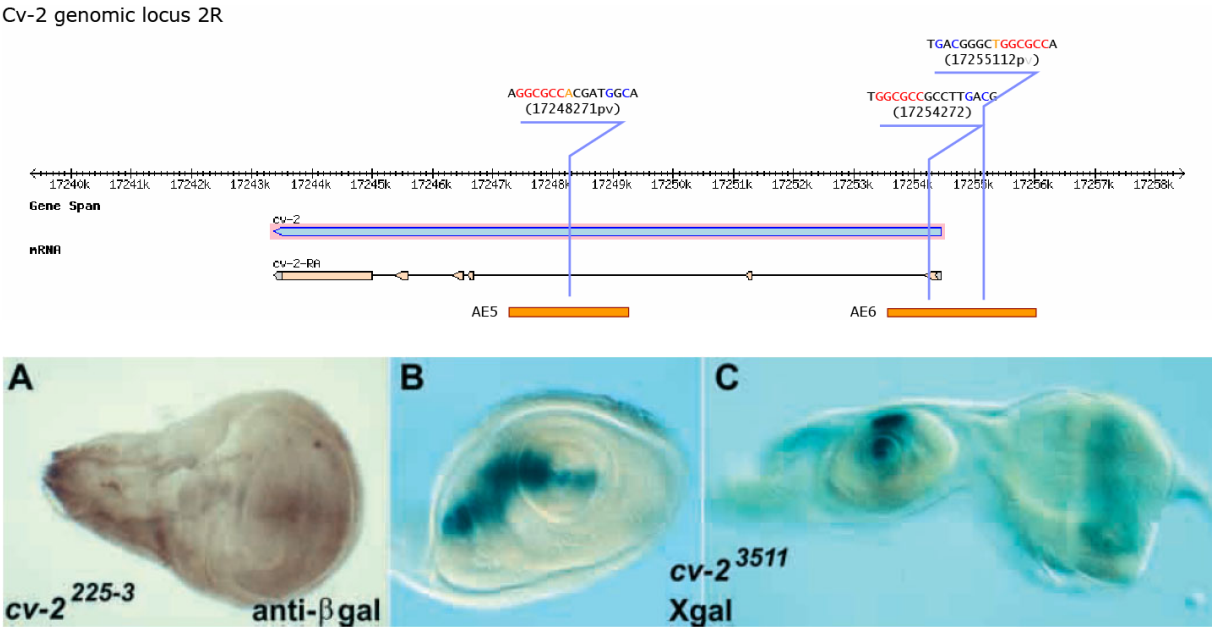

Figure 6.34
Genomic locus and expression of *cv-2*. The *cv-2* gene is located on the second chromosome. Two reporter constructs, AE5 and AE6, were designed, including three potential AEs. Two *lacZ* enhancer traps positioned in the first (3511) and second intron (225-3) show expression within the anterior-posterior border of the wing imaginal disc as well as dorsal regions of the leg and eye-antennal disc. Figures A to C adapted from Conley et al (2000).

To our disappointment, neither AE5 nor AE6 showed expression in larval imaginal discs (data not shown). For AE5, due to its high conservation a promising candidate, no specific staining could be observed in the embryo either (Fig. 6.35, G to I). This was not the case for AE6. AE6 is expressed already in the early gastrulating embryo anteriorly and in a broad dorso-lateral domain (J, K). Later, expression refines to a segmented lateral stripe and increases anteriorly (L). In the older embryo, two stripes become visible (M, N), though the specific expression in the leading edge of dorsal closure is most striking (O). To test whether the

Brinker site in AE6 was functional, we expressed BrkVP16 under the control of the *paired* enhancer. This led to an ectopic striped expression (R, S), indicating that Brinker indeed binds to AE6.

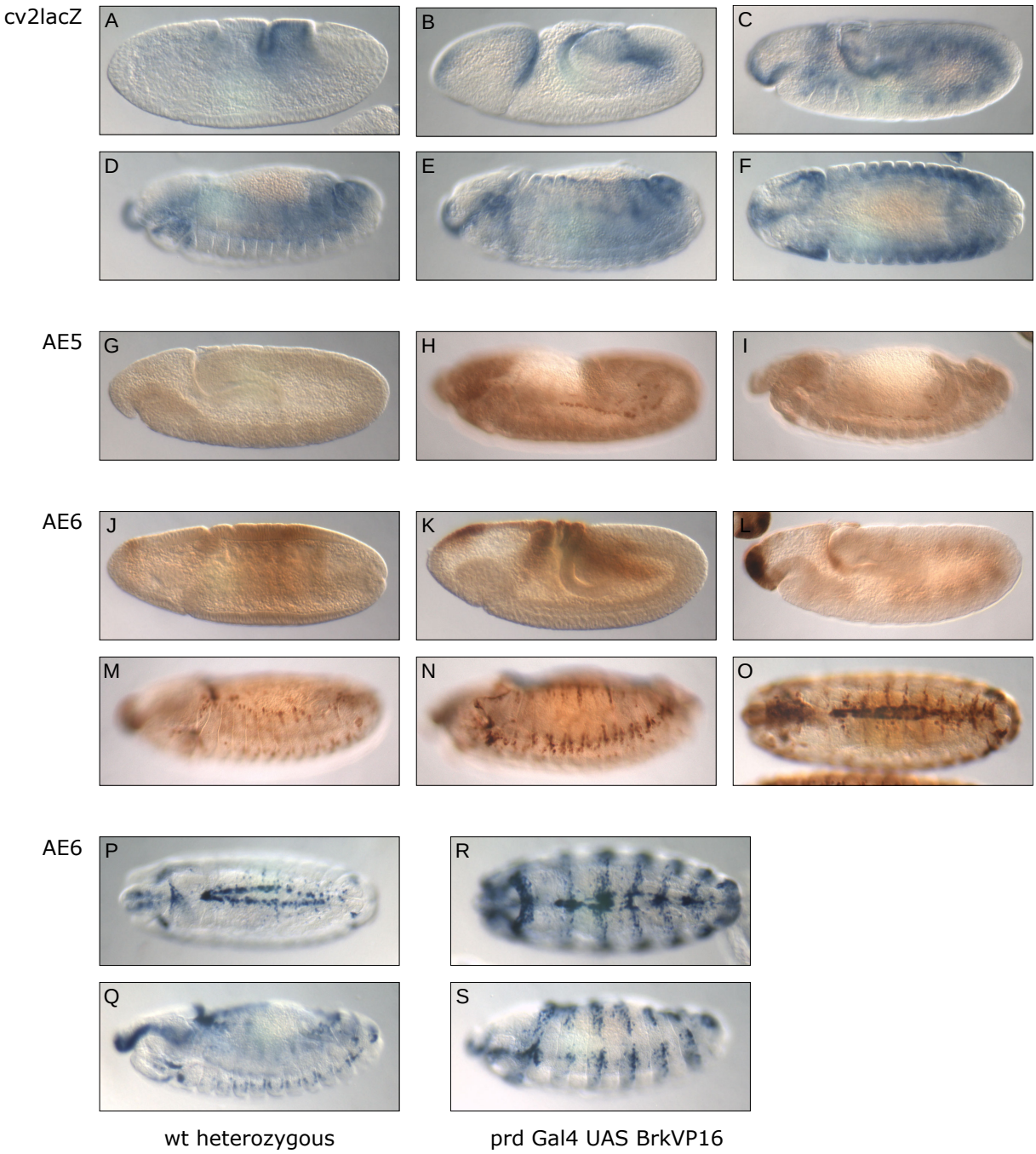

Figure 6.35
Expression of *cv-2* reporter constructs AE5/AE6 and enhancer trap. AE5 does not induce any expression in the embryo (G to I). AE6 mediated *lacZ* expression (J to O) differs in several aspects from that of the enhancer trap cv-$2^{225\text{-}3}$ (A to C). Unlike all other tested AE enhancers, AE6 induces *lacZ* expression already as early as stage 6 (J). The most prominent feature is the strong staining within the leading edge cells of the late embryo (O). Striped expression of a transgene encoding BrinkerVP16 is able to ectopically activate AE6 (R, S). All embryos were stained using an anti-βgal antibody.

6.4.3 Elbow B

The *elbow B* (*elb*) gene encodes a nuclear zinc finger protein and is expressed in the tracheal pits and later in a specific subset of tracheal cells (Dorfman et al., 2002). Embryos mutant for *elB* show a tracheal phenotype similar to that caused by defects in the Dpp pathway. However, an interaction of Dpp and Elb or a mutual dependence could not be found (Dorfman et al., 2002). Two potential AEs were identified within the largest intron of the *elB* gene, both conserved in *D. pseudoobscura*. We designed two constructs, AE11 and AE12, centered on each AE (Fig. 6.36). While expression data for AE12 is not yet available, AE11 shows a strong expression in the ectoderm and mesoderm, which initiates at the beginning of germ-band retraction. Two initially distinct stripes fuse to give rise to a wide lateral stripe that also encompasses the Brinker domain (Fig. 6.36). This was surprising. A closer look at AE11, however, revealed that the AE there carries the non-perfect Brinker site AGGCGTC, instead of (T)GGCGCC, and thus might not be sensitive to Brinker regulation. This proved to be the case - ectopic expression of both Brinker and BrinkerVP16 under the control of the *paired* enhancer had no effect on the expression of AE11. Further investigations have to be carried out, but chances are high that the AE11 thus contains a natural HASE – an AE that lacks the Brinker binding site.

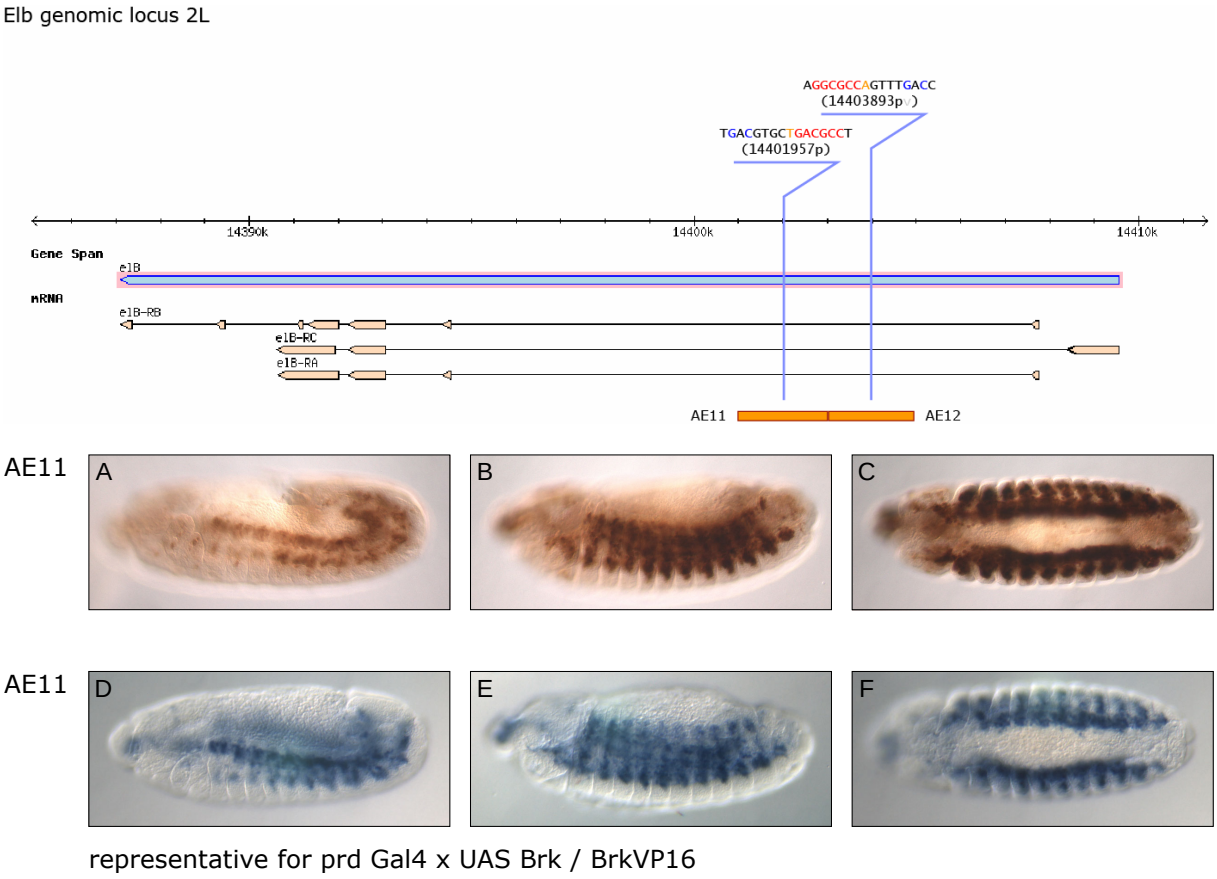

Figure 6.36
Expression of the *elB* enhancer construct AE11. After stage 10, AE11 is expressed in two distinct lateral stripes (A) that soon fuse to one wide stripe (B, C). The expression of AE11 is independent of Brinker, as shown by the ectopic expression of Brinker and BrinkerVP16 (D to F show representative embryos). All embryos were stained using an anti-βgal antibody.

6.4.4 Dorsocross

The *Dorsocross* gene cluster consists of three closely related genes (*Dorsocross1*, *Dorsocross2* and *Dorsocross3*) of redundant function that code for transcription factors of the T-box protein family. *Dorsocross* has been shown to act downstream of Dpp (Hamaguchi et al., 2004; Reim et al., 2003) and was considered a candidate for a gene directly regulated by Dpp. The gene name results from its characteristic dorsal cross-like expression in the early embryo. Later, *Dorsocross* is expressed in a fashion similar to *dad*, in two metameric stripes (Fig. 6.37). Also in the wing imaginal disc *Dorsocross* is expressed along the anterior-posterior border like *dad* (Fig. 6.37). However, expression is not continuous, since *Dorsocross* is repressed by Wingless (Reim et al., 2003). In no other genomic locus than that of *Dorsocross*, so many potential AEs were found (Fig. 6.37). We designed four constructs including five putative AEs, two constructs in the major introns of *Doc2* and *Doc3* and two within their intergenic region. All four fragments were able to activate the *lacZ* reporter gene in both embryo and imaginal discs (Fig. 6.39). None of them completely resembled endogenous *Doc* expression, which indicates a modular organization of the *Doc* enhancer. AE7 and AE10 are expressed in two lateral ectodermal stripes in the embryo, whereas AE9 displays only the more ventral stripe. AE7, AE8 and AE10 also show a very specific

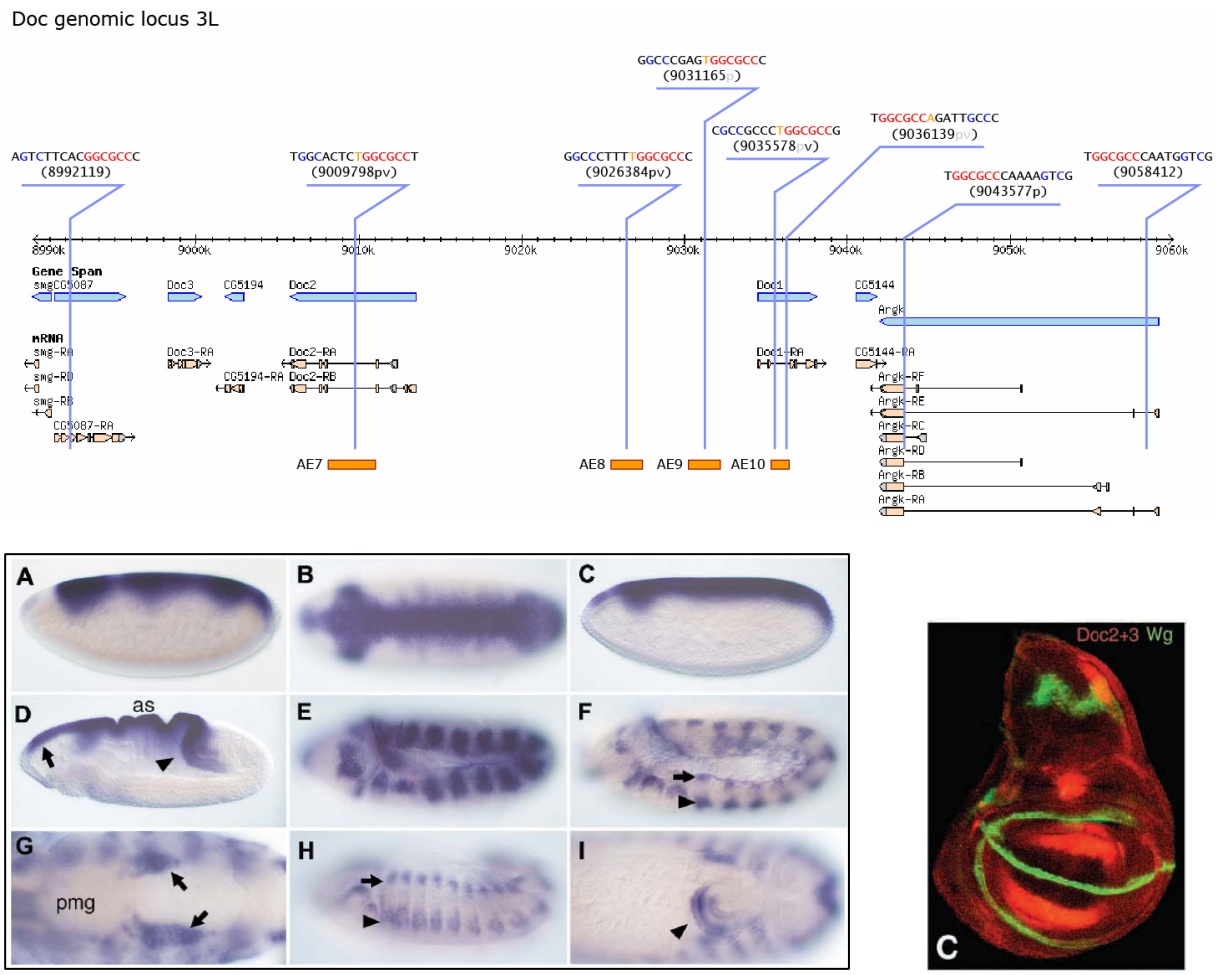

Figure 6.37
Organization of the *Dorsocross* locus and endogenous expression. The three genes *Dorsocross1*, *Dorsocross2* and *Dorsocross3* form the *Dorsocross* locus. They are expressed in a very similar pattern and show redundant function. *Dorsocross* is expressed characteristically in the early embryo in dorsal regions and later in two ectodermal stripes as well as the hindgut (*Doc1 in situ* hybridization; images adapted from Hamaguchi et al., 2004). In the wing disc Dorsocross can be detected along the anterior-posterior border with local repression within the Wingless domains (anti-Doc2+3 and anti-Wingless antibodies, image adapted from Reim et al., 2003).

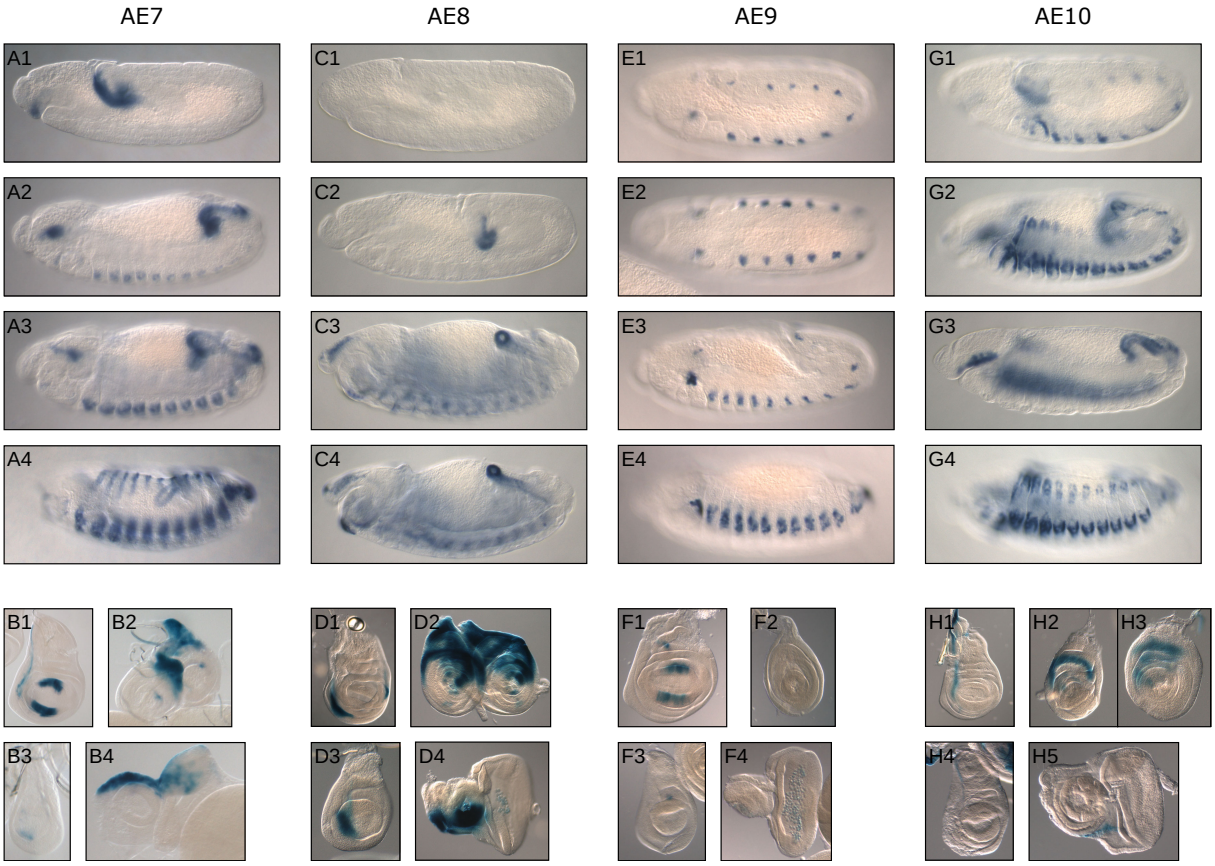

Figure 6.38
Expression of *Doc* enhancer constructs AE7 to AE10. All constructs induce expression in tissues and regions known to be exposed to Dpp signalling, in the embryo as well as larval imaginal discs. All embryos were stained using an anti-βgal antibody, expression in discs was detected by XGal stainings.

individual staining of the hindgut. In the imaginal disc, expression can be seen in dorsal domains of leg and eye-antennal disc for AE7, AE8 and AE10 and in the wing and haltere discs for AE7, AE8 and AE9.
Our next aim was to mutate the AE. By this means we hoped to abolish the activity of the enhancer constructs. As done before, the core nucleotides of the Brk/Mad site GGCGCC were mutated to GGatCC. However, no effect was seen for the two AEs tested, AE7 and AE9 (data not shown), neither in the imaginal discs nor in the embryo. Since the linker length of the AE was shown to be flexible, this could be explained with the existence of more AEs. To decrease the number of additional candidate sites we first reduced the size of AE7 from 2.9kb

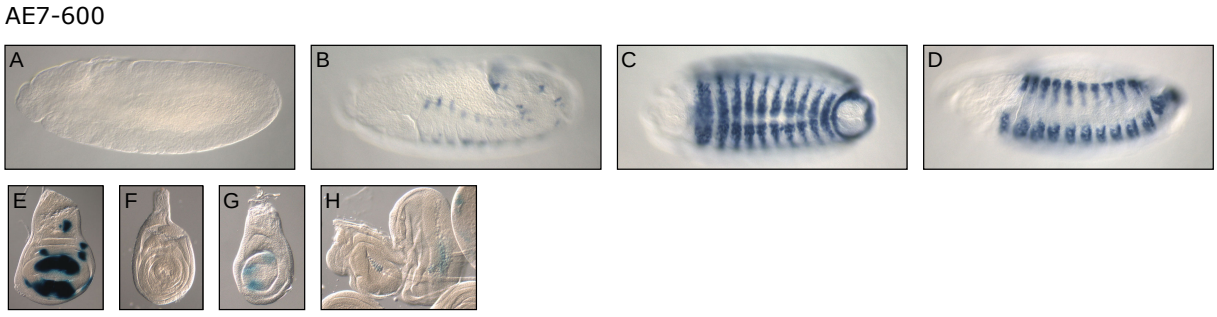

Figure 6.39
Expression of the AE7 subconstruct AE7-600. Compared to AE7, expression in leg and eye-antennal discs is lost (F to H), as well as in the embryonic hindgut (A to D). Expression in the wing dics is expanded (E). All embryos were stained using an anti-βgal antibody, discs using an XGal protocol.

to less than 600bp (position 1458 to 2038). This construct, AE7-600, differed in its expression from AE7, as it was not active anymore in the embryonic hindgut and in larval leg and eye-antennal discs (Fig. 6.39). Expression in the wing disc was expanded, suggesting the removal of repressive sites. In the embryo, the expression in two ectodermal stripes was maintained. Still, also mutation of AE7-600 did not result in changes in the wing disc expression (the analysis of the embryonic expression is pending). A look on the sequence of the AE7-600 construct revealed again the existence of further AE-like sequences (Fig. 6.40). Striking was the high number of Smad binding elements (SBEs), since the *dad* minimal enhancer only has two of them. However, only one SBE is conserved in other distantly related *Drosophila* species (Fig. 6.40). In the next step, we plan to test an even smaller construct, AE7-300, which includes the initial potential AE and excludes two other possible AEs that differ in linker length and composition of the Brinker/Mad site (Fig. 6.40).

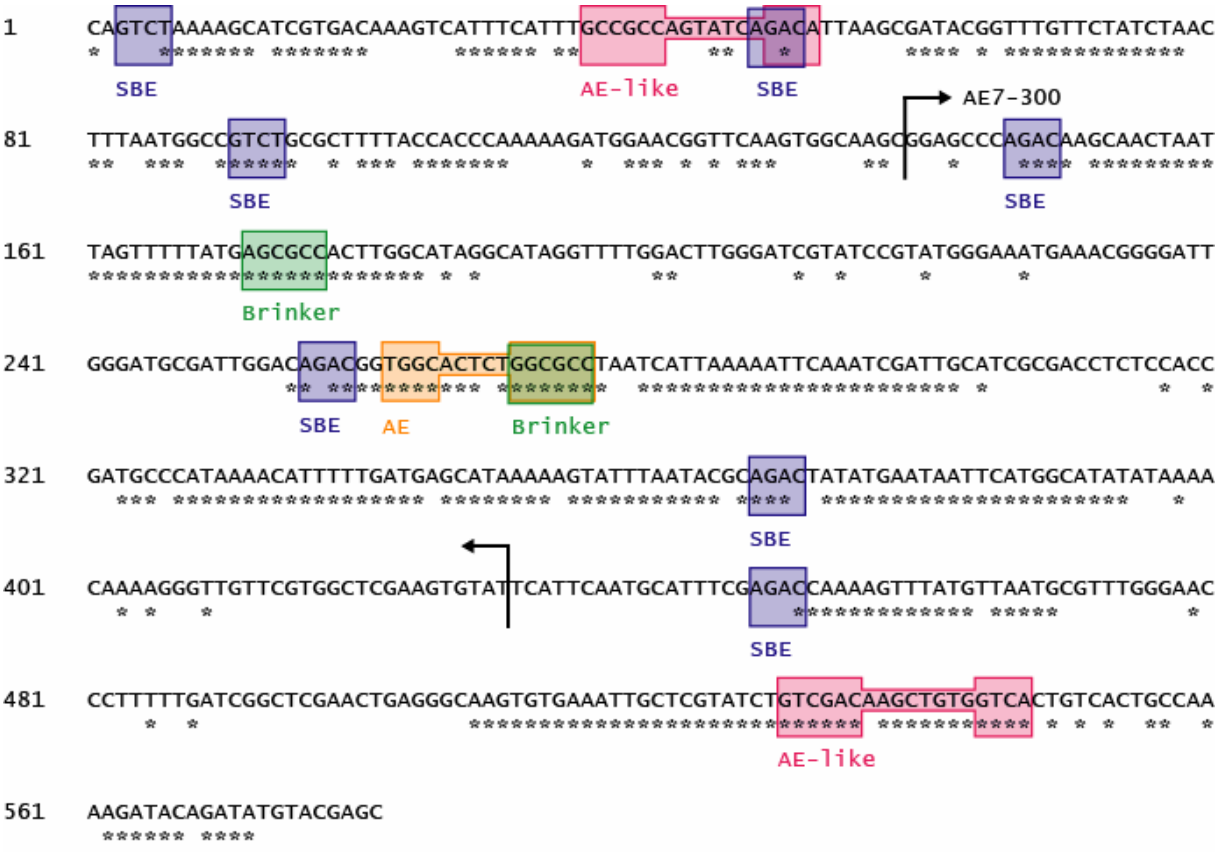

Figure 6.40
Putative transcription factor binding sites in AE7-600. The initially identified AE is depicted in orange, AE-like sequences in pink, putative Brinker sites in green and SBEs in blue. The high number of SBEs is striking and exceeds the average statistical number by three. The position of a smaller construct AE7-300 is indicated by arrows. Asterisks mark bases conserved in D. *pseudoobscura*, *mojavensis* and *virilis*. Position 1 refers to position position 1458 in AE7.

6.4.5 Knirps

The *knirps* gene belongs to the group of zygotic gap genes and encodes a zinc finger transcription factor (Rothe et al., 1989). It has been intensively studied for its role in patterning the early embryo. However, it also functions in the formation of the tracheal system later in embryogenesis, where it mediates Dpp-regulated cell migration, together with its close homolog *knirps-related* (*knrl*) (Chen et al., 1998). Two potential AEs, perfectly conserved in *D. pseudoobscura* and *D. virilis*, were found in the *kni* locus, one upstream of *kni* in proximity to the stripe-enhancer (Pankratz et al., 1992) and one between the *kni* and *knrl* genes, 18kb downstream of *kni* (Fig. 6.41). Both enhancer constructs showed trachea-specific expression. Whereas AE19 was expressed in ventral cells of the trachea placodes and branches and the visceral branch, AE20 was expressed in both dorsal and ventral cells of trachea placodes and branches. To analyse the dependence of AE20 on Smad and Brinker input, we introduced several kinds of mutations. In one construct we intended to destroy the enhancer activity by mutating the core nucleotides of the Brinker/Mad site (AE20AEd). In the second we introduced nucleotides shown to be important for Schnurri recruitment, thus transforming the AE into a repressive SE (AE20SE). The third mutation aimed to convert the

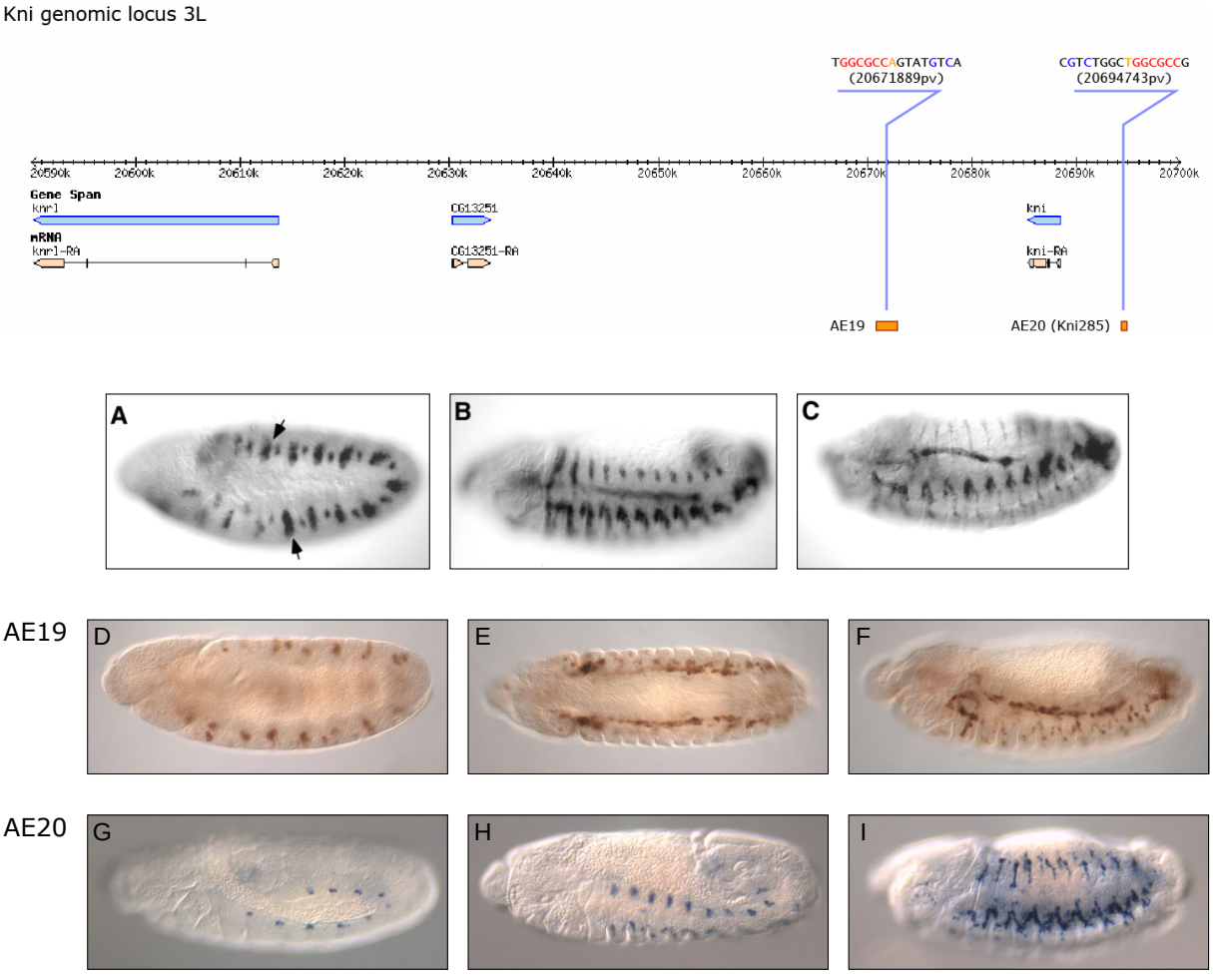

Figure 6.41
Expression of *kni* and the enhancer constructs AE19 and AE20. Two constructs AE19 and AE20 were designed, with AE20 based on unpublished data provided by Reinhard Schuh. *kni* and *knrl* are expressed in the tracheal placodes and later in the cells of dorsal, visceral, and lateral trunk and ganglionic branches (images A, B, C *kni in situ* hybridization, adapted from Chen et al., 1998). The expression patterns of AE19 and AE20 reflect aspects of the endogenous *kni* expression, with AE19 expressed in cells of the ventral placodes and branches as well as in the visceral branch, and AE20 expressed in cells of dorsal and ventral placodes and branches. All embryos were stained using an anti-βgal antibody.

putative Brinker/Mad site into an exclusive Mad binding site (AE20BtM). As seen in Figure 6.42, expression of the reporter gene was strongly reduced upon destruction of the AE (B) and completely gone when the AE was turned into an SE (C). Strikingly, our attempt to remove the Brinker input without destroying the Mad site resulted in a dramatic expansion of the expression pattern (D). Reporter expression was not only detected in the dorsal and ventral branches (though at slightly lower levels), but also in the connective trachea, as the dorsal trunk, where Brinker is active (Markus Affolter, personal communication). To further test the functionality of the Brinker binding site, we expressed the strong activator BrinkerVP16 under the control of the *paired* enhancer. The result was a striped ectopic upregulation of the wild type enhancer as well as the mutated version, where the AE was converted into an SE. This strongly indicated the existence of a Brinker binding site and demonstrated the integrity of the SE construct. Altogether, our results suggest that the AE of this enhancer is an important site for regulative activating input.

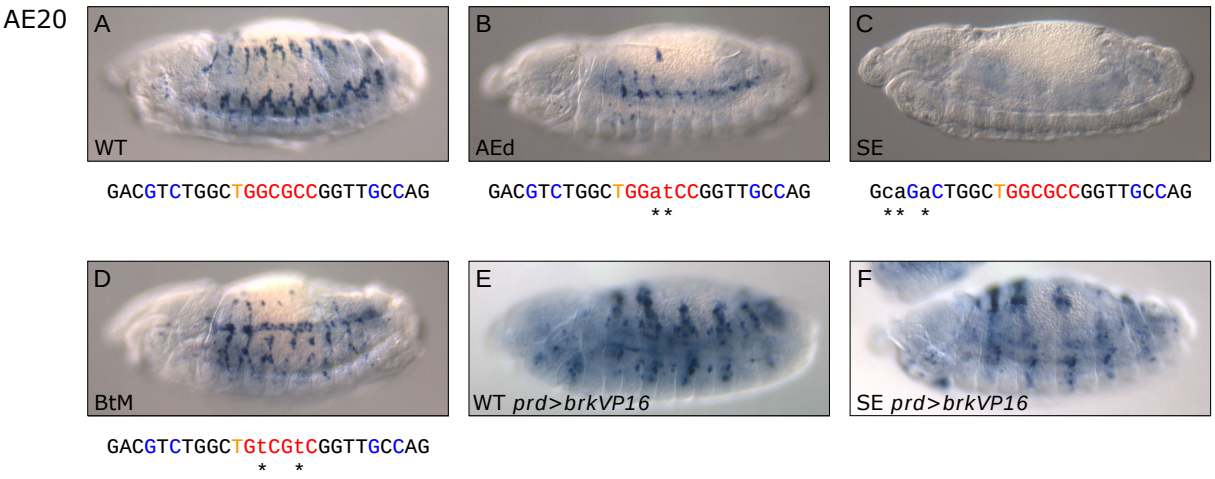

Figure 6.42
Expression of mutated forms of AE20. The AE within this only 285bp large enhancer construct was mutated in three different ways. Destruction of the AE (B) strongly reduced expression levels, while conversion of the AE into a repressive SE completely abolished them (C). Mutations that turn the Brinker/Mad site into a pure Mad site led to a drastic expansion of the staining into the dorsal trunk (D). Striped expression of BrkVP16 induced ectopic reporter gene expression in the wild type construct (E) as well as in the otherwise non-active SE construct (F). Asterisks mark mutated sites. All embryos were stained using an anti-βgal antibody.

6.4.6 Pannier

The *pannier* (*pnr*) gene encodes a zinc finger transcription factor of the GATA family (Ramain et al., 1993; Winick et al., 1993). Its function has been analysed mostly in the wing imaginal disc, where it is expressed in the presumptive notum, which forms the dorsal mesothorax of the adult fly. Within the notum, Pannier is involved in a regulatory network with Dpp, Wingless and U-Shaped (Calleja et al., 1996; Sato et al., 1999; Sato and Saigo, 2000; Tomoyasu et al., 2000), where Dpp regulates *wg* by induction of *pnr*. Overexpression of the constitutively active Dpp receptor Tkv^{QD} induces ectopic *pnr* expression, whereas expression of pannier is mostly lost in Tkv mutant clones (Sato and Saigo, 2000; Tomoyasu et al., 2000). *pnr* is also expressed in dorsal regions of the eye-antennal disc (Heitzler et al., 1996). In the embryo, *pannier* plays an important function in heart development (Gajewski et al., 1999). It is also involved in formation of dorsal ectoderm and amnioserosa (Heitzler et al., 1996; Winick et al., 1993) where it is regulated by Dpp (Ashe et al., 2000) and later itself activates *dpp* in cells necessary for dorsal closure (Herranz and Morata, 2001). Furthermore, *pnr* expression expands in early *brinker* mutant embryos (Jazwinska et al., 1999b)

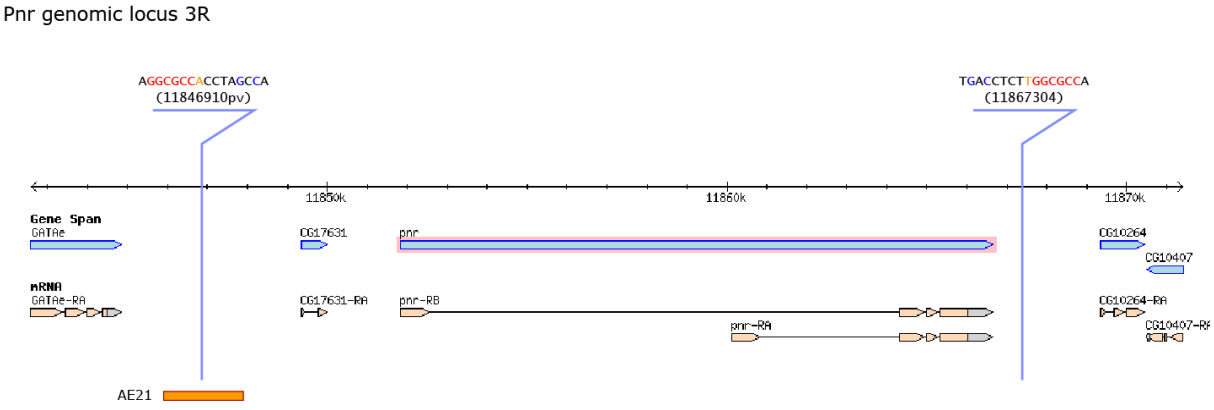

Figure 6.43
Genomic locus of *pannier*. The *pannier* gene on the third chromosome encodes for two differently regulated transcripts (Fromental-Ramain et al., 2008). Two putative AEs, were identified. The 2kb enhancer construct AE21 surrounding the better conserved AE is situated between *pnr* and the neighboring gene *GATAe*.

Two potential AEs were found in the *pannier* locus, upstream and downstream of the largest *pnr* transcript (Fig. 6.43). The first one is perfectly conserved in *D. pseudoobscura* and *D. virilis* and situated within a 5.6kb fragment shown to be genetically regulated by Dpp and to reflect several aspects of endogenous *pnr* expression in wing disc and the older embryo (Fromental-Ramain et al., 2008). Expression of the respective construct AE21 could be observed in the presumptive notum of the wing imaginal disc and in the center of the wing pouch, presumably where *dpp* and *wg* expression domains meet (Fig. 6.44). This dot-like expression does not reflect the endogenous expression. Furthermore, AE21 was expressed in the dorsal-most regions of haltere and eye-antennal discs. In the embryo, expression can not be detected before germ-band retraction. AE21 is strongly expressed in the dorsal-most cells, later a second, weaker lateral stripe becomes evident, which is not included in the endogenous *pnr* expression and might reflect the lack of (Brinker) repressor sites resulting from the design of AE21.

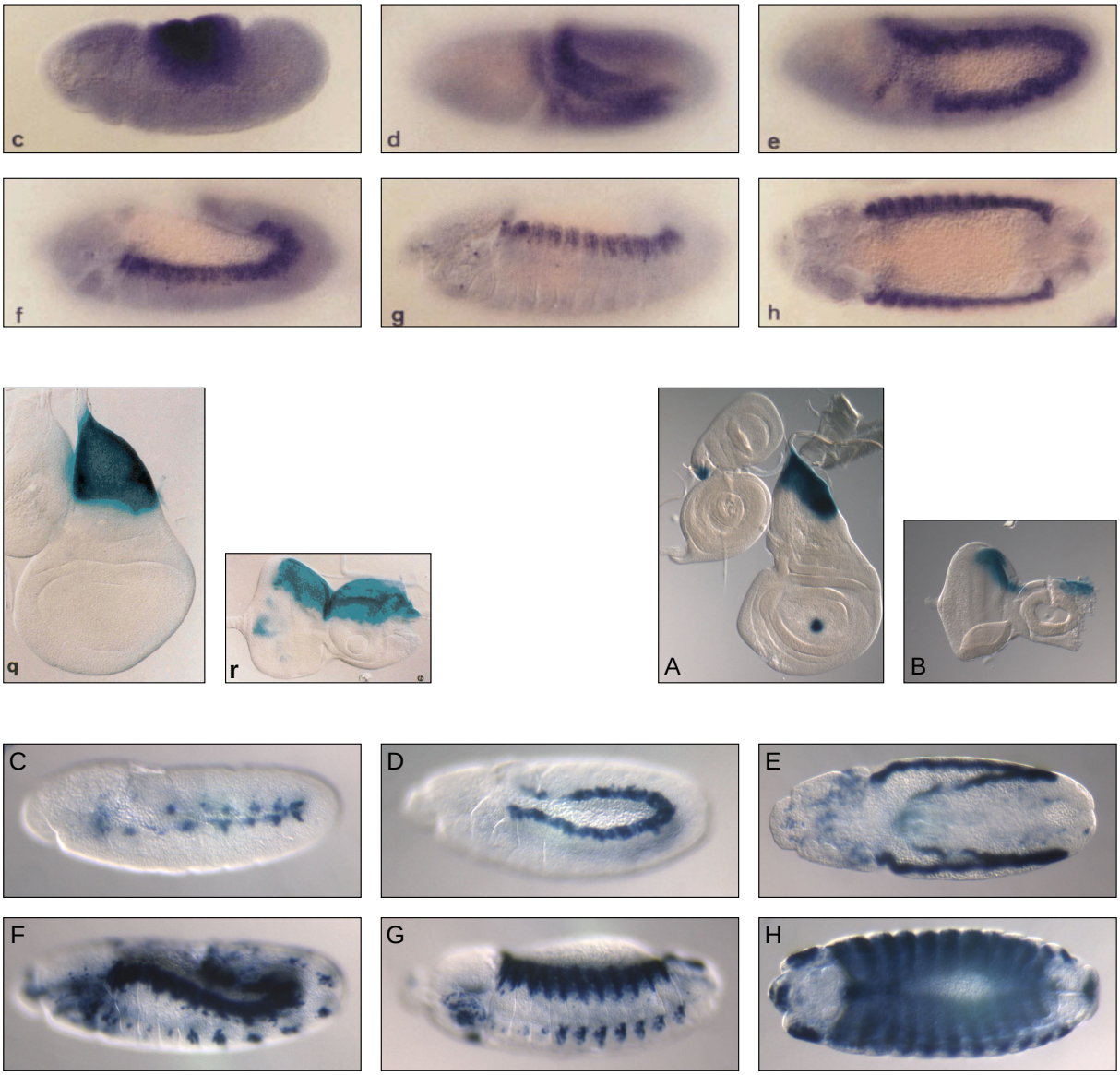

Figure 6.44
Endogenous *pnr* expression and AE21 expression. Images c to h, q and r are adapted from Heitzler et al. (1996) and show endogenous embryonic *pnr* expression (*in situ* hybridization) and imaginal disc XGal staining of a *pnr* enhancer trap. AE21 resembles several aspects of the *pnr* expression in the imaginal discs (A, B) and the embryo (C to H), although expression in the early embryo before germband extension is lacking. All embryos were stained using an anti-βgal antibody, discs using an XGal protocol.

6.4.7 Another *dad* enhancer

When we performed the *in silico* search for other AEs in the *Drosophila* genome, we surprisingly detected another putative AE in the *dad* locus, at the beginning of the fifth intron (Fig. 6.45). The 1kb enhancer construct DadInt52 including this AE drives the *lacZ* reporter gene in a very characteristic manner in both larval imaginal discs and the embryo. Expression in the wing and haltere imaginal discs resembles the expression of the Dpp target gene *Dorsocross* (Fig. 6.45, compare Fig. 6.37). In the embryo, DadInt52 induces expression of the *lacZ* reporter gene in the head region as well as in endodermal cells, similarly to lab550, a known Dpp-regulated enhancer found upstream of the *labial* gene (Grieder et al., 1997; Marty et al., 2001). Furthermore, expression is found the hindgut and in four characteristic spots in proximity to the posterior spiracles and the anal plate. No ectodermal striped expression as for the minimal Dad13 enhancer can be detected.

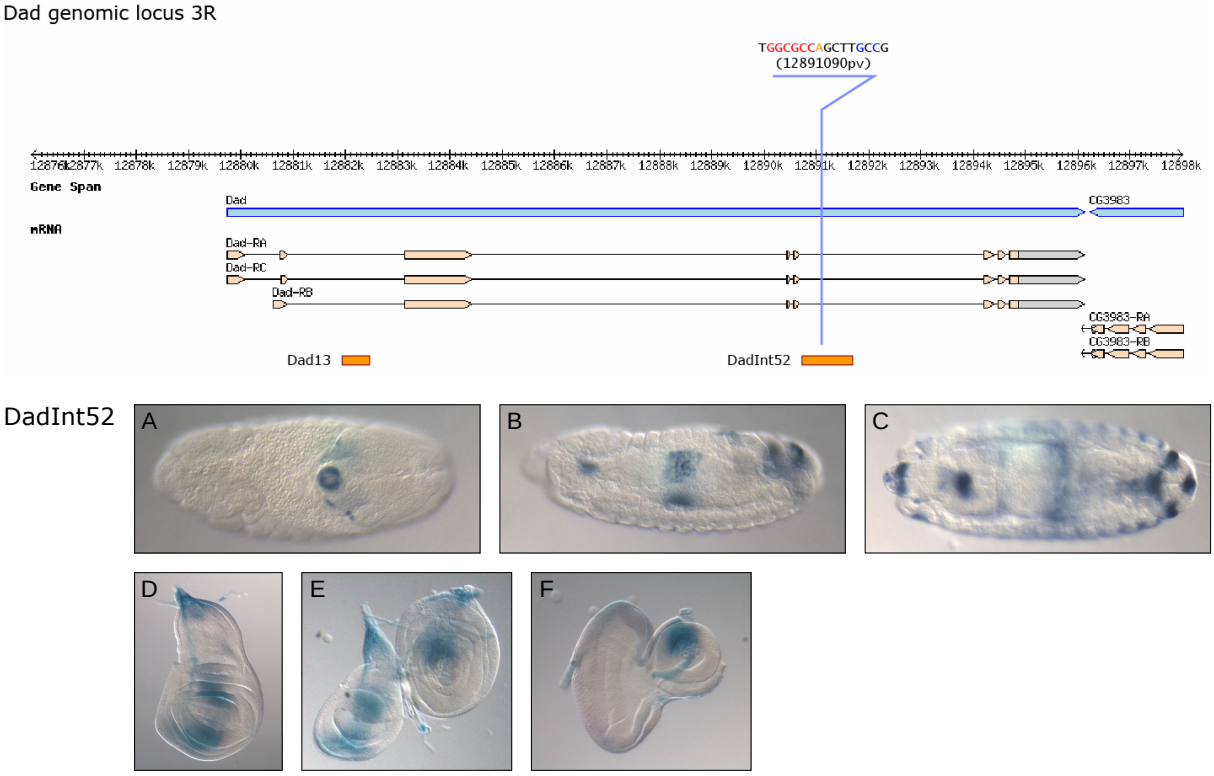

Figure 6.45
Expression of a different enhancer found in the *dad* locus. The enhancer construct DadInt52 contains another AE found in the fifth intron of the *dad* gene. Its expression pattern differs from that of Dad13, but partially overlaps. DadInt52 drives expression of a *lacZ* reporter in the embryo and in larval imaginal discs. All embryos were stained using an anti-βgal antibody, discs using an XGal protocol.

We again applied the same mutations to DadInt52 as before to the *knirps* enhancer and other constructs, first mutating the core nucleotides of the Brinker/Mad site of the AE from GGCGCC to GGatCC for complete destruction (termed AEd), and second introducing the nucleotides required for Schnurri recruitment (Fig. 6.46) (termed SE). The effect was striking in both larval and embryonic tissues. Expression in all imaginal discs decreased dramatically upon mutation of the AE and was totally abolished, when the AE was turned into an SE. In the embryo, expression was lacking nearly completely for the construct with the destroyed AE and entirely for the one with an introduced SE, except of the characteristic four spots at the posterior end that remained unaffected for both constructs. This expression is most probably Dpp-independent, but served as an internal control that the reporter gene was indeed inducible.

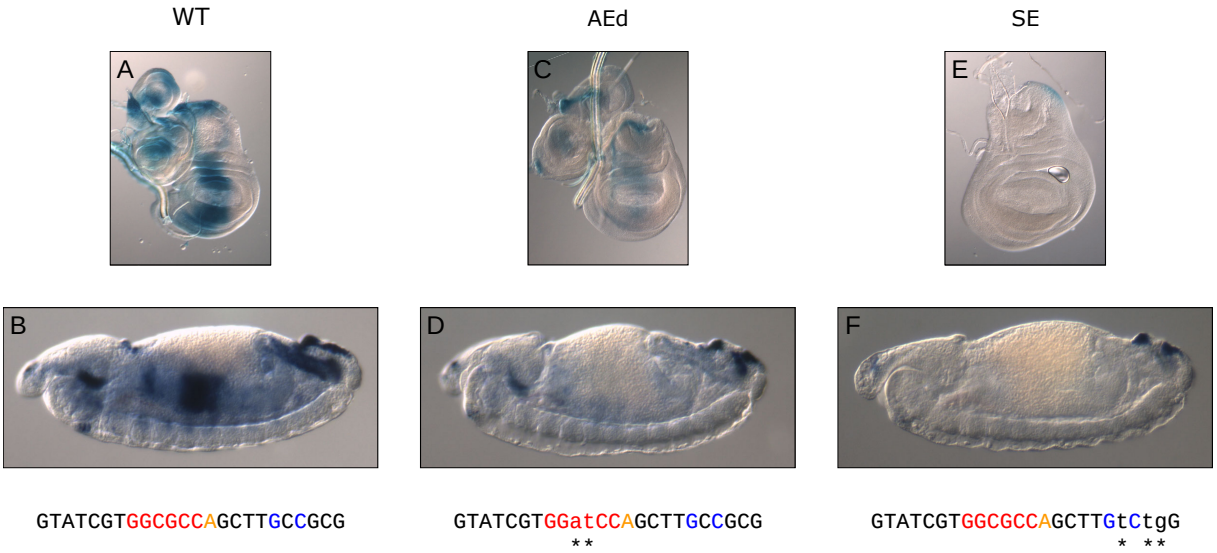

Figure 6.46
Expression of DadInt52 mutants. Destruction of the Mad/Brinker site (AEd) almost abolished the expression of the *lacZ* reporter gene in imaginal discs (C) and the embryo (D), while transformation of the AE into a repressive SE completely removed it (E, F). Only expression in the posterior domains next to the anal plate remained unaffected in the embryo (D, F). All embryos were stained using an anti-βgal antibody, discs using an XGal protocol.

In summary, the AE identified within this enhancer is crucial for its functionality. Mutation of as few as two or three out of one thousand nucleotides is sufficient to completely abolish its activity.

6.5 The function of the AE is pylogenetically conserved

The AE resembles the SE-like (but activating) BMP response elements (BREs) found in the context of BMP-regulated vertebrate genes (see 4.4.2) and it has been reported that a BRE in the *Xenopus Vent2* promoter is able to recruit *Drosophila* Mad/Medea and respond to BMP signalling *in vivo* when oligomerized (von Bubnoff et al., 2005; Yao et al., 2006).
Given this background, we were interested to find out whether the 5xAE, shown to be able to read-out BMP signalling in Drosophila, also induced expression of a *lacZ* reporter gene in a vertebrate model organism. Linearized plasmids used for the transformation of *Drosophila* embryos were injected into 1- to 2-cell zebrafish embryos. At approximately 60% epiboly, embryos were fixed and *lacZ* activity was determined by an XGal staining. 5xAE as well as 5xSE led to ventral expression of the reporter gene within the BMP2/4 domain (Fig. 6.47), indicating a role of BMP in the activation. To verify this, we applied Dorsomorphin, a drug identical to the AMP-activated Kinase (AMPK) inhibitor Compound C, to the developing embryos. Dorsomorphin has been shown to specifically counteract BMP-mediated phosphorylation of Smad1, 5 and 8 (Yu et al., 2008) and thus BMP target gene activation. Indeed, we registered a dramatic decrease in activity for 5xAE, while the expression domain remained unchanged (Fig. 6.47).

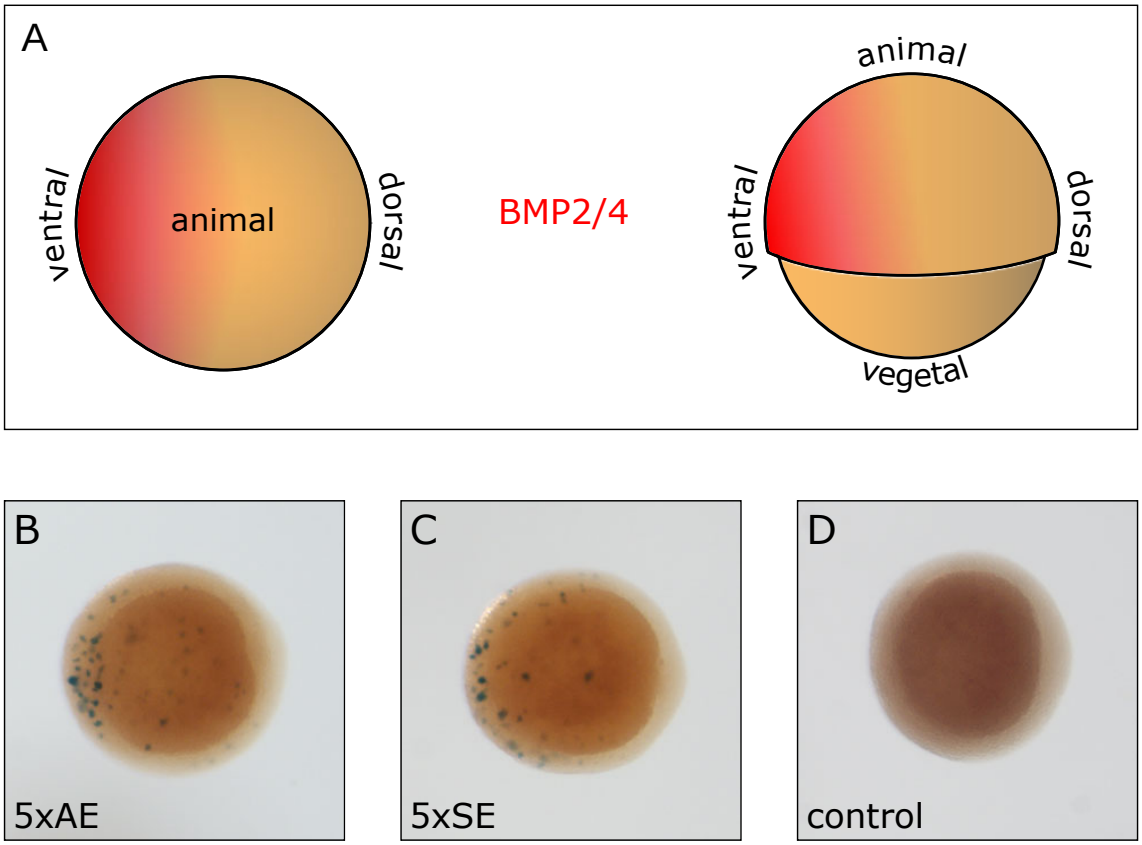

Expression pattern

	n	ventral	dorsal	not localized	lateral
5xAE	44	66%	5%	20%	9%
5xAE + Dm	37	64%	2%	16%	2%

Expression strength

	n	none	1 to 10 cells	>40 cells
5xAE	68	3%	26%	71%
5xAE + Dm	86	5%	66%	29%

Figure 6.47
Expression of 5xAE and 5xSE in zebrafish embryos. (A) The schematic drawings of a 60% epiboly zebrafish embryo show the BMP2/4 distribution from the animal pole and a lateral view. A *lacZ* reporter gene driven by 5xAE (B) or 5xSE (C) is expressed within the BMP domain, which is also statistically confirmed. Application of the BMP inhibitor Dorsomorphin does not alter the expression pattern, but strongly reduces expression strength. Embryos were stained using XGal and photographed from the animal pole.

7 Discussion

7.1 The genetic basis of evolution

The discovery of genes as units of inheritable information, the identification of the DNA as the carrier of these genes and the subsequent cloning of protein coding sequences from various organisms quickly led to the widespread belief that it was significant variations in these genes that could explain the morphological differences between distinct animals. Accordingly, a fruit fly would possess completely dissimilar proteins (and thus genes) than a cow. And the driving force of evolution would be the constant development of new genes with novel functions, by duplication, alteration and mutation of pre-existing ones.
With the dramatic increase in sequence data and the subsequent successful sequencing of whole genomes, however, it became evident that genes in different animals were not as dissimilar as they were thought to be. The same genes were found to control development and morphogenesis in phylogenetically distant species, and proteins were shown to have conserved functions in animals whose last common ancestor lived several hundred million years ago. The mouse Pax-6 protein, for example, is able to induce eye formation in *Drosophila*, like the *Drosophila* homolog Eyeless (Halder et al., 1995). And human BMP-4 can rescue the early patterning defects of *dpp* mutant fly embryos (Padgett et al., 1993). In fact, it turned out that signalling pathways involved in development and form-giving processes are highly conserved over the whole metazoan kingdom.
More recent studies revealed that morphological differences among animal taxa were more due to variations in the *cis*-regulatory elements and transcriptional control than differences in coding sequences (reviewed in Carroll, 2008). One example where this has been demonstrated in great detail is the divergent body pigmentation pattern of two closely related *Drosophila* species. The different morphology was tracked down to a mutation in one specific *cis*-regulatory element of the *tan* gene, whereas the tan protein sequence was unchanged (Jeong et al., 2008). New microarray screens and more powerful bioinformatic techniques draw the image of large regulatory networks in which each transcription factor controls the expression of hundreds of genes. It is obvious that any mutation in the DNA binding behavior of a transcription factor would lead to a drastic change (if not collapse) of the respective regulatory network. This is evolutionary unfavorable and most probably the reason why the function of transcription factors tends to be substantially better conserved among distant species than that of other proteins.
Rather than by introducing mutations into DNA-binding proteins, evolutionary changes can be achieved more subtly by mutations in the respective binding sites. Remodeling of existing regulatory sequences or the transfer of spatially distant *cis*-regulatory elements by genomic rearrangement can suddenly put a gene under the control of a hitherto not associated signalling pathway or abolish an existing linkage, without affecting the whole regulatory network. Instead of creating completely novel genes and functions, organisms are thus able to recruit existing genes to another context. The recurring redeployment of basically every signalling pathways and transcription factor during *Drosophila* development is a well-studied phenomenon. The Dpp pathway, for example, is important for dorso-ventral patterning of the embryo as well as growth and patterning of larval imaginal discs (Spencer et al., 1982). And the transcription factor Knirps does not only function as a zygotic gap gene, but is also crucial for development of the tracheal system (Chen et al., 1998; Rothe et al., 1989).
The dissection of an enhancer in the attempt to gain molecular understanding of the regulatory input is a tedious task. But if successful, it can lead to the identification of a novel *cis*-regulatory element and the discovery of a whole new regulatory network. The analysis of the *brinker* enhancer revealed the existence of the Silencer Element as a small repressive Dpp

response element (Pyrowolakis et al., 2004). Here, we analysed the enhancer of *dad*, a gene activated by Dpp, and report the identification of an analogous Activating Element.

7.2 Regulation of the Dpp-antagonist Dad

7.2.1 Function of Dad

Dad is the only inhibitory Smad found in Drosophila (Tsuneizumi et al., 1997) and a close homolog of the vertebrate I-Smads, Smad6 and Smad7. I-Smads are negative regulators of TGF-β signalling, due to their ability to interact with the type I receptor and block phosphorylation of R-Smads (Hayashi et al., 1997; Imamura et al., 1997; Nakao et al., 1997). Initially, Dad was identified as an antagonist of Dpp signalling. Misexpression of *dad* in the wing disc strongly affects growth and leads to the formation of tiny winglets, which can be counterbalanced by overexpressing a transgene encoding the constitutively active Dpp receptor Tkv^{QD} (Tsuneizumi et al., 1997).

Studies on the molecular functions of inhibitory Smads mainly focused on the vertebrate members. It was revealed that I-Smads do not only compete with R-Smads for receptor binding, but also cooperate with ubiquitin ligases, so called Smurfs (for Smad ubiquitin regulatory factors), to target activated receptor complexes to proteasomal degradation (Kavsak et al., 2000). I-Smads are also able to form complexes with R-Smads and lead to ubiquitination and degradation of the latter (Murakami et al., 2003). Other functions include the recruitment of specific phosphatases to deactivate the type I receptor (Shi et al., 2004). While Smad7 acts as a general inhibitor of TGF-β and BMP signalling, Smad6 preferentially inhibits the BMP type I receptors ALK-3 and ALK-6. Besides their fundamental role in blocking type I receptor signalling, there is also evidence for functions in transcriptional regulation. Although I-Smads lack the Smad-specific MH1 DNA-binding domain, they are known to be located in the nucleus of most cell types. Smad6 was shown to interact with the homeobox transcription factors Hoxc-8 and Hoxc-9 to repress target gene transcription (Bai et al., 2000) and to bind DNA, together with Histone deacetylases (Bai and Cao, 2002). Interaction with histone deacetylases was also reported for Smad7 (Bai and Cao, 2002). Furthermore, Smad6 is able to recruit the transcriptional corepressor CtBP to the promoter of the *Id1* gene (possibly by interaction with Smad1) and inhibit its transcription (Lin et al., 2003).

The function of inhibitory Smads is not restricted to TGF-β signalling. Smad 7 has also been associated with the TNF-α and MAPK pathway, where it was reported to inhibit the transcriptional activity of NF-κB, induce activation of JNK and activate p38 MAP kinase (Edlund et al., 2003; Lallemand et al., 2001; Mazars et al., 2001). A link to the Wnt/Wingless pathway was also established when Smad7 was shown to interact with β-catenin and LEF1/TCF in a TGF-β dependent manner (Edlund et al., 2005) and induce the degradation of β-catenin by direct binding and subsequent recruitment of the E3 ubiquitin ligase Smurf2 (Han et al., 2006).

Since inhibitory Smads are crucial for regulating the intensity and duration of TGF-β signalling, their dysfunction or misexpression is associated with various diseases classically assigned to TGF-β signalling. This includes fibrosis, inflammatory diseases as well as tumor progression. Indeed, increased expression levels of Smad7 correlate with a poor prognosis for several types of cancers.

Compared to the enormous body of data gathered about the function, regulation and expression of vertebrate inhibitory Smads in physiological and pathological conditions (Miyazono, 2007), our knowledge of the Drosophila I-Smad Dad is negligible. Very few studies have dealt with the function of Dad. Due to the high structural conservation of fly and

vertebrate I-Smads, it is tempting to speculate that Dad acts similarly to Smad6 and Smad7. Indeed, it has been shown that Dad binds to the cytosolic domain of the Dpp receptor Thickveins and thereby blocks phosphorylation of Mad (Inoue et al., 1998). Recently it has been reported that Dad is not able to inhibit signalling of the Activin receptor Baboon in heterologous cell culture, but is restricted to the receptors of the BMP pathway, Thickveins and Saxophone (Kamiya et al., 2008). Notably, and in contrast to vertebrate I-Smads, Dad seems not to recruit dSmurf, the *Drosophila* homolog of vertebrate Smurfs, since dSmurf interacts with Mad but not Dad in a signal-dependent manner (Liang et al., 2003b).

7.2.2 Genetic control of *dad* expression

The transcription of genes encoding vertebrate inhibitory Smads is directly induced by BMP signalling (see 4.4.2), and also *dad* is upregulated in cells receiving Dpp signalling (Tsuneizumi et al., 1997). However, until now it has not been shown that this upregulation is due to direct Smad binding to the *dad* enhancer. This is important in light of the discovery that another gene, *omb*, which had been regarded as the prototype of a gene directly activated by the Dpp pathway, is actually only derepressed by Dpp signalling via the removal of the repressor Brinker and induced by other, hitherto unknown, factors (Sivasankaran et al., 2000). Brinker is the default antagonist of the Dpp pathway and represses the majority of Dpp target genes in the absence of Dpp signalling (Campbell and Tomlinson, 1999; Jazwinska et al., 1999a; Jazwinska et al., 1999b; Minami et al., 1999). Consequently, one of the main effects in cells responding to Dpp is the downregulation of *brinker* (Marty et al., 2000). The outcome of

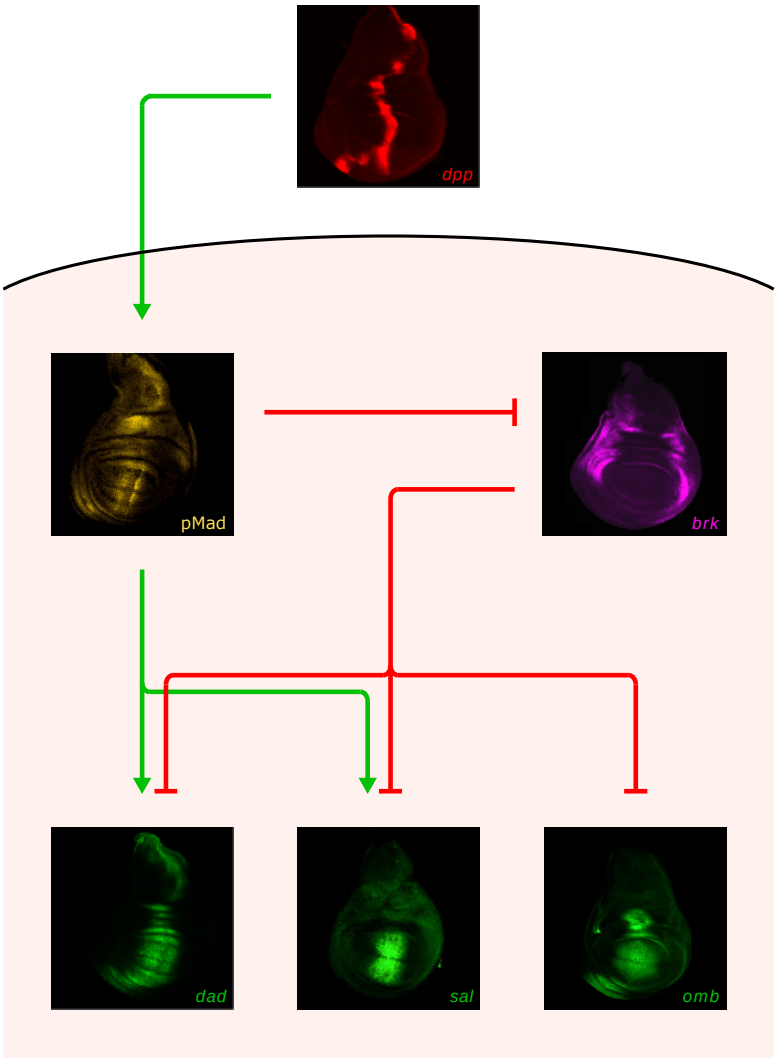

Figure 7.1
Regulation of Dpp/Brinker target genes in the wing imaginal disc. The diffusible extracellular ligand Dpp is produced in a narrow stripe of cells along the anterior-posterior border. Its activity gradient can be visualized by antibody-detection of phospho-Mad. The *brinker* gene, which encodes a nuclear repressor, is repressed by the Dpp pathway and thus expressed in a complementary manner. The sensitivity of gene expression to the Dpp gradient can be due to activation by the Dpp pathway or repression by Brinker. We were able to characterize *dad* as a gene integrating both inputs, similar to *sal* and unlike *omb*, that is only repressed by Brinker and induced by unknown activators.

genetic experiments suggests that *dad* is a Brinker target as well (Marty et al., 2000; Torres-Vazquez et al., 2001). Our findings reveal that, upon Dpp signalling, *dad* is not only derepressed by removal of Brinker, but also activated by Dpp in a Brinker-independent fashion. Thus, *dad* can be assigned to the member-rich class of genes that are both activated by the Dpp pathway and repressed by Brinker (see Fig. 7.1).

7.2.3 Regulation of a minimal *dad* enhancer

Analysing the expression pattern of *lacZ* reporter transgenes, we were able to identify a 520bp enhancer (Dad13) within the second intron of *dad* that induces an expression pattern very similarly to that of the endogenous *dad* gene. Although we did not perform any rescue experiments yet, we consider it to be the minimal enhancer due to this truthful recapitulation. Dad13 is inducible by Dpp signalling and sensitive to *brinker* expression in cell culture experiments as well as *in vivo*. Using purified recombinant DNA-binding domains of Brinker, Mad and Medea, we demonstrated the existence of well conserved and largely overlapping binding sites for Smads and Brinker. Mad as well as Medea compete with Brinker for binding to these sites, which implies a similar regulative mechanism for the regulation of *dad* as it has already been proposed for a *zen* and a *Ubx* enhancer element (Kirkpatrick et al., 2001; Rushlow et al., 2001). By precise mutations we were able to selectively abolish Brinker binding (see Fig. 7.2) and demonstrate that it is possible to unlink Smad and Brinker input. Importantly, we did not only show the binding of rather promiscuously interacting protein domains, but also the assembly of a full-length Mad/Medea complex on at least three different sites within the Dad13. This kind of complex formation has been demonstrated only in the context of the SE before (Pyrowolakis et al., 2004). Several genes have been reported to be directly activated by Smads. However, the experimental evidence was based on the binding of bacterially produced DNA-binding domains. Therefore, our work presents the first example of formation of such a complex in the context of a gene activated by Dpp.

Figure 7.2
Mutation of a Brk/Mad into an exclusive Mad site. The consensus binding sequences of Brinker and Mad share great similarity, and the major binding sites within the *dad* enhancer (WT) fulfill both. However, we demonstrated that it is possible to mutate such a site to an exclusive Mad site (BtM), thereby abrogating the Brinker input and preserving the Mad input.

Mutation of two of the sites able to recruit the Mad/Medea complex strongly reduced the activity of Dad13 in cell culture assays as well as its capability to drive the expression of a *lacZ* reporter in the embryo. Expression in the wing disc, however, was only mildly affected. This might be due to a certain level of redundancy and modularity of the minimal *dad* enhancer and is in accordance with the fact that successive reduction of the size of Dad13 leads to a constant, but not abrupt, loss of activity. It might also reflect functionally overlapping, but still slightly differing mechanisms for regulating *dad* expression in larval imaginal discs and the embryo.

```
D.melanogaster     CCTCAACCTTAA--ATTGTTGATTCTT-CAACTTGTCAAACCGGCTGACAAACCGACCG
D.pseudoobscura    CCTCAACCTTAAATATTGTTGATTCTT-CAACTTGTCAAACCGGCTGACAAACCAACCG
D.virilis          --TTCACCTCAA--ATTGTTGATTCTT-CAACTTGTCAAACCGGCTGACAAACCGACTG
D.mojavensis       --TTCACCTCAG--ATTTTTGATTCTTCCAACTTGTCAAACCGGCTGACAAAACGACCG
D.yakuba           CCTCAACCTTAA--ATTGTTGATTCTT-CAACTTGTCAAACCGGCTGACAAACCGACCG
D.erecta           CCTCAACCTTAA--ATTGTTGATTCTT-CAACTTGTCAAACCGGCTGACAAACCGACCG
consensus          ..*..****.*.  ***.********* ************************.*.**.*
AP1-like site                                        TGACAAA      TGACAAA
```

Figure 7.3
Conservation of the 5' region of Dad13. The first sixty nucleotides of Dad13 are highly conserved among different Drosophila species, although they are not absolutely essential for the activity of the enhancer. Remarkable is a duplicated stretch of ten nucleotides (violet) that resembles an AP1-like binding site (Tsuji et al., 1998).

Due to its ability to control the intensity of Dpp signaling and thus growth and patterning in general, *dad* is a very good candidate for a gene that computes regulatory input from multiple factors and signaling pathways, as it has been reported for the enhancers of the vertebrate inhibitory I-Smads. Interestingly, Dad13 not only comprises two highly conserved clusters of Brinker and Smad sites, separated by a poorly conserved nucleotide stretch, but also a perfectly conserved region at the 5' end that does not include any putative Smad or Brinker binding sites. This region contains a duplicated motif of ten nucleotides (Fig 7.3) that resembles an AP1-like binding site shown to recruit a Jun/Fos complex (Tsuji et al., 1998). It is noteworthy that AP1 has also been reported to bind to the *smad7* promoter (Brodin et al., 2000). However, removal of these sites by designing a construct smaller than Dad13 only weakly affected enhancer activity.
Our results also indicate a role of the TEA-domain transcription factor Scalloped in the transcriptional control of *dad* in the wing imaginal disc. Scalloped has been shown to interact with Vestigial (Halder et al., 1998) as well as Yorkie (Goulev et al., 2008; Wu et al., 2008; Zhang et al., 2008b) in the regulation of its target genes. Yorkie is a potent activator of cell growth and proliferation and is tightly regulated by the Hippo pathway (reviewed by Saucedo and Edgar, 2007). Thus, our findings might elucidate a new level of interaction of the Hippo and Dpp pathways, two important regulatory networks involved in growth control. Future experiments will shed more light on this potential cross-regulation.

7.2.4 The AE as an integrative activating Dpp response element

Further dissection of the minimal *dad* enhancer led to the discovery of a short motif with less than twenty nucleotides that was able to recruit a Mad/Medea complex *in vitro* and drive

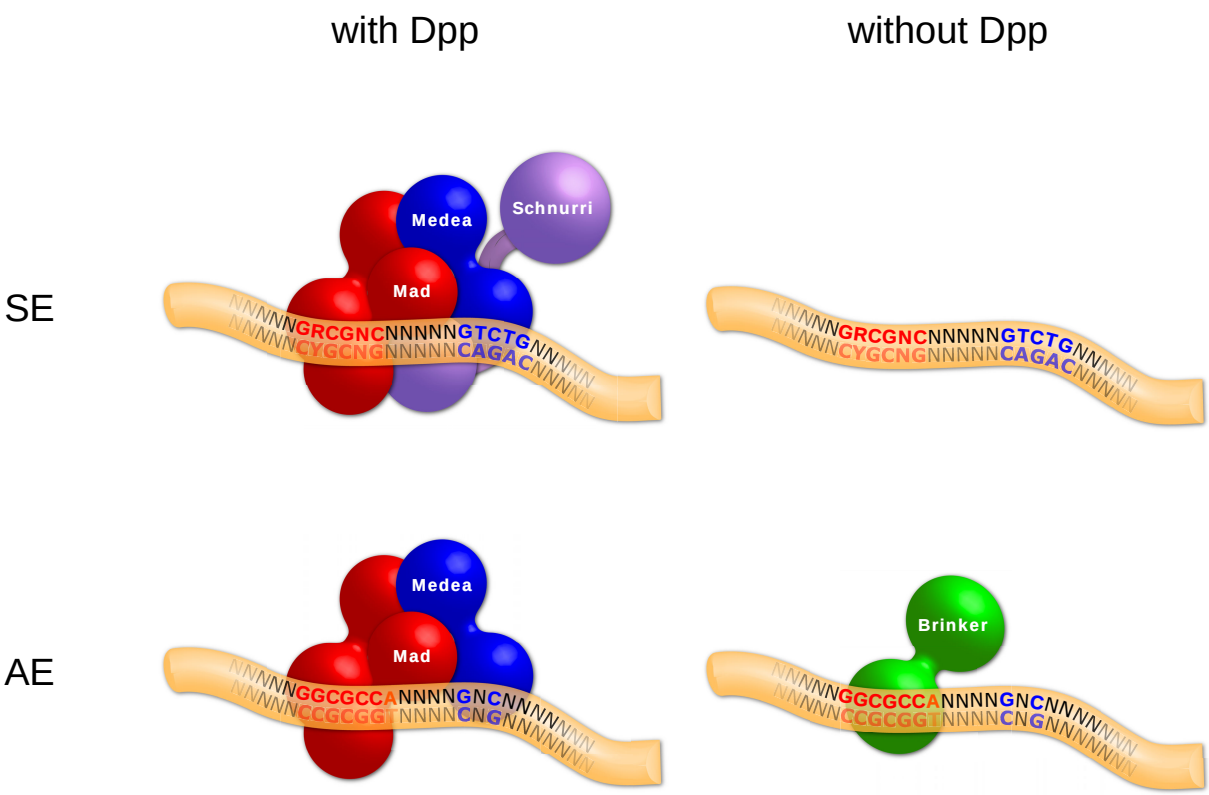

Figure 7.4
Architecture of the AE and SE. Although they exert completely contrary effects, the architecture of the AE and SE is very similar. Both are able to recruit a complex of Mad and Medea upon Dpp signaling. The Smad/SE complex, however, additionally recruits the repressor Schnurri. This is not the case for the AE that lacks the second T in the blue box. Without Dpp signaling, the repressor Brinker binds to the AE to inhibit transcription, whereas genes regulated by an SE are activated by other factors.

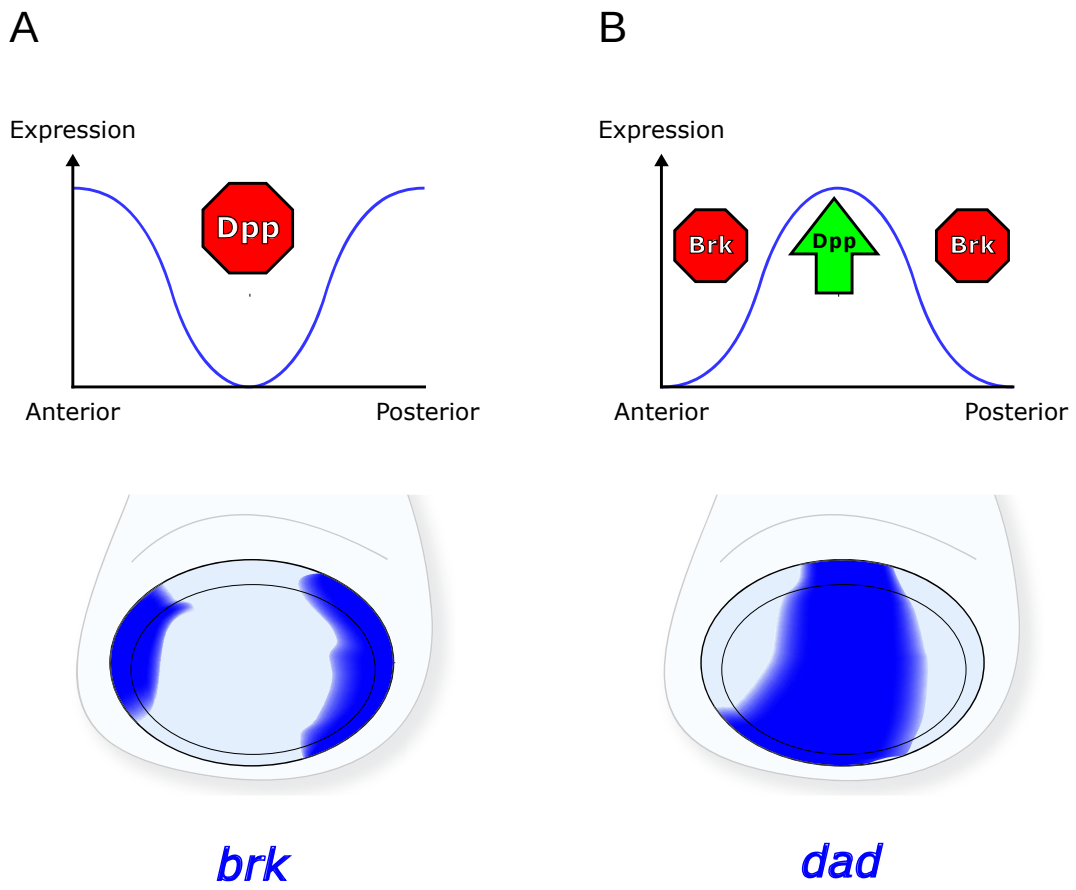

Figure 7.5
Comparison of SE- and AE-mediated transcriptional regulation. The two genes *brinker* and *dad* are prototypes of genes whose transcription is regulated by an SE and AE, respectively. (A) In the wing imaginal disc, *brinker* is generally activated by unknown factors, but repressed within the Dpp domain by a Mad/Medea/Schnurri complex recruited to the SE. (B) *dad* expression is complementary, because it is induced within the Dpp domain by direct activation via the AE and downregulated outside the Dpp domain by the repressor Brinker (B).

expression of a reporter gene in a *dad*-like fashion *in vivo*. Because of its striking similarity to the Silencer Element (SE), we termed it Activating Element (AE). The AE very closely resembles the SE, which came as a big surprise. We had chosen *dad* for our studies because of its characteristic expression and were totally unbiased when we started the molecular dissection of its enhancer. Despite their analogy, the SE and AE differ in several key aspects. Due to the arrangement of the Smad binding sites, they are both able to recruit a complex of Mad and Medea. But only the SE comprises the second T within the “blue box” (see Fig 7.4), which is essential for the recruitment of the repressor Schnurri (Pyrowolakis et al., 2004). Furthermore, the AE identified in the *dad* enhancer is able to interact with the repressor Brinker. Brinker competes with Mad for binding to the “red box” of the AE, which fulfills the consensus sequence derived from analysis of the SE (GRCGNC) as well as the one of the Brinker binding site (TGGCGYY). Thus, the AE and SE are using a very similar sequence to exert opposite effects (see Fig 7.5). While genes comprising an SE are consequently repressed upon Dpp signaling, the AE allows for Dpp-mediated activation in various developmental contexts and at the same time ensures downregulation in the absence of Dpp signalling by recruitment of Brinker.
So far we do not have any evidence that Schnurri, which has been associated also with activation (see 4.3.4), acts on the AE. Schnurri^{CT} is not able to bind to the AE. Domains of human Schnurri with homology to the N-terminal regions of Schnurri (that are not included in Schnurri^{CT}) were shown to bind to the SE (Yao et al., 2006), which might indicate other, so

far unknown, functions of *Drosophila* Schnurri. However, this is probably not the case in the context of the *dad* enhancer. The observation that expression of *dad* is lacking in *shn* mutants, can be explained with the derepression of *brinker*. This becomes evident when looking at *brk*; *shn* double mutants, where transcription of *dad* is reconstituted (Marty et al., 2000).

7.2.5 Flexibility and adaptability of the AE

The AE consensus sequence GGCGCCA(N)$_4$GNCV is based on the analysis of the AE that we found in the *dad* enhancer. We successfully demonstrated its usefulness for prediction of other genes directly activated by the Dpp pathway. In addition, we could also show that variants of this sequence as well allow for activation upon Dpp signalling. The length of the linker, for example, is not invariant, which is in sharp contrast to the SE. It has been reported that Mad and Medea are still able to form a complex on the DNA when the red box and blue box within the SE are distantly spaced (Gao and Laughon, 2007). In accordance with this, reduction of the linker length by one nucleotide retains activity of the synthetic pentamerized construct 5xAE-1. Interestingly, linker extension of one nucleotide is sufficient to convert the repressive SE into an activating element. These data indicate that the function of the AE is not totally dependent on the linker length, as it is the case for the SE. However, five nucleotides might be the optimal spacing for the AE.
By creating the HASE construct, we were able to show that the activating Smad input can be separated from the Brinker input. This raises of course the question: is such an element of physiological relevance? Many Dpp target genes are at the same time repressed by Brinker, which could be explained with the need to tightly regulate gene transcription and precisely define expression boundaries. However, there are genes known such as *Race* that lack Brinker input and rely solely on regulation upon Dpp signalling (Ashe et al., 2000). It is thus reasonable to speculate that *Drosophila* also possesses functional HASEs. The enhancer found within the *elbow B* gene might contain such an endogenous HASE and will be subjected to further experiments.
If there are functional AEs, SEs and HASEs *in vivo*, what about NASEs? Or with other words, are there SEs that at the same time recruit Brinker? The NASE reads out Smad-mediated repression as well as Brinker repression and leads to constant downregulation. It is not easy to imagine situations where such an element would be of use. However, three out of nine SEs found in the vicinity of *brinker* are actually NASEs. It has been shown that Brinker represses its own transcription in a negative autoregulatory loop and that this, besides regulation via Mad/Medea/Schnurri, is essential for formation of the Brinker gradient (Hasson et al., 2001; Moser and Campbell, 2005). The NASEs might represent such sites where Brinker and Smad-mediated repression converge.
Since Smads have been reported to interact with other transcription factors in the induction of their target genes, and considering that transcriptional activation is believed to depend on local co-activators (Barolo and Posakony, 2002), it came as a surprise that a simple pentamerized AE was sufficient to drive expression in such a specific pattern. This brings up the question, whether this is due to an intrinsic activation capability of the Smad proteins or the recruitment of an unknown co-activator. Interestingly, the expression pattern of 5xHASE in the wing imaginal disc pinpoints a regulative role of the selector protein Scalloped. Scalloped very likely binds to a motif comprised of the linker and parts of the Mad binding site. This potential function for the spacer of the AE might indicate a general concept. The spacer is highly variant, often not conserved and differs between different AEs/SEs. Due to its flexibility it might offer the possibility to integrate the input of other transcription factors such as Scalloped to establish or increase tissue-specificity.
The AE, SE and derived elements are fascinating examples of how minimal changes in *cis*-regulatory sequences provoke dramatic changes in their function. Only few response elements

are known that harbor this feature. In the case of the mouse POU domain protein Pit-1, the distinction between repression or activation depends on the existence of two base pairs within the bipartite binding site (Scully et al., 2000). Also for NFκB binding sites it has been shown that a single base pair determines co-factor specificity and whether the expression of the respective target gene is induced or restricted (Leung et al., 2004; Luecke and Yamamoto, 2005). Additionally, it has been demonstrated for the Wingless pathway that mutation of a TCF binding site can induce activation instead of repression. However, this requires the exchange of an AGAWAW motif by a SCTTTGWW motif, which recruits the same protein, but by an uncharacterized, different binding mechanism (Blauwkamp et al., 2008).

7.2.6 Discovery of a Dpp synregulation group

We initially attempted to identify an element that is able to read out Dpp signalling independent of tissue restrictions, analogous to the SE. The AE gets very close to fulfill these criteria. The expression pattern of none of the genes we identified in our genome-wide *in silico* search for AEs (see Fig. 7.6) reflects all domains where Dpp is active. Instead, their diversified expression patterns indicate that the AE is able to confer Dpp signalling activity in various tissues and at different developmental stages. The expression domains of *pannier* and *knirps*, for example, are very dissimilar. However, both have been shown (*knirps*) or are very likely (*pannier*) to be regulated by an AE and depend on Mad/Medea input. Thus, we would rather suggest the term synregulation than synexpression, as underlying regulatory mechanisms are the same for both genes, but they are not necessarily expressed in

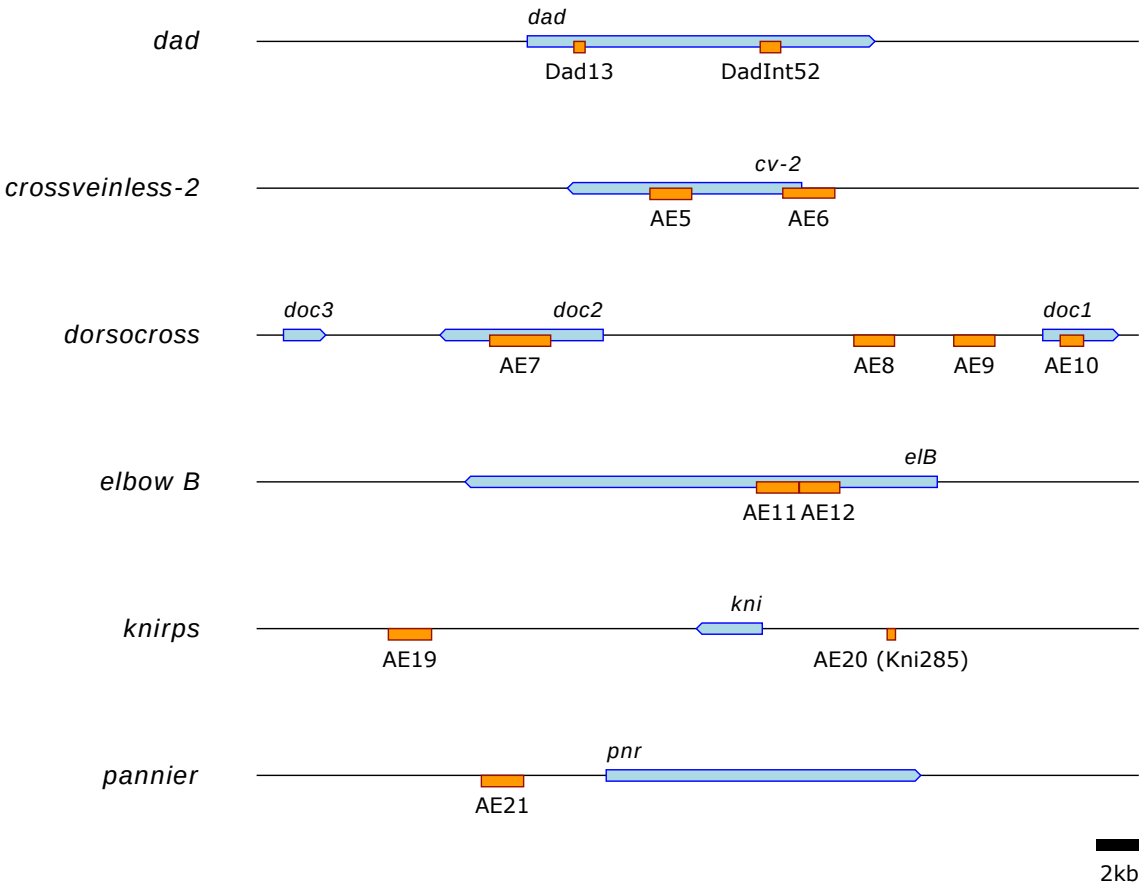

Figure 7.6
Overview of AE containing enhancer. The comparative list shows all enhancer elements analysed in this work (excluding subfragments) and the corresponding genes. All elements depicted induce expression in domains known to be regulated by Dpp (except AE5, which showed no activity). AE12 has not been tested yet. Besides Dad13, the importance of the AE for enhancer activity was unequivocally demonstrated for DadInt52 and AE20. Analysis of the other enhancer elements is ongoing.

overlapping domains.
The observation that the expression patterns of putative AE containing genes fall into regions of Dpp activity, but differ greatly, suggests that the AE acts in concert with other (local) activators and repressors to temporally and spatially control transcription. In the case of the Kni285 enhancer, this co-activation might depend on Trachealess (Trh), a regulator of tracheal cell fates (Isaac and Andrew, 1996; Wilk et al., 1996) that interacts with the basic helix-loop-helix (bHLH)-PAS protein dARNT (Ohshiro and Saigo, 1997; Sonnenfeld et al., 1997; Zelzer et al., 1997). A complex of Trh and dARNT (also known as Tango) has been shown to bind to a putative binding site within Kni285 *in vitro*, and expression of a 444bp enhancer construct comprising Kni285 significantly decreased when this site was mutated (Reinhard Schuh, personal communication).
The importance of our findings is substantiated by the fact that most of the enhancer fragments predicted to contain a functional AE induce expression in a fashion that implies regulation by the Dpp pathway. This was, for example, the case for all constructs derived from the *Dorsocross* locus, the genomic region with the most AE hits. The *Dorsocross* genes have been implied to be directly regulated by Dpp (Hamaguchi et al., 2004; Reim et al., 2003) and our study might provide the molecular basis for this assumption.
However, initial attempts to destroy the central AEs in the *Dorsocross* enhancer fragments by mutating the two central nucleotides of the Mad binding site was not efficient in abrogating the activity of the enhancer. This might be due to the insufficiency of the introduced mutation, which we are planning to test by more dramatic changes. But the reason is more likely to be the redundancy of AEs. The minimal *dad* enhancer already contains at least three AEs, and more careful analysis of the *Dorsocross* enhancers revealed the existence of several more potential AEs. Hence, the redundant and modular nature of the enhancers seems to be a common theme for genes that are activated by the Dpp pathway via an AE. This makes mutational analysis more difficult. Two exceptions are the 285bp *knirps* enhancer and the second enhancer found in the *dad* locus, DadInt52. Both include only a single AE, whose mutation completely abolishes activity of the enhancer.
Further experiments will also focus on an enhancer identified in the proximity of *pannier*. The regulatory interactions of *dpp* and *pannier,* an important dorsal selector gene in the embryo, are not well understood and our findings might help to shed more light on them.

7.2.7 Phylogenetic conservation of the AE

Due to the high conservation of the Dpp/BMP pathway and the molecular properties of the Smad proteins, it is not unlikely that the function of the AE/SE is phylogenetically conserved. The AE impressively shows how the DNA-binding sites of two distinct proteins (Mad and Brinker) evolutionarily converged into one motif. No Brinker homolog has been identified in vertebrates so far. However, SE-like (and thus AE-like) motifs have been found in the enhancers of several vertebrate genes activated by BMP signalling, such as *smad7* or the *Id* genes (Karaulanov et al., 2004; Korchynskyi and ten Dijke, 2002). An AE-including BMP response element isolated from the *Id1* enhancer is even sufficient to drive a reporter gene in a pattern partially overlapping with regions of BMP activity in the mouse (Monteiro et al., 2004). Recently, it has been reported that the function of an SE-like activating element from the *Xenopus Vent2* promoter is subjected to the same restrictions as the *Drosophila* SE considering the spacer length, and that vertebrate Schnurri is able to form a complex with Mad and Medea on this element. These findings imply that vertebrate AE/SE sequences are activated by the vertebrate Schnurri homologs. Our experiments with zebrafish embryos do not necessarily support this idea, because the pentamerized AE induces *lacZ* expression ventrally in a BMP-dependent manner, also when the linker length is varied. There are several explanations possible for this discrepancy. Vertebrate Schnurri proteins might act only on a

subset of AE/SE like sequences, or only in a certain developmental context. It is also possible that the limitation of the spacer length is specific to the *Xenopus Vent2* motif and even caused by other reasons. More efforts will have to be made to elucidate the functions of Schnurri, not only in vertebrates (where the possible functional redundancy of the three vertebrate Schnurri homologs complicates the analysis), but also in *Drosophila*.

7.2.8 Open questions

One of the greatest unanswered questions is certainly which factors bind to the AE besides Mad and Medea. Several approaches are conceivable to investigate this issue. We demonstrated that it is possible to specifically co-precipitate phosphorylated Mad bound to biotinylated AE. It is likely that also other unknown factors can be isolated by this means and detected by subjection of the bound complexes to mass spectrometry.
Alternatively, we are planning a cell culture based RNAi screen. The cell culture assay has already been established in this work and is based on the induction of a luciferase gene fused to the *dad* minimal enhancer. This construct is co-transfected with a plasmid encoding the constitutively active Dpp receptor Tkv^{QD}. A library of double-stranded RNA molecules, targeting the majority of the *Drosophila* genes, is then applied and the effect on the reporter gene expression analysed. RNAs directed against genes that are involved in activation of *dad* should lead to a decreased luciferase signal and allow for their identification.
Probably linked to the prior question, it remains to be elucidated why the 5xAE is able to induce diverse and specific expression patterns in the embryo (although absent or only weak at early stages), but not in the wing imaginal disc. In this context, it will be insightful to illuminate the role of Scalloped.
The expression of the minimal *dad* enhancer truthfully recapitulates Dpp signalling activity. Classically, activity of the Dpp pathway is visualized using an antibody directed against phosphorylated Mad. With the generation of transgenic flies carrying a Dad4::GFP construct, we for the first time provide a way to visualize Dpp activity in living tissues. We are convinced that this will be of great use to the *Drosophila* community.
One question that could be addressed using such a tool is little obvious but of great importance. Why is *dad* ubiquitously and seemingly constantly activated upon Dpp signalling? As intensively discussed, the major role of Dad is to antagonize Dpp signalling. However, continuous Dpp signalling is required for growth of the wing imaginal disc. And inhibition of Dpp signalling leads to loss of *dad* transcription. What is the consequence of this feedback loop? Do cells reacting to Dpp permanently produce Dad and degrade it, together with the bound receptor/Smad complex? Or do cells constantly cycle through periods of high activity of the Dpp pathway/low levels of Dad and low activity of the Dpp pathway/high levels of Dad?
Addressing these questions will be the aim of future experiments. We believe that the work presented here will be of great guidance in successfully answering them.

8 Acknowledgements

My greatest thanks are dedicated to Markus Affolter, for his support and patience as well as his encouragement and enthusiasm. His points of view and scientific attitude inspired me a lot and I appreciate that he did not pursue his plans to turn me into an early bird.
I am also very thankful to Georgios, Jorgos, George and Giorgos Pyrowolakis, for their amicable supervision, friendship and 24/7 knowledge supply, even after their postdoc to group leader transition.

Furthermore, I would like to highly acknowledge the help of Elín Ellertsdóttir with the zebrafish experiments and the efforts of Enrica Charbonnier to produce the lovely colorful images. I am also grateful to Reinhard Schuh and Christian Wolf for providing helpful unpublished data about the *knirps* enhancer.

I want to thank the former and present members of the Affolter lab for their contribution to an enjoyable and productive atmosphere, scientific support and non-scientific distraction. Special thanks go to Fisun for careful proofreading and phrase finding, as well as rescuing me when I locked myself out the night before handing in this thesis. I am also indebted to members of the neighboring labs, namely the Keller and Gehring lab, for providing help and materials.

Moreover, I am thankful to Rolf Zeller and Walter Gehring for happily volunteering to join my thesis committee.

Last, but definitively not least, I want to thank Daria for guiding me through the organisational obstacles during the last months before obtaining my PhD and my family for their emotional and financial support during the last three decades.

9 References

Abramoff, M.D., Magelhaes, P.J., and Ram, S.J. (2004). Image Processing with ImageJ. Biophotonics Int *11*, 36-42.
Affolter, M., and Basler, K. (2007). The Decapentaplegic morphogen gradient: from pattern formation to growth regulation. Nat Rev Genet *8*, 663-674.
Arora, K., Dai, H., Kazuko, S.G., Jamal, J., O'Connor, M.B., Letsou, A., and Warrior, R. (1995). The Drosophila schnurri gene acts in the Dpp/TGF beta signaling pathway and encodes a transcription factor homologous to the human MBP family. Cell *81*, 781-790.
Ashe, H.L., Mannervik, M., and Levine, M. (2000). Dpp signaling thresholds in the dorsal ectoderm of the Drosophila embryo. Development *127*, 3305-3312.
Bachmeyer, C., Mak, C.H., Yu, C.Y., and Wu, L.C. (1999). Regulation by phosphorylation of the zinc finger protein KRC that binds the kappaB motif and V(D)J recombination signal sequences. Nucleic Acids Res *27*, 643-648.
Bai, S., and Cao, X. (2002). A nuclear antagonistic mechanism of inhibitory Smads in transforming growth factor-beta signaling. J Biol Chem *277*, 4176-4182.
Bai, S., Shi, X., Yang, X., and Cao, X. (2000). Smad6 as a transcriptional corepressor. J Biol Chem *275*, 8267-8270.
Baldwin, A.S., Jr., LeClair, K.P., Singh, H., and Sharp, P.A. (1990). A large protein containing zinc finger domains binds to related sequence elements in the enhancers of the class I major histocompatibility complex and kappa immunoglobulin genes. Mol Cell Biol *10*, 1406-1414.
Barolo, S., Carver, L.A., and Posakony, J.W. (2000). GFP and beta-galactosidase transformation vectors for promoter/enhancer analysis in Drosophila. Biotechniques *29*, 726, 728, 730, 732.
Barolo, S., and Posakony, J.W. (2002). Three habits of highly effective signaling pathways: principles of transcriptional control by developmental cell signaling. Genes Dev *16*, 1167-1181.
Barrio, R., and de Celis, J.F. (2004). Regulation of spalt expression in the Drosophila wing blade in response to the Decapentaplegic signaling pathway. Proc Natl Acad Sci U S A *101*, 6021-6026.
Belenkaya, T.Y., Han, C., Yan, D., Opoka, R.J., Khodoun, M., Liu, H., and Lin, X. (2004). Drosophila Dpp morphogen movement is independent of dynamin-mediated endocytosis but regulated by the glypican members of heparan sulfate proteoglycans. Cell *119*, 231-244.
Benchabane, H., and Wrana, J.L. (2003). GATA- and Smad1-dependent enhancers in the Smad7 gene differentially interpret bone morphogenetic protein concentrations. Mol Cell Biol *23*, 6646-6661.
Biemar, F., Nix, D.A., Piel, J., Peterson, B., Ronshaugen, M., Sementchenko, V., Bell, I., Manak, J.R., and Levine, M.S. (2006). Comprehensive identification of Drosophila dorsal-ventral patterning genes using a whole-genome tiling array. Proc Natl Acad Sci U S A *103*, 12763-12768.
Bischof, J., Maeda, R.K., Hediger, M., Karch, F., and Basler, K. (2007). An optimized transgenesis system for Drosophila using germ-line-specific phiC31 integrases. Proc Natl Acad Sci U S A *104*, 3312-3317.
Blauwkamp, T.A., Chang, M.V., and Cadigan, K.M. (2008). Novel TCF-binding sites specify transcriptional repression by Wnt signalling. Embo J *27*, 1436-1446.
Brand, A.H., and Perrimon, N. (1993). Targeted gene expression as a means of altering cell fates and generating dominant phenotypes. Development *118*, 401-415.

Brodin, G., Ahgren, A., ten Dijke, P., Heldin, C.H., and Heuchel, R. (2000). Efficient TGF-beta induction of the Smad7 gene requires cooperation between AP-1, Sp1, and Smad proteins on the mouse Smad7 promoter. J Biol Chem *275*, 29023-29030.
Calleja, M., Moreno, E., Pelaz, S., and Morata, G. (1996). Visualization of gene expression in living adult Drosophila. Science *274*, 252-255.
Campbell, G., and Tomlinson, A. (1999). Transducing the Dpp morphogen gradient in the wing of Drosophila: regulation of Dpp targets by brinker. Cell *96*, 553-562.
Campbell, S., Inamdar, M., Rodrigues, V., Raghavan, V., Palazzolo, M., and Chovnick, A. (1992). The scalloped gene encodes a novel, evolutionarily conserved transcription factor required for sensory organ differentiation in Drosophila. Genes Dev *6*, 367-379.
Carroll, S.B. (2008). Evo-devo and an expanding evolutionary synthesis: a genetic theory of morphological evolution. Cell *134*, 25-36.
Chai, J., Wu, J.W., Yan, N., Massague, J., Pavletich, N.P., and Shi, Y. (2003). Features of a Smad3 MH1-DNA complex. Roles of water and zinc in DNA binding. J Biol Chem *278*, 20327-20331.
Chen, C.K., Kuhnlein, R.P., Eulenberg, K.G., Vincent, S., Affolter, M., and Schuh, R. (1998). The transcription factors KNIRPS and KNIRPS RELATED control cell migration and branch morphogenesis during Drosophila tracheal development. Development *125*, 4959-4968.
Chen, X., Weisberg, E., Fridmacher, V., Watanabe, M., Naco, G., and Whitman, M. (1997). Smad4 and FAST-1 in the assembly of activin-responsive factor. Nature *389*, 85-89.
Conley, C.A., Silburn, R., Singer, M.A., Ralston, A., Rohwer-Nutter, D., Olson, D.J., Gelbart, W., and Blair, S.S. (2000). Crossveinless 2 contains cysteine-rich domains and is required for high levels of BMP-like activity during the formation of the cross veins in Drosophila. Development *127*, 3947-3959.
Cordier, F., Hartmann, B., Rogowski, M., Affolter, M., and Grzesiek, S. (2006). DNA recognition by the brinker repressor--an extreme case of coupling between binding and folding. J Mol Biol *361*, 659-672.
Dai, H., Hogan, C., Gopalakrishnan, B., Torres-Vazquez, J., Nguyen, M., Park, S., Raftery, L.A., Warrior, R., and Arora, K. (2000). The zinc finger protein schnurri acts as a Smad partner in mediating the transcriptional response to decapentaplegic. Dev Biol *227*, 373-387.
de Larco, J.E., and Todaro, G.J. (1978). Growth factors from murine sarcoma virus-transformed cells. Proc Natl Acad Sci U S A *75*, 4001-4005.
Denissova, N.G., and Liu, F. (2004). Repression of endogenous Smad7 by Ski. J Biol Chem *279*, 28143-28148.
Denissova, N.G., Pouponnot, C., Long, J., He, D., and Liu, F. (2000). Transforming growth factor beta -inducible independent binding of SMAD to the Smad7 promoter. Proc Natl Acad Sci U S A *97*, 6397-6402.
Derynck, R., and Miyazono, K. (2007). TGF-beta and the TGF-beta Family. In The TGF-beta Family, R. Derynck, and K. Miyazono, eds. (Cold Spring Harbor Laboratory Press), pp. 29-43.
Dorfman, R., Glazer, L., Weihe, U., Wernet, M.F., and Shilo, B.Z. (2002). Elbow and Noc define a family of zinc finger proteins controlling morphogenesis of specific tracheal branches. Development *129*, 3585-3596.
Dosch, R., Gawantka, V., Delius, H., Blumenstock, C., and Niehrs, C. (1997). Bmp-4 acts as a morphogen in dorsoventral mesoderm patterning in Xenopus. Development *124*, 2325-2334.
Doyle, H.J., Kraut, R., and Levine, M. (1989). Spatial regulation of zerknullt: a dorsal-ventral patterning gene in Drosophila. Genes Dev *3*, 1518-1533.
Dürr, U., Henningfeld, K.A., Hollemann, T., Knöchel, W., and Pieler, T. (2004). Isolation and characterization of the Xenopus HIVEP gene family. Eur J Biochem *271*, 1135-1144.

Edlund, S., Bu, S., Schuster, N., Aspenstrom, P., Heuchel, R., Heldin, N.E., ten Dijke, P., Heldin, C.H., and Landstrom, M. (2003). Transforming growth factor-beta1 (TGF-beta)-induced apoptosis of prostate cancer cells involves Smad7-dependent activation of p38 by TGF-beta-activated kinase 1 and mitogen-activated protein kinase kinase 3. Mol Biol Cell *14*, 529-544.

Edlund, S., Lee, S.Y., Grimsby, S., Zhang, S., Aspenstrom, P., Heldin, C.H., and Landstrom, M. (2005). Interaction between Smad7 and beta-catenin: importance for transforming growth factor beta-induced apoptosis. Mol Cell Biol *25*, 1475-1488.

Eldar, A., Dorfman, R., Weiss, D., Ashe, H., Shilo, B.Z., and Barkai, N. (2002). Robustness of the BMP morphogen gradient in Drosophila embryonic patterning. Nature *419*, 304-308.

Entchev, E.V., Schwabedissen, A., and Gonzalez-Gaitan, M. (2000). Gradient formation of the TGF-beta homolog Dpp. Cell *103*, 981-991.

Ericson, J., Briscoe, J., Rashbass, P., van Heyningen, V., and Jessell, T.M. (1997). Graded sonic hedgehog signaling and the specification of cell fate in the ventral neural tube. Cold Spring Harb Symp Quant Biol *62*, 451-466.

Feng, X.H., and Derynck, R. (2005). Specificity and versatility in tgf-beta signaling through Smads. Annu Rev Cell Dev Biol *21*, 659-693.

Frazer, K.A., Pachter, L., Poliakov, A., Rubin, E.M., and Dubchak, I. (2004). VISTA: computational tools for comparative genomics. Nucleic Acids Res *32*, W273-279.

Fromental-Ramain, C., Vanolst, L., Delaporte, C., and Ramain, P. (2008). pannier encodes two structurally related isoforms that are differentially expressed during Drosophila development and display distinct functions during thorax patterning. Mech Dev *125*, 43-57.

Gajewski, K., Fossett, N., Molkentin, J.D., and Schulz, R.A. (1999). The zinc finger proteins Pannier and GATA4 function as cardiogenic factors in Drosophila. Development *126*, 5679-5688.

Galant, R., Walsh, C.M., and Carroll, S.B. (2002). Hox repression of a target gene: extradenticle-independent, additive action through multiple monomer binding sites. Development *129*, 3115-3126.

Gao, S., and Laughon, A. (2007). Flexible interaction of Drosophila Smad complexes with bipartite binding sites. Biochim Biophys Acta *1769*, 484-496.

Gao, S., Steffen, J., and Laughon, A. (2005). Dpp-responsive silencers are bound by a trimeric Mad-Medea complex. J Biol Chem *280*, 36158-36164.

Gilbert, S.F. (2000). Developmental Biology, 6th edn (Sunderland, Mass., Sinauer).

Goulev, Y., Fauny, J.D., Gonzalez-Marti, B., Flagiello, D., Silber, J., and Zider, A. (2008). SCALLOPED interacts with YORKIE, the nuclear effector of the hippo tumor-suppressor pathway in Drosophila. Curr Biol *18*, 435-441.

Grieder, N.C., Marty, T., Ryoo, H.D., Mann, R.S., and Affolter, M. (1997). Synergistic activation of a Drosophila enhancer by HOM/EXD and DPP signaling. Embo J *16*, 7402-7410.

Grieder, N.C., Nellen, D., Burke, R., Basler, K., and Affolter, M. (1995). Schnurri is required for Drosophila Dpp signaling and encodes a zinc finger protein similar to the mammalian transcription factor PRDII-BF1. Cell *81*, 791-800.

Guss, K.A., Nelson, C.E., Hudson, A., Kraus, M.E., and Carroll, S.B. (2001). Control of a genetic regulatory network by a selector gene. Science *292*, 1164-1167.

Halder, G., Callaerts, P., and Gehring, W.J. (1995). Induction of ectopic eyes by targeted expression of the eyeless gene in Drosophila. Science *267*, 1788-1792.

Halder, G., and Carroll, S.B. (2001). Binding of the Vestigial co-factor switches the DNA-target selectivity of the Scalloped selector protein. Development *128*, 3295-3305.

Halder, G., Polaczyk, P., Kraus, M.E., Hudson, A., Kim, J., Laughon, A., and Carroll, S. (1998). The Vestigial and Scalloped proteins act together to directly regulate wing-specific gene expression in Drosophila. Genes Dev *12*, 3900-3909.

Hamaguchi, T., Yabe, S., Uchiyama, H., and Murakami, R. (2004). Drosophila Tbx6-related gene, Dorsocross, mediates high levels of Dpp and Scw signal required for the development of amnioserosa and wing disc primordium. Dev Biol *265*, 355-368.
Han, G., Li, A.G., Liang, Y.Y., Owens, P., He, W., Lu, S., Yoshimatsu, Y., Wang, D., Ten Dijke, P., Lin, X., *et al.* (2006). Smad7-induced beta-catenin degradation alters epidermal appendage development. Dev Cell *11*, 301-312.
Hartmann, B. (2004). Characterization of Schnurri, an integral component of the Dpp-signaling pathway in Drosophila melanogaster. In Biozentrum (Basel, University of Basel).
Hasson, P., Muller, B., Basler, K., and Paroush, Z. (2001). Brinker requires two corepressors for maximal and versatile repression in Dpp signalling. Embo J *20*, 5725-5736.
Hata, A., Lo, R.S., Wotton, D., Lagna, G., and Massague, J. (1997). Mutations increasing autoinhibition inactivate tumour suppressors Smad2 and Smad4. Nature *388*, 82-87.
Hata, A., Seoane, J., Lagna, G., Montalvo, E., Hemmati-Brivanlou, A., and Massague, J. (2000). OAZ uses distinct DNA- and protein-binding zinc fingers in separate BMP-Smad and Olf signaling pathways. Cell *100*, 229-240.
Hayashi, H., Abdollah, S., Qiu, Y., Cai, J., Xu, Y.Y., Grinnell, B.W., Richardson, M.A., Topper, J.N., Gimbrone, M.A., Jr., Wrana, J.L., *et al.* (1997). The MAD-related protein Smad7 associates with the TGFbeta receptor and functions as an antagonist of TGFbeta signaling. Cell *89*, 1165-1173.
Heitzler, P., Haenlin, M., Ramain, P., Calleja, M., and Simpson, P. (1996). A genetic analysis of pannier, a gene necessary for viability of dorsal tissues and bristle positioning in Drosophila. Genetics *143*, 1271-1286.
Heldin, C.-H. (2007). TGF-beta Signaling from Receptors to Smads. In The TGF-beta Family, R. Derynck, and K. Miyazono, eds. (Cold Spring Harbor Laboratory Press), pp. 259-285.
Herranz, H., and Morata, G. (2001). The functions of pannier during Drosophila embryogenesis. Development *128*, 4837-4846.
Hogan, B.L. (1996). Bone morphogenetic proteins: multifunctional regulators of vertebrate development. Genes Dev *10*, 1580-1594.
Hua, X., Miller, Z.A., Benchabane, H., Wrana, J.L., and Lodish, H.F. (2000). Synergism between transcription factors TFE3 and Smad3 in transforming growth factor-beta-induced transcription of the Smad7 gene. J Biol Chem *275*, 33205-33208.
Imamura, T., Takase, M., Nishihara, A., Oeda, E., Hanai, J., Kawabata, M., and Miyazono, K. (1997). Smad6 inhibits signalling by the TGF-beta superfamily. Nature *389*, 622-626.
Inoue, H., Imamura, T., Ishidou, Y., Takase, M., Udagawa, Y., Oka, Y., Tsuneizumi, K., Tabata, T., Miyazono, K., and Kawabata, M. (1998). Interplay of signal mediators of decapentaplegic (Dpp): molecular characterization of mothers against dpp, Medea, and daughters against dpp. Mol Biol Cell *9*, 2145-2156.
Isaac, D.D., and Andrew, D.J. (1996). Tubulogenesis in Drosophila: a requirement for the trachealess gene product. Genes Dev *10*, 103-117.
Ishida, W., Hamamoto, T., Kusanagi, K., Yagi, K., Kawabata, M., Takehara, K., Sampath, T.K., Kato, M., and Miyazono, K. (2000). Smad6 is a Smad1/5-induced smad inhibitor. Characterization of bone morphogenetic protein-responsive element in the mouse Smad6 promoter. J Biol Chem *275*, 6075-6079.
Jazwinska, A., Kirov, N., Wieschaus, E., Roth, S., and Rushlow, C. (1999a). The Drosophila gene brinker reveals a novel mechanism of Dpp target gene regulation. Cell *96*, 563-573.
Jazwinska, A., Rushlow, C., and Roth, S. (1999b). The role of brinker in mediating the graded response to Dpp in early Drosophila embryos. Development *126*, 3323-3334.
Jeong, S., Rebeiz, M., Andolfatto, P., Werner, T., True, J., and Carroll, S.B. (2008). The evolution of gene regulation underlies a morphological difference between two Drosophila sister species. Cell *132*, 783-793.

Jin, W., Takagi, T., Kanesashi, S.N., Kurahashi, T., Nomura, T., Harada, J., and Ishii, S. (2006). Schnurri-2 controls BMP-dependent adipogenesis via interaction with Smad proteins. Dev Cell *10*, 461-471.
Jones, D.C., Wein, M.N., Oukka, M., Hofstaetter, J.G., Glimcher, M.J., and Glimcher, L.H. (2006). Regulation of adult bone mass by the zinc finger adapter protein Schnurri-3. Science *312*, 1223-1227.
Jungert, K., Buck, A., Buchholz, M., Wagner, M., Adler, G., Gress, T.M., and Ellenrieder, V. (2006). Smad-Sp1 complexes mediate TGFbeta-induced early transcription of oncogenic Smad7 in pancreatic cancer cells. Carcinogenesis *27*, 2392-2401.
Kamiya, Y., Miyazono, K., and Miyazawa, K. (2008). Specificity of the inhibitory effects of Dad on TGF-beta family type I receptors, Thickveins, Saxophone, and Baboon in Drosophila. FEBS Lett *582*, 2496-2500.
Karaulanov, E., Knochel, W., and Niehrs, C. (2004). Transcriptional regulation of BMP4 synexpression in transgenic Xenopus. Embo J *23*, 844-856.
Karess, R.E., and Rubin, G.M. (1984). Analysis of P transposable element functions in Drosophila. Cell *38*, 135-146.
Kavsak, P., Rasmussen, R.K., Causing, C.G., Bonni, S., Zhu, H., Thomsen, G.H., and Wrana, J.L. (2000). Smad7 binds to Smurf2 to form an E3 ubiquitin ligase that targets the TGF beta receptor for degradation. Mol Cell *6*, 1365-1375.
Kim, J., Johnson, K., Chen, H.J., Carroll, S., and Laughon, A. (1997). Drosophila Mad binds to DNA and directly mediates activation of vestigial by Decapentaplegic. Nature *388*, 304-308.
Kirkpatrick, H., Johnson, K., and Laughon, A. (2001). Repression of dpp targets by binding of brinker to mad sites. J Biol Chem *276*, 18216-18222.
Korchynskyi, O., and ten Dijke, P. (2002). Identification and functional characterization of distinct critically important bone morphogenetic protein-specific response elements in the Id1 promoter. J Biol Chem *277*, 4883-4891.
Ku, M., Howard, S., Ni, W., Lagna, G., and Hata, A. (2006). OAZ regulates bone morphogenetic protein signaling through Smad6 activation. J Biol Chem *281*, 5277-5287.
Kuhnlein, R.P., Bronner, G., Taubert, H., and Schuh, R. (1997). Regulation of Drosophila spalt gene expression. Mech Dev *66*, 107-118.
Labbe, E., Silvestri, C., Hoodless, P.A., Wrana, J.L., and Attisano, L. (1998). Smad2 and Smad3 positively and negatively regulate TGF beta-dependent transcription through the forkhead DNA-binding protein FAST2. Mol Cell *2*, 109-120.
Lallemand, F., Mazars, A., Prunier, C., Bertrand, F., Kornprost, M., Gallea, S., Roman-Roman, S., Cherqui, G., and Atfi, A. (2001). Smad7 inhibits the survival nuclear factor kappaB and potentiates apoptosis in epithelial cells. Oncogene *20*, 879-884.
Leung, T.H., Hoffmann, A., and Baltimore, D. (2004). One nucleotide in a kappaB site can determine cofactor specificity for NF-kappaB dimers. Cell *118*, 453-464.
Liang, J., Lints, R., Foehr, M.L., Tokarz, R., Yu, L., Emmons, S.W., Liu, J., and Savage-Dunn, C. (2003a). The Caenorhabditis elegans schnurri homolog sma-9 mediates stage- and cell type-specific responses to DBL-1 BMP-related signaling. Development *130*, 6453-6464.
Liang, Y.Y., Lin, X., Liang, M., Brunicardi, F.C., ten Dijke, P., Chen, Z., Choi, K.W., and Feng, X.H. (2003b). dSmurf selectively degrades decapentaplegic-activated MAD, and its overexpression disrupts imaginal disc development. J Biol Chem *278*, 26307-26310.
Lin, X., Liang, Y.Y., Sun, B., Liang, M., Shi, Y., Brunicardi, F.C., Shi, Y., and Feng, X.H. (2003). Smad6 recruits transcription corepressor CtBP to repress bone morphogenetic protein-induced transcription. Mol Cell Biol *23*, 9081-9093.
Lin, X., and Perrimon, N. (1999). Dally cooperates with Drosophila Frizzled 2 to transduce Wingless signalling. Nature *400*, 281-284.

Luecke, H.F., and Yamamoto, K.R. (2005). The glucocorticoid receptor blocks P-TEFb recruitment by NFkappaB to effect promoter-specific transcriptional repression. Genes Dev *19*, 1116-1127.
Maekawa, T., Sakura, H., Sudo, T., and Ishii, S. (1989). Putative metal finger structure of the human immunodeficiency virus type 1 enhancer binding protein HIV-EP1. J Biol Chem *264*, 14591-14593.
Markstein, M., Markstein, P., Markstein, V., and Levine, M.S. (2002). Genome-wide analysis of clustered Dorsal binding sites identifies putative target genes in the Drosophila embryo. Proc Natl Acad Sci U S A *99*, 763-768.
Marty, T., Muller, B., Basler, K., and Affolter, M. (2000). Schnurri mediates Dpp-dependent repression of brinker transcription. Nat Cell Biol *2*, 745-749.
Marty, T., Vigano, M.A., Ribeiro, C., Nussbaumer, U., Grieder, N.C., and Affolter, M. (2001). A HOX complex, a repressor element and a 50 bp sequence confer regional specificity to a DPP-responsive enhancer. Development *128*, 2833-2845.
Mayor, C., Brudno, M., Schwartz, J.R., Poliakov, A., Rubin, E.M., Frazer, K.A., Pachter, L.S., and Dubchak, I. (2000). VISTA : visualizing global DNA sequence alignments of arbitrary length. Bioinformatics *16*, 1046-1047.
Mazars, A., Lallemand, F., Prunier, C., Marais, J., Ferrand, N., Pessah, M., Cherqui, G., and Atfi, A. (2001). Evidence for a role of the JNK cascade in Smad7-mediated apoptosis. J Biol Chem *276*, 36797-36803.
Minami, M., Kinoshita, N., Kamoshida, Y., Tanimoto, H., and Tabata, T. (1999). brinker is a target of Dpp in Drosophila that negatively regulates Dpp-dependent genes. Nature *398*, 242-246.
Miyazono, K. (2007). Regulation of TGF-beta Family Signaling by I-Smads. In The TGF-beta Family, R. Derynck, and K. Miyazono, eds. (Cold Spring Harbor Laboratory Press), pp. 363-387.
Monteiro, R.M., de Sousa Lopes, S.M., Korchynskyi, O., ten Dijke, P., and Mummery, C.L. (2004). Spatio-temporal activation of Smad1 and Smad5 in vivo: monitoring transcriptional activity of Smad proteins. J Cell Sci *117*, 4653-4663.
Moser, M., and Campbell, G. (2005). Generating and interpreting the Brinker gradient in the Drosophila wing. Dev Biol *286*, 647-658.
Moses, H.L., Branum, E.L., Proper, J.A., and Robinson, R.A. (1981). Transforming growth factor production by chemically transformed cells. Cancer Res *41*, 2842-2848.
Müller, B., Hartmann, B., Pyrowolakis, G., Affolter, M., and Basler, K. (2003). Conversion of an extracellular Dpp/BMP morphogen gradient into an inverse transcriptional gradient. Cell *113*, 221-233.
Murakami, G., Watabe, T., Takaoka, K., Miyazono, K., and Imamura, T. (2003). Cooperative inhibition of bone morphogenetic protein signaling by Smurf1 and inhibitory Smads. Mol Biol Cell *14*, 2809-2817.
Nagarajan, R.P., Zhang, J., Li, W., and Chen, Y. (1999). Regulation of Smad7 promoter by direct association with Smad3 and Smad4. J Biol Chem *274*, 33412-33418.
Nakao, A., Afrakhte, M., Moren, A., Nakayama, T., Christian, J.L., Heuchel, R., Itoh, S., Kawabata, M., Heldin, N.E., Heldin, C.H.*, et al.* (1997). Identification of Smad7, a TGFbeta-inducible antagonist of TGF-beta signalling. Nature *389*, 631-635.
Nellen, D., Burke, R., Struhl, G., and Basler, K. (1996). Direct and long-range action of a DPP morphogen gradient. Cell *85*, 357-368.
Nüsslein-Volhard, C., Wieschaus, E., and Klundig, H. (1984). Mutations affecting the pattern of the larval cuticle in Drosophila melanogaster. I. Zygotic loci on the second chromosome. Roux's Arch Dev Biol *193*, 267–282.

Ohshiro, T., and Saigo, K. (1997). Transcriptional regulation of breathless FGF receptor gene by binding of TRACHEALESS/dARNT heterodimers to three central midline elements in Drosophila developing trachea. Development *124*, 3975-3986.
Oukka, M., Kim, S.T., Lugo, G., Sun, J., Wu, L.C., and Glimcher, L.H. (2002). A mammalian homolog of Drosophila schnurri, KRC, regulates TNF receptor-driven responses and interacts with TRAF2. Mol Cell *9*, 121-131.
Oukka, M., Wein, M.N., and Glimcher, L.H. (2004). Schnurri-3 (KRC) interacts with c-Jun to regulate the IL-2 gene in T cells. J Exp Med *199*, 15-24.
Padgett, R.W., Wozney, J.M., and Gelbart, W.M. (1993). Human BMP sequences can confer normal dorsal-ventral patterning in the Drosophila embryo. Proc Natl Acad Sci U S A *90*, 2905-2909.
Panganiban, G.E., Reuter, R., Scott, M.P., and Hoffmann, F.M. (1990). A Drosophila growth factor homolog, decapentaplegic, regulates homeotic gene expression within and across germ layers during midgut morphogenesis. Development *110*, 1041-1050.
Pankratz, M.J., Busch, M., Hoch, M., Seifert, E., and Jackle, H. (1992). Spatial control of the gap gene knirps in the Drosophila embryo by posterior morphogen system. Science *255*, 986-989.
Parker, L., Stathakis, D.G., and Arora, K. (2004). Regulation of BMP and activin signaling in Drosophila. Prog Mol Subcell Biol *34*, 73-101.
Pyrowolakis, G., Hartmann, B., and Affolter, M. (2007). TGF-beta Family Signaling in Drosophila. In The TGF-beta Family, R. Derynck, and K. Miyazono, eds. (Cold Spring Harbor Laboratory Press), pp. 493-526.
Pyrowolakis, G., Hartmann, B., Muller, B., Basler, K., and Affolter, M. (2004). A simple molecular complex mediates widespread BMP-induced repression during Drosophila development. Dev Cell *7*, 229-240.
Ramain, P., Heitzler, P., Haenlin, M., and Simpson, P. (1993). pannier, a negative regulator of achaete and scute in Drosophila, encodes a zinc finger protein with homology to the vertebrate transcription factor GATA-1. Development *119*, 1277-1291.
Reim, I., Lee, H.H., and Frasch, M. (2003). The T-box-encoding Dorsocross genes function in amnioserosa development and the patterning of the dorsolateral germ band downstream of Dpp. Development *130*, 3187-3204.
Roberts, A.B., Anzano, M.A., Lamb, L.C., Smith, J.M., and Sporn, M.B. (1981). New class of transforming growth factors potentiated by epidermal growth factor: isolation from non-neoplastic tissues. Proc Natl Acad Sci U S A *78*, 5339-5343.
Rothe, M., Nauber, U., and Jackle, H. (1989). Three hormone receptor-like Drosophila genes encode an identical DNA-binding finger. Embo J *8*, 3087-3094.
Rusch, J., and Levine, M. (1997). Regulation of a dpp target gene in the Drosophila embryo. Development *124*, 303-311.
Rushlow, C., Colosimo, P.F., Lin, M.C., Xu, M., and Kirov, N. (2001). Transcriptional regulation of the Drosophila gene zen by competing Smad and Brinker inputs. Genes Dev *15*, 340-351.
Saller, E., and Bienz, M. (2001). Direct competition between Brinker and Drosophila Mad in Dpp target gene transcription. EMBO Rep *2*, 298-305.
Sambrook, J., and Russell, D.W. (2001). Molecular cloning a laboratory manual, 3rd edn (Cold Spring Harbor, (N.Y.), Cold Spring Harbor Laboratory Press).
Sato, M., Kojima, T., Michiue, T., and Saigo, K. (1999). Bar homeobox genes are latitudinal prepattern genes in the developing Drosophila notum whose expression is regulated by the concerted functions of decapentaplegic and wingless. Development *126*, 1457-1466.
Sato, M., and Saigo, K. (2000). Involvement of pannier and u-shaped in regulation of decapentaplegic-dependent wingless expression in developing Drosophila notum. Mech Dev *93*, 127-138.

Saucedo, L.J., and Edgar, B.A. (2007). Filling out the Hippo pathway. Nature reviews *8*, 613-621.
Scully, K.M., Jacobson, E.M., Jepsen, K., Lunyak, V., Viadiu, H., Carriere, C., Rose, D.W., Hooshmand, F., Aggarwal, A.K., and Rosenfeld, M.G. (2000). Allosteric effects of Pit-1 DNA sites on long-term repression in cell type specification. Science *290*, 1127-1131.
Segalat, L., Berger, G., and Lepesant, J.A. (1994). Dissection of the Drosophila pourquoi-pas? promoter: complex ovarian expression is driven by distinct follicle cell- and germ line-specific enhancers. Mech Dev *47*, 241-251.
Sekelsky, J.J., Newfeld, S.J., Raftery, L.A., Chartoff, E.H., and Gelbart, W.M. (1995). Genetic characterization and cloning of mothers against dpp, a gene required for decapentaplegic function in Drosophila melanogaster. Genetics *139*, 1347-1358.
Seki, K., and Hata, A. (2004). Indian hedgehog gene is a target of the bone morphogenetic protein signaling pathway. J Biol Chem *279*, 18544-18549.
Serpe, M., Umulis, D., Ralston, A., Chen, J., Olson, D.J., Avanesov, A., Othmer, H., O'Connor, M.B., and Blair, S.S. (2008). The BMP-binding protein Crossveinless 2 is a short-range, concentration-dependent, biphasic modulator of BMP signaling in Drosophila. Dev Cell *14*, 940-953.
Shi, W., Sun, C., He, B., Xiong, W., Shi, X., Yao, D., and Cao, X. (2004). GADD34-PP1c recruited by Smad7 dephosphorylates TGFbeta type I receptor. J Cell Biol *164*, 291-300.
Shi, Y., and Massague, J. (2003). Mechanisms of TGF-beta signaling from cell membrane to the nucleus. Cell *113*, 685-700.
Shi, Y., Wang, Y.F., Jayaraman, L., Yang, H., Massague, J., and Pavletich, N.P. (1998). Crystal structure of a Smad MH1 domain bound to DNA: insights on DNA binding in TGF-beta signaling. Cell *94*, 585-594.
Sivasankaran, R., Vigano, M.A., Muller, B., Affolter, M., and Basler, K. (2000). Direct transcriptional control of the Dpp target omb by the DNA binding protein Brinker. Embo J *19*, 6162-6172.
Small, S., Blair, A., and Levine, M. (1992). Regulation of even-skipped stripe 2 in the Drosophila embryo. Embo J *11*, 4047-4057.
Sonnenfeld, M., Ward, M., Nystrom, G., Mosher, J., Stahl, S., and Crews, S. (1997). The Drosophila tango gene encodes a bHLH-PAS protein that is orthologous to mammalian Arnt and controls CNS midline and tracheal development. Development *124*, 4571-4582.
Spencer, F.A., Hoffmann, F.M., and Gelbart, W.M. (1982). Decapentaplegic: a gene complex affecting morphogenesis in Drosophila melanogaster. Cell *28*, 451-461.
Srinivasan, S., Rashka, K.E., and Bier, E. (2002). Creation of a Sog morphogen gradient in the Drosophila embryo. Dev Cell *2*, 91-101.
Staehling-Hampton, K., Laughon, A.S., and Hoffmann, F.M. (1995). A Drosophila protein related to the human zinc finger transcription factor PRDII/MBPI/HIV-EP1 is required for dpp signaling. Development *121*, 3393-3403.
Tabata, T. (2001). Genetics of morphogen gradients. Nat Rev Genet *2*, 620-630.
Takagi, T., Harada, J., and Ishii, S. (2001). Murine Schnurri-2 is required for positive selection of thymocytes. Nat Immunol *2*, 1048-1053.
Teleman, A.A., and Cohen, S.M. (2000). Dpp gradient formation in the Drosophila wing imaginal disc. Cell *103*, 971-980.
ten Dijke, P., and Hill, C.S. (2004). New insights into TGF-beta-Smad signalling. Trends Biochem Sci *29*, 265-273.
Thuringer, F., Cohen, S.M., and Bienz, M. (1993). Dissection of an indirect autoregulatory response of a homeotic Drosophila gene. Embo J *12*, 2419-2430.
Tomancak, P., Beaton, A., Weiszmann, R., Kwan, E., Shu, S., Lewis, S.E., Richards, S., Ashburner, M., Hartenstein, V., Celniker, S.E., *et al.* (2002). Systematic determination of

patterns of gene expression during Drosophila embryogenesis. Genome Biol *3*, RESEARCH0088.
Tomoyasu, Y., Ueno, N., and Nakamura, M. (2000). The decapentaplegic morphogen gradient regulates the notal wingless expression through induction of pannier and u-shaped in Drosophila. Mech Dev *96*, 37-49.
Torres-Vazquez, J., Park, S., Warrior, R., and Arora, K. (2001). The transcription factor Schnurri plays a dual role in mediating Dpp signaling during embryogenesis. Development *128*, 1657-1670.
Traka, M., Gasper, A.V., Melchini, A., Bacon, J.R., Needs, P.W., Frost, V., Chantry, A., Jones, A.M., Ortori, C.A., Barrett, D.A.*, et al.* (2008). Broccoli consumption interacts with GSTM1 to perturb oncogenic signalling pathways in the prostate. PLoS ONE *3*, e2568.
Tsuda, M., Kamimura, K., Nakato, H., Archer, M., Staatz, W., Fox, B., Humphrey, M., Olson, S., Futch, T., Kaluza, V.*, et al.* (1999). The cell-surface proteoglycan Dally regulates Wingless signalling in Drosophila. Nature *400*, 276-280.
Tsuji, Y., Torti, S.V., and Torti, F.M. (1998). Activation of the ferritin H enhancer, FER-1, by the cooperative action of members of the AP1 and Sp1 transcription factor families. J Biol Chem *273*, 2984-2992.
Tsukazaki, T., Chiang, T.A., Davison, A.F., Attisano, L., and Wrana, J.L. (1998). SARA, a FYVE domain protein that recruits Smad2 to the TGFbeta receptor. Cell *95*, 779-791.
Tsuneizumi, K., Nakayama, T., Kamoshida, Y., Kornberg, T.B., Christian, J.L., and Tabata, T. (1997). Daughters against dpp modulates dpp organizing activity in Drosophila wing development. Nature *389*, 627-631.
Udagawa, Y., Hanai, J., Tada, K., Grieder, N.C., Momoeda, M., Taketani, Y., Affolter, M., Kawabata, M., and Miyazono, K. (2000). Schnurri interacts with Mad in a Dpp-dependent manner. Genes to cells *5*, 359-369.
van Helden, J., Andre, B., and Collado-Vides, J. (2000). A web site for the computational analysis of yeast regulatory sequences. Yeast *16*, 177-187.
von Bubnoff, A., Peiffer, D.A., Blitz, I.L., Hayata, T., Ogata, S., Zeng, Q., Trunnell, M., and Cho, K.W. (2005). Phylogenetic footprinting and genome scanning identify vertebrate BMP response elements and new target genes. Dev Biol *281*, 210-226.
von Gersdorff, G., Susztak, K., Rezvani, F., Bitzer, M., Liang, D., and Bottinger, E.P. (2000). Smad3 and Smad4 mediate transcriptional activation of the human Smad7 promoter by transforming growth factor beta. J Biol Chem *275*, 11320-11326.
Walsh, C.M., and Carroll, S.B. (2007). Collaboration between Smads and a Hox protein in target gene repression. Development *134*, 3585-3592.
Wang, Q., Wei, X., Zhu, T., Zhang, M., Shen, R., Xing, L., O'Keefe, R.J., and Chen, D. (2007). Bone morphogenetic protein 2 activates Smad6 gene transcription through bone-specific transcription factor Runx2. J Biol Chem *282*, 10742-10748.
Wharton, S.J., Basu, S.P., and Ashe, H.L. (2004). Smad affinity can direct distinct readouts of the embryonic extracellular Dpp gradient in Drosophila. Curr Biol *14*, 1550-1558.
Wieser, R., Wrana, J.L., and Massague, J. (1995). GS domain mutations that constitutively activate T beta R-I, the downstream signaling component in the TGF-beta receptor complex. Embo J *14*, 2199-2208.
Wilk, R., Weizman, I., and Shilo, B.Z. (1996). trachealess encodes a bHLH-PAS protein that is an inducer of tracheal cell fates in Drosophila. Genes Dev *10*, 93-102.
Winick, J., Abel, T., Leonard, M.W., Michelson, A.M., Chardon-Loriaux, I., Holmgren, R.A., Maniatis, T., and Engel, J.D. (1993). A GATA family transcription factor is expressed along the embryonic dorsoventral axis in Drosophila melanogaster. Development *119*, 1055-1065.
Wolpert, L. (1969). Positional information and the spatial pattern of cellular differentiation. J Theor Biol *25*, 1-47.

Wozney, J.M., Rosen, V., Celeste, A.J., Mitsock, L.M., Whitters, M.J., Kriz, R.W., Hewick, R.M., and Wang, E.A. (1988). Novel regulators of bone formation: molecular clones and activities. Science *242*, 1528-1534.
Wu, S., Liu, Y., Zheng, Y., Dong, J., and Pan, D. (2008). The TEAD/TEF family protein Scalloped mediates transcriptional output of the Hippo growth-regulatory pathway. Dev Cell *14*, 388-398.
Xu, M., Kirov, N., and Rushlow, C. (2005). Peak levels of BMP in the Drosophila embryo control target genes by a feed-forward mechanism. Development *132*, 1637-1647.
Xu, X., Yin, Z., Hudson, J.B., Ferguson, E.L., and Frasch, M. (1998). Smad proteins act in combination with synergistic and antagonistic regulators to target Dpp responses to the Drosophila mesoderm. Genes Dev *12*, 2354-2370.
Yao, L.C., Blitz, I.L., Peiffer, D.A., Phin, S., Wang, Y., Ogata, S., Cho, K.W., Arora, K., and Warrior, R. (2006). Schnurri transcription factors from Drosophila and vertebrates can mediate Bmp signaling through a phylogenetically conserved mechanism. Development *133*, 4025-4034.
Yao, L.C., Phin, S., Cho, J., Rushlow, C., Arora, K., and Warrior, R. (2008). Multiple modular promoter elements drive graded brinker expression in response to the Dpp morphogen gradient. Development *135*, 2183-2192.
Yu, P.B., Hong, C.C., Sachidanandan, C., Babitt, J.L., Deng, D.Y., Hoyng, S.A., Lin, H.Y., Bloch, K.D., and Peterson, R.T. (2008). Dorsomorphin inhibits BMP signals required for embryogenesis and iron metabolism. Nat Chem Biol *4*, 33-41.
Zawel, L., Dai, J.L., Buckhaults, P., Zhou, S., Kinzler, K.W., Vogelstein, B., and Kern, S.E. (1998). Human Smad3 and Smad4 are sequence-specific transcription activators. Mol Cell *1*, 611-617.
Zecca, M., Basler, K., and Struhl, G. (1995). Sequential organizing activities of engrailed, hedgehog and decapentaplegic in the Drosophila wing. Development *121*, 2265-2278.
Zelzer, E., Wappner, P., and Shilo, B.Z. (1997). The PAS domain confers target gene specificity of Drosophila bHLH/PAS proteins. Genes Dev *11*, 2079-2089.
Zhang, H., Levine, M., and Ashe, H.L. (2001). Brinker is a sequence-specific transcriptional repressor in the Drosophila embryo. Genes Dev *15*, 261-266.
Zhang, J.L., Qiu, L.Y., Kotzsch, A., Weidauer, S., Patterson, L., Hammerschmidt, M., Sebald, W., and Mueller, T.D. (2008a). Crystal structure analysis reveals how the Chordin family member crossveinless 2 blocks BMP-2 receptor binding. Dev Cell *14*, 739-750.
Zhang, L., Ren, F., Zhang, Q., Chen, Y., Wang, B., and Jiang, J. (2008b). The TEAD/TEF family of transcription factor Scalloped mediates Hippo signaling in organ size control. Dev Cell *14*, 377-387.